University of Alberta

Molecular Mechanisms of Peroxisome Inheritance

In the Yeast *Saccharomyces cerevisiae*

by

©

Monica Eliza Fagarasanu,

A thesis submitted to the Faculty of Graduate Studies and Research in partial fulfillment

of the requirements for the degree of *Doctor of Philosophy*

Department of Cell Biology

Edmonton, Alberta

FALL, 2008

Preface

This thesis reports and discusses findings on the molecular mechanisms controlling peroxisome inheritance in the budding yeast, *Saccharomyces cerevisiae*. Two proteins, Inp1p and Yjl185p, involved in peroxisome retention in cells are highlighted.

Abstract

The inheritance of cellular organelles from mother cell to daughter cell is critical for eukaryotic cells to maintain the metabolic benefits of compartmentalization. Because of its asymetrical division, the budding yeast *Saccharomyces cerevisiae* has been used extensively to understand the molecular pathways involved in the inheritance of different organelles. The inheritance of peroxisomes is dependent on Inp1p, which is directly involved in tethering peroxisomes to anchoring structures at the cell cortex. Inp1p is a peroxisomal protein of *Saccharomyces cerevisiae* that affects both the morphology of peroxisomes and their partitioning during cell division. While Inp1p plays a central role in the peroxisomal retention pathway, its interaction partner protein encoded by the open reading frame *YJL185c* is required for the partial retention of peroxisomes on the distal region of the cell cortex. Cells deleted for *YJL185c* exhibit an altered peroxisome morphology and a preferred localization of peroxisomes to the bud neck. Thus, apart from its role in peroxisomal partitioning during cell division, Yjl185p also regulates the size and number of peroxisomes. In conclusion, our studies identified and characterized two new members involved in the peroxisomal inheritance pathway, namely the peroxisomal proteins Inp1p and Yjl185p.

Acknowledgements

I am greatly indebted to Dr. Richard Rachubinski for his excellent mentoring during my Ph.D. program. His guidance and encouragement led my way through the exciting and challenging world of graduate studies. I will always remember to look at the "big picture", as he taught me.

I would also like to thank Andrei Fagarasanu for being a team player and for everything else that he taught me (except subcellular fractionation). We had good times and we had difficult times, but in the end I respect him deeply and I hope we will both find our ways again.

As well, I thank Richard Poirier not only for his excellent technical assistance but for being such a fun person with whom to work. He always tackled my tehnical problems with a good laugh.

I thank Dwayne Weber as well for his excellent technical assistance and for keeping the laboratory a highly ordered space by meticulously labeling everything. He was a good friend who listened to me for hours about everything that bothered me at the time, especially the unforgiving climate during the winter.

I am also thankful to Fred Mast for being a good friend and lunch buddy and for his helpful feedback on defending my thesis. I found inspiration in his genuine interest for science as well as his drive to always make things better (deconvolved or not).

The president of the postdoc association of Cell Biology, Ryan Perry, was a good friend of mine and I thank him for the laughs that we shared and for the very interesting scientific and non-scientific conversations that we had.

Table of Contents

List of Tables

List of Figures and Illustrations

List of Symbols, Abbreviations and Nomenclature

20KgP	pellet obtained from centrifugation at 20,000x g
20KgS	20KgS supernatant obtained from centrifugation at 20,000x g
4D	four dimensional
bp	base pair
BSA	bovin serum albumin
Da	dalton
DRP	dynamin related protein
DMF	N, N-Dimethylformamide
dNTP	Deoxyribonucleoside triphosphate
ECL	Enhanced Chemiluminescence
ER	Endoplasmic reticulum
F-actin	filamentous actin
g	gram
g	gravitational force
G1	stage G1 of the cell cycle
G6PDH	glucose-6-phosphate dehydrogenase
GFP	green fluorescent protein
GST	glutathione S-transferase
h	hour
HRP	horseradish peroxidase
IgG	immunoglobulin G
IPTG	isopropyl β-D-thiogalactoside
PTS	peroxisomal targeting signal
M	stage M of the cell cycle
mRFP	monomeric red fluorescence protein
OD	optical density
pA	protein A
PAGE	polyacrylamide gel electrophoresis
PBD	peroxisome biogenesis disorder
PCR	polymerase chain reaction
PEX#	wild-type gene encoding *Pex#*p
pex#	mutant *PEX#* gene
PI-(3,4)/P2	phosphatidylinositol 3,4,5-trisphosphate
Pot1	thiolase
PNS	post-nuclear supernatant
S	stage S of the cell cycle

S. cerevisiae	*Saccharomyces cerevisiae*
Sdh2	succinate dehydrogenase
SDS	sodium dodecyl sulphate
TAP	tandem affinity purification
TCA	trichloroacetic
U	unit of enzyme activity
v	volume
w	weight
X-gal	5-bromo-4-chloro-3-indolyl-β-D-galactopyranoside
Y. lipolytica	*Yarrowia lipolytica*

CHAPTER ONE: INTRODUCTION

A version of this chapter has been published.

1.1 Compartmentalization of eukaryotic cells

Eukaryotic cells contain several membrane-enclosed compartments called organelles that perform diverse metabolic functions to ensure cell survival. The highly organized nature of the intracellular space established itself over time as the best way for cells to adapt to their environment. The compartmentalization of eukaryotic cells separates antagonistic biochemical reactions and facilitates complementary biochemical reactions by bringing their components into close proximity, thus increasing the overall competency of the cell.

1.2 Peroxisomes

Peroxisomes are round, single membrane-bounded organelles containing an enzymatic matrix and are found in almost all eukaryotic cells. Peroxisomes were first reported in the literature in the thesis of a Swedish graduate student, J. Rhodin (Rhodin, J. 1954, Doctoral Thesis). He described a new type of cytoplasmic organelle present in the proximal convoluted tubule cells of the mouse kidney and called it a "microbody". de Duve and coworkers later characterized peroxisomes morphologically and biochemically by isolating enriched fractions containing these organelles from rat liver, along with mitochondria and lysosomes (Schrader and Fahimi, 2008). The name "peroxisome" derives from the initial description of the chemical reactions of synthesis and degradation of hydrogen peroxide within peroxisomes.

Peroxisomal proteins are encoded by nuclear genes, synthesized on free polysomes and post-translationally imported (Purdue and Lazarow, 2001). In yeasts, plants, human and other mammals, peroxisome biogenesis involves at least 32 proteins,

known as peroxins, that are encoded by the PEX genes (Table 1-1). Peroxins are required for the assembly and maintenance of peroxisomes, which involves several events, including the initial formation of the peroxisomal membrane, the import of membrane as well as matrix proteins, and the proliferation of peroxisomes.

Table 1-1. Peroxins and their functions

Peroxin	Functions
Pex1p	Fusion of preperoxisomal vesicles
Pex2p	Peroxisomal matrix protein import
Pex3p	Peroxisomal membrane assembly
Pex4p	Peroxisomal matrix protein import
Pex5p	PTS1 receptor
Pex6p	Fusion of preperoxisomal vesicles
Pex7p	PTS2 receptor
Pex8p	Peroxisomal matrix protein import
Pex9p	Peroxisomal matrix protein import
Pex10p	Peroxisomal matrix protein import
Pex11p	Peroxisome proliferation
Pex12p	Peroxisomal matrix protein import
Pex13p	Peroxisomal matrix protein import
Pex14p	Peroxisomal matrix protein import
Pex15p	Peroxisomal matrix protein import

Pex16p	Peroxisome proliferation and/or peroxisomal membrane assembly
Pex17p	Peroxisomal matrix protein import
Pex18p	Facilitation of PTS2 protein import
Pex19p	Peroxisomal membrane assembly
Pex20p	Thiolase oligomerization and import
Pex21p	Facilitation of PTS2 protein import
Pex22p	Peroxisomal matrix protein import
Pex23p	Peroxisomal matrix protein import
Pex24p	Peroxisomal matrix and membrane protein import
Pex25p	Peroxisome proliferation
Pex26p	Recruitment of Pex1p and Pex6p to the peroxisomal membrane
Pex27p	Peroxisome proliferation
Pex28p	Peroxisome morphology
Pex29p	Peroxisome morphology
Pex30p	Peroxisome proliferation
Pex31p	Peroxisome proliferation
Pex32p	Peroxisome proliferation

1.3 Metabolic roles

Peroxisomes contain more than 50 enzymes that perform various biochemical reactions depending on the cell type (Purdue and Lazarow, 2001). Two reactions that are found in all peroxisomes are the metabolism of hydrogen peroxide and the β-oxidation of fatty acids. Fatty acid β-oxidation occurs exclusively in peroxisomes in fungi and plants,

while mitochondria are also involved in this reaction in mammalian cells. Other roles for peroxisomes are the α-oxidation of some fatty acids; the catabolism of purines, polyamines, prostaglandins, and eicosanoids; the biosynthesis of plasmalogens and sterols; and the final steps of penicillin biosynthesis in some filamentous fungi (Purdue and Lazarow, 2001). The diverse activities of peroxisomes are required for the proper functioning of cells under different conditions. For example, yeast mutants that contain nonfunctional peroxisomes do not survive on media containing carbon sources like oleic acid (*Saccharomyces cerevisiae, Yarrowia lipolytica, Pichia pastoris, Candida boidinii* and *Candida albicans*) or methanol (*Hansenula polymorpha, C. boidinii* and *P. pastoris*), which require peroxisomal enzymes for their metabolism. Alternatively, wild-type yeasts incubated in oleic acid- or methanol-containing medium have the ability to adjust the number and size of peroxisomes according to the increased demand of peroxisomal enzymes. These characteristics have made yeast an advantageous model organism for the identification of key peroxisomal components (van der Klei and Veenhuis, 2006). Since the pathways of peroxisome biogenesis are conserved from yeasts to human, yeast research has contributed greatly to the elucidation of the molecular mechanisms governing human peroxisomal diseases.

1.4 Peroxisomal disorders

The association of peroxisomes with human disease was made in 1973 by Sidney Goldfischer and colleagues while studying patients with kidney and liver malfunction (Steinberg et al., 2006). Loss of peroxisomal function has severe clinical consequences, and patients often die soon after birth. Since peroxisomes are responsible for key

biochemical pathways in embryogenesis, impaired peroxisome biogenesis leads to important developmental anomalies that are apparent at birth. The dramatic outcome of these disorders has exposed the vital role of peroxisomes in human health and at the same time stimulated intense medical research into the molecular bases of the different peroxisomal disorders.

The peroxisomal disorders are divided into two major groups: assembly deficiencies and single peroxisomal enzyme deficiencies. Assembly deficiencies, also known as peroxisome biogenesis disorders (PBD), are characterized by abnormal peroxisome assembly. There are four PBDs: Zellweger syndrome, neonatal adrenoleukodystrophy, infantile Refsum's disease and rhizomelic chondrodysplasia punctata. Historically, the PBDs represent the first described malformation disorders caused by a defect in a biochemical reaction. Zellweger syndrome is representative of the PBDs, being characterized by multiple hereditary abnormalities, notably craniofacial and eye malformations, neuronal migration defects, hepatomegaly, and chondrodysplasia punctata. The multitude of organ systems affected in Zellweger syndrome highlights the ubiquitous nature of peroxisomes. The second group of peroxisomal disorders is characterized by structurally intact peroxisomes having a faulty peroxisomal protein and has at least ten members, including X-linked adrenoleukodystrophy, acyl-CoA oxidase deficiency and bifunctional enzyme deficiency (Steinberg et al., 2006).

1.5 Peroxisome biogenesis

The severity of peroxisomal disorders emphasizes the significant contribution of peroxisomes to human development and health. Accordingly, eukaryotic cells have

developed elaborate molecular mechanisms for the biogenesis of peroxisomes. As diagrammed in Figure 1-1, peroxisome biogenesis ensures the formation and maintenance of peroxisomes through:

- *de novo* formation of peroxisomes from the ER

- peroxisome proliferation

- segregation of peroxisomes between mother cell and bud at cell division (not shown).

1.5.1 Towards a unified model of peroxisome formation and proliferation

1.5.1.1 The "growth and division" model

For more than 20 years, the accepted model in the field described the formation of peroxisomes by the "growth and division" of pre-existing peroxisomes (Purdue and Lazarow, 2001). This model considered peroxisomes as autonomous organelles, like mitochondria and chloroplasts, that are not made *de novo*. The formation of an autonomous organelle involves the steady import of lipids and proteins that permit membrane expansion. In the "growth and division" model, peroxisomal proteins are post-translationally imported into peroxisomes, while peroxisomal lipids are made in the ER.
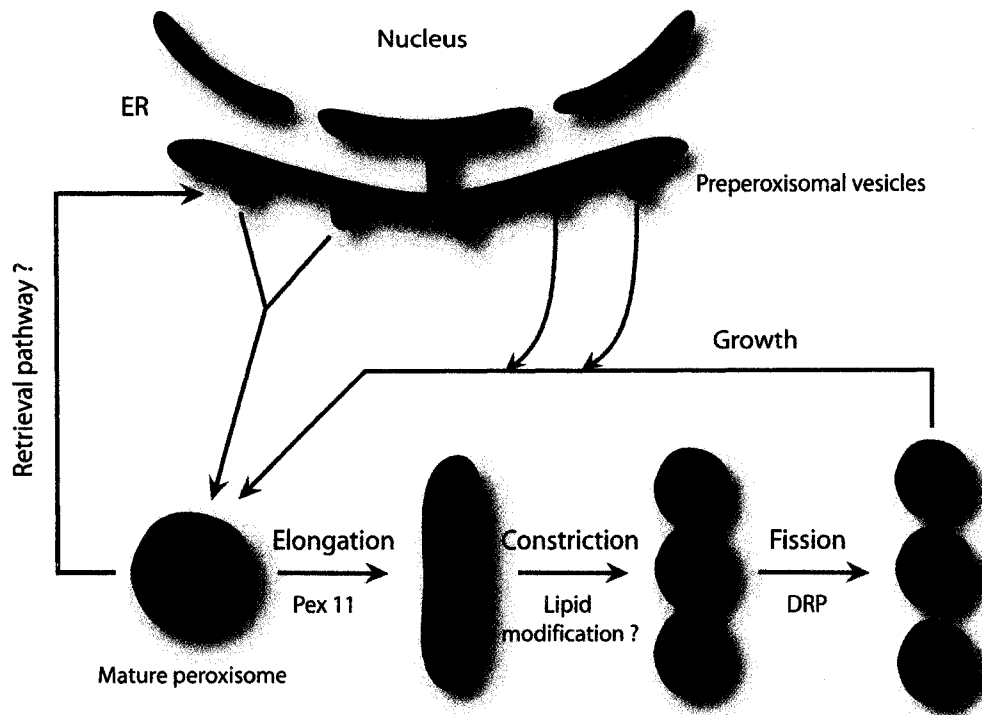
Figure 1-1. The de novo ER formation and proliferation of peroxisomes. A model for peroxisome biogenesis and division. Preperoxisomal vesicles originate in specialized compartments of the endoplasmic reticulum (ER). Fusion of these preperoxisomes is probably required to form a mature, metabolically active peroxisome. A retrograde pathway can be envisioned for the retrieval of escaped ER proteins and recycling of the preperoxisome assembly machinery. The division of peroxisomes proceeds through three distinct steps: elongation of peroxisomes, membrane constriction, and final fission of peroxisomal tubules. Pex11 proteins are implicated in the elongation step of peroxisome division, whereas dynamin-related proteins (DRPs) catalyze the fission event. A modification in membrane lipid composition probably underlies the membrane curvature necessary for membrane constriction. Peroxisomes grow by fusion with preperoxisomal vesicles and through the direct import of matrix and membrane proteins.

1.5.1.2 The *de novo* peroxisome formation model

Numerous findings challenged the view of the autonomous peroxisome by demonstrating the ER as a source for the *de novo* formation of peroxisomes (Titorenko and Rachubinski, 1998; Titorenko et al., 1997; Geuze et al., 2003; Hoepfner et al., 2005; Tam et al., 2005; Kim et al., 2006). These studies showed the targeting of several peroxisomal membrane proteins, *e.g.* Pex2p, Pex3p and Pex16p, to the ER. In *S. cerevisiae*, only one peroxisomal membrane protein, Pex3p, was shown to transit through the ER to peroxisomes (Hoepfner et al., 2005; Tam et al., 2005). While yeast cells lacking Pex3p were unable to form peroxisomes, reintroduction of Pex3p into these cells re-established the formation of peroxisomes. Microscopy showed that the reintroduced Pex3p initially localized to the ER, concentrating in foci. Vesicle formation from the ER then occurs, followed by incorporation of peroxisomal membrane proteins into these so-called preperoxisomal vesicles. Preperoxisomal vesicles then develop into mature peroxisomes through a number of steps. In the yeasts *Y. lipolytica* (Titorenko et al., 2000) and *P. pastoris* (Faber et al., 1998), preperoxisomal vesicles were shown to develop into mature peroxisomes by a series of vesicular fusion, as well as protein import, events.

1.5.1.3 The dual nature of peroxisome biogenesis

The current view of peroxisome biogenesis encompasses elements of both the "growth and division" and "*de novo* formation" models and views the peroxisome as a semi-autonomous organelle. ER-derived preperoxisomal vesicles are envisioned to fuse both homotypically, to form "new" peroxisomes, and with mature peroxisomes. Mature

peroxisomes eventually divide once they reach a certain size or when environmental conditions require it. In this way, peroxisomal membrane proteins that pass constitutively through the ER could also be integrated into actively dividing peroxisomes. Peroxisomal membrane protein import would help to maintain an appropriate apportioning of peroxisomal membrane during repeated cycles of "growth and division" (Fagarasanu et al., 2007).

As mentioned above, the molecular mechanisms governing these processes are beginning to be defined, but little is known about their relative contributions to maintaining peroxisome homeostasis. That peroxisomes divide constitutively at each cell division cycle independently of external stimuli is well established (Titorenko and Rachubinski, 2001). Which mechanism of peroxisome biogenesis is responsible for the cell-cycle-related division of peroxisomes? To what extent does each of these biogenesis pathways participate in the doubling of peroxisomes at cell division? These questions were answered at least in part by a recent study in mammalian cells that demonstrated how both processes participate in the constitutive division of peroxisomes (Kim et al., 2006). While the necessity of both the division and *de novo* formation of peroxisomes is not yet apparent, these processes are probably complementary. The continuous *de novo* formation of peroxisomes might ensure certain heterogeneity of peroxisomes at different stages of growth. During maturation, peroxisomes might acquire components that confer distinctive properties needed for various functions in the cell. Therefore, cells invest not only in maintaining the number of peroxisomes at each cell division but also in keeping distinct proportions of peroxisomes at different stages of maturation (Fagarasanu et al., 2007).

In *S. cerevisiae*, the maintenance of peroxisomes may be achieved primarily through peroxisome division and inheritance. *De novo* formation from the ER does not appear to be a major source of new peroxisomes in wild-type cells during normal cell growth (Motley and Hettema, 2007). *De novo* formation may be a rescue mechanism for peroxisomes that is activated when peroxisomes are lost, such as when there are defects in peroxisome inheritance. Therefore, at least in the case of *S. cerevisiae*, an absolute requirement for *de novo* peroxisome formation from the ER has been challenged.

1.5.2 Peroxisome proliferation and inheritance

1.5.2.1 Peroxisome proliferation

Peroxisome proliferation can be divided into two types: constitutive division of peroxisomes, which is cell-cycle-coordinated and maintains a constant number of peroxisomes after each cell division, and adaptive division of peroxisomes, which is responsible for the synthesis of sufficient amounts of peroxisomal enzymes to respond to environmental stimuli. The signaling pathways controlling both types of peroxisome division probably share the same factors (Yan et al., 2005). The extent of participation of the ER in the *de novo* formation of peroxisomes in constitutive and adaptive division is not yet well understood. There is an apparent correlation between the maturation of peroxisomes and their division, and the order of occurrence of the two processes varies in different yeast species. In *Y. lipolytica* and *H. polymorpha*, immature peroxisomes divide only after they have matured through matrix protein import, while in *C. boidinii*, peroxisomes undergo division before developing into mature peroxisomes (Sakai et al., 1998). Interestingly, both mature and immature peroxisomes have the capacity to divide

in mammalian cells (Thoms and Erdmann, 2005). A dividing population of peroxisomes presents three distinct morphologies (Li and Gould, 2002): peroxisomes of regular size, long elongated peroxisomes, and small peroxisomes. Consequently, one can assume that peroxisome division proceeds through three sequential stages: the elongation of peroxisomes, the constriction of the peroxisomal membrane, and the fission of peroxisomes (Li and Gould, 2002). The elongation process is influenced by the Pex11 family of proteins, while the dynamin-related proteins (DRP) function in the fission of peroxisomal tubules.

1.5.2.1.1. The role of Pex11 proteins

The first protein to be implicated in peroxisome division was Pex11p (Erdmann and Blobel, 1995; Marshall et al., 1995). *S. cerevisiae* cells deleted for the *PEX11* gene exhibited fewer and enlarged peroxisomes compared to wild-type cells. In contrast, overexpression of *PEX11* led to increased numbers of small peroxisomes. Interestingly, peroxisomes in cells overexpressing *PEX11* also formed long tubular structures that spanned the entire cytoplasm, suggesting the involvement of Pex11p in the elongation stage of peroxisome division; (Yan et al., 2005). *S. cerevisiae* contains two additional proteins, Pex25p (Smith et al., 2002) and Pex27p (Rottensteiner et al., 2003; Tam et al., 2003), that share amino acid sequence similarity to Pex11p. Pex25p and Pex27p have also been implicated in peroxisome division and, together with Pex11p, form the Pex11 protein family that controls the division of peroxisomes. Single, double or triple deletions of the *PEX11* gene family members affect the size and number of peroxisomes, with mutant cells containing a few enlarged peroxisomes.

Mammalian PEX11 protein has three isoforms, PEX11α, PEX11β and PEX11γ (Li and Gould, 2002), that are all integral to the peroxisomal membrane and have both their amino and carboxyl termini exposed to the cytosol (Li and Gould, 2002). In cells overexpressing the PEX11β gene, peroxisomes form long tubular structures and eventually increase dramatically in number (Schrader et al., 1998). Overproduction of Pex11β in cells lacking a functional DRP led to the appearance of long tubular peroxisomes but without a concomitant increase in the number of peroxisomes. Thus, PEX11 proteins act upstream of DRPs in an early step of the peroxisome tubulation process and are unable to completely divide peroxisomes by themselves (Koch et al., 2003, 2004; Schrader and Fahimi, 2006).

1.5.2.1.2 The role of DRPs

The dynamins constitute a superfamily of large GTPases that have multiple functions in cells; however, their main role is in the scission of vesicles. Dynamins are classified into classical dynamins and DRPs depending on the presence of specific domains in their protein structure (Praefcke and McMahon, 2004). Both dynamins and DRPs are able to bend membranes, leading to membrane constriction and ultimately scission. Often, additional factors prepare the membrane for constriction, and dynamins are recruited in the final step in the fission event (Praefcke and McMahon, 2004; McMahon and Gallop, 2005). Peroxisomes in mammalian or yeast cells lacking the corresponding peroxisomal DRPs resemble "beads on a string" (Hoepfner et al., 2001); (Koch et al., 2003), indicating the ability of peroxisomes to constrict, but not to divide, by membrane scission whenever DRPs are absent. Thus, DRPs act in the final scission event

of peroxisome division after constriction of the peroxisomal membrane (Yan et al., 2005). Although the details of the molecular mechanisms involved in peroxisome division remain poorly defined, peroxisome constriction and scission events can be clearly distinguished in the process (Schrader and Fahimi, 2006).

S. cerevisiae has three DRPs, Dnm1p, Mgm1p and Vps1p, and peroxisome fission is dependent on Vps1p (Hoepfner et al., 2001). Cells lacking Vps1p show reduced numbers of enlarged peroxisomes, with a typical cell exhibiting only one or two giant peroxisomes that sometimes appear as elongated tubular structures. Electron microscopy analysis has revealed the above mentioned peroxisome "beads on a string" morphology in vps1Δ cells, suggesting the ability of the peroxisomal membrane to constrict but not to complete division in the absence of Vps1p. Microscopic studies showed a partial and transient colocalization of Vps1p with peroxisomes. Peroxisome fission requires Vps1p under both peroxisome-inducing and -noninducing conditions (Hoepfner et al., 2001; Li and Gould, 2003). Interestingly, Dnm1p, a DRP known to mediate mitochondrial fission (Purdue and Lazarow, 2001), is also involved in peroxisome fission, mostly under peroxisome-inducing conditions (Kuravi et al., 2006). Deletion of the DNM1 gene in vps1Δ cells further decreased the number of peroxisomes and increased their size (Kuravi et al., 2006). Remarkably, the giant peroxisomes observed in vps1Δ and vps1Δ/dnm1Δ mutants are able to divide at the time of cell division. In vivo time-lapse microscopy showed that the division of peroxisomes in these cells is preceded by the formation of a long tubule that reaches towards the new bud. The peroxisome tubule eventually divides and is then correctly distributed between mother and daughter cells (Hoepfner et al., 2001; Kuravi et al., 2006). This finding suggests that Vps1p and Dnm1p are not involved

directly in peroxisome distribution and inheritance and also suggests the existence of other factors apart from Vps1p and Dnm1p that control the constitutive division of peroxisomes.

1.5.2.1.3. Other proteins that regulate the size and number of peroxisomes

Although the Pex11 family of proteins and DRPs are central to peroxisome division, other peroxisomal proteins affect the size and number of peroxisomes. In *S. cerevisiae*, Pex28p and Pex29p may be involved in the separation of peroxisomes after peroxisome division (Vizeacoumar et al., 2003). Yeast cells with single or double deletions of *PEX28* and *PEX29* contain clusters of peroxisomes that often exhibit thickened membranes between adjacent peroxisomes. However, the distribution of peroxisomes at cell division is not perturbed by lack of either Pex28p or Pex29p, and therefore these proteins are not required for peroxisome inheritance. Another family of peroxins implicated in the regulation of peroxisome size and number in *S. cerevisiae* includes Pex30p, Pex31p and Pex32p (Vizeacoumar et al., 2004). Peroxisomes are more numerous in cells lacking Pex30p, whereas loss of either Pex31p or Pex32p results in enlarged peroxisomes. The triple-deletion mutant strain *pex30Δ/pex31Δ/pex32Δ* exhibits a pronounced increase in the number of peroxisomes per cell. The molecular mechanisms by which these proteins regulate peroxisome size and number have yet to be determined.

1.5.2.2 Peroxisome inheritance

The accurate inheritance of organelles at cell division is essential to maintain the advantages of increased metabolic efficiency afforded to eukaryotic cells by subcellular

compartmentalization. A typical eukaryotic cell contains a variety of organelles, and each has to be delivered to a specific destination at a specific time. Ensuring the correct organization and synchronization of these processes requires a tightly regulated molecular mechanism. Studies in *S. cerevisiae* have led to many recent advances in understanding how organelles are distributed between mother cell and daughter cell (Fagarasanu and Rachubinski, 2007). *S. cerevisiae* undergoes an asymmetrical cell division, with the formation of a bud or daughter cell that is initially much smaller than its mother. In contrast to cells that divide by fission, *S. cerevisiae* must dynamically and vectorially deliver its organelles to the growing bud (Rossanese and Glick, 2001).

In order to partition their organelles, cells use a transport system composed of a cytoskeletal "track" to support movement and a "motor" to provide the necessary energy. In *S. cerevisiae*, peroxisomes are transported along a track of actin cables by the motor Myo2p, a class V myosin (Hoepfner et al., 2001). Approximately half of the peroxisomes is transferred in this manner from the mother cell to the arising bud. Furthermore, an active retention mechanism is in place in the mother cell to keep the remaining peroxisome population anchored at the cell cortex (Fagarasanu et al., 2005). The segregation of peroxisomes is closely synchronized with the cell division cycle and thus occurs in stages (Hoepfner et al., 2001; Fagarasanu et al., 2005, 2006a).

Peroxisome dynamics at cell division follows a specific sequence of events. In a nondividing cell, most peroxisomes are immobile at the periphery. As the bud starts to form, some peroxisomes gather at the new bud site. During development of the bud, about half of the peroxisomes is recruited one by one from their static cortical positions and transported towards the bud. At the time of cytokinesis, only half of the peroxisome

population remains in the mother cell and is anchored at the cell cortex. Interestingly, peroxisomes in the bud concentrate at sites of polarized cell growth, initially clustering at the bud tip. During cytokinesis, a few peroxisomes in both the bud and in the mother cell relocate to the bud-neck region, while the remaining peroxisomes are immobile and localized to the bud and mother cell cortices (Hoepfner et al., 2001; Fagarasanu et al., 2005, 2006a).

The retention of a subset of organelles in the mother cell is an essential feature of organelle inheritance in *S. cerevisiae*. Although the anchoring of organelles in the mother cell was long postulated, the identification of components that function directly in this process has remained elusive.

Studies of mitochondria in *S. cerevisiae* provided the first evidence for the presence of a mechanism that actively anchors organelles within the mother cell during cell division (Yang et al., 1999). Mitochondrial tubules are immobilized at a specific anchoring area in the mother cell during cell division. This area is situated at the cell pole distal to the bud site and was designated the "retention zone". Retention at this location prevents a subset of mitochondria from being transferred to the bud, resulting in effective segregation of mitochondria upon cytokinesis. Moreover, mitochondrial retention was shown to be dependent on the actin cytoskeleton, as mitochondria in the retention zone colocalized with actin cables and a specific mutation affecting actin dynamics disturbed their retention (Yang et al., 1999). This was the first demonstration that organelles need to be actively retained in the mother cell to ensure their correct partitioning during cell division.

1.6 Inheritance of other organelles

1.6.1 Mitochondrial inheritance

Mitochondria are essential organelles with crucial roles in metabolism, cellular growth and survival. Mitochondria cannot be made *de novo* and must therefore be inherited at cell division (Boldogh et al., 2005). In most cell types, mitochondria form complex tubular networks that uniformly distribute throughout the cell and are continuously remodeled through fusion and fission of their membranes (Hoppins et al., 2007). In *S. cerevisiae,* the tubular mitochondrial networks are localized at the cell periphery near the plasma membrane (Warren and Wickner, 1996).

Mitochondrial dynamics follows characteristic cell cycle-dependent stages (Boldogh et al., 2005; Boldogh and Pon, 2006). Initially, the formation of a new bud triggers an accumulation of mitochondria at the bud site. As the bud grows, part of the mitochondrial network is transferred into it, while the remaining mitochondria remain anchored in the mother cell. Interestingly, throughout the cell cycle, mitochondria display both anterograde movement toward the bud tip and retrograde movement toward the mother distal pole. Upon reaching the bud tip and the distal pole of the mother cell, mitochondria are immobilized at these locations until the start of the next cell cycle (Boldogh et al., 2005; Boldogh and Pon, 2006; Fehrenbacher et al., 2004). The end result of this process is the equal sharing of the mitochondrial population between the two resulting cells.

In *S. cerevisiae*, mitochondrial movement is dependent on actin cables (Boldogh et al., 2005; Boldogh and Pon, 2006; Simon et al., 1997). Actin monomers polymerize to generate actin filaments, and these are then transformed into different actin structures as

cables or patches (Young et al., 2004). Actin cables are long tracks that span the entire mother cell parallel to the mother-bud axis to assist the movement of cellular material to the bud. Actin patches are cortical sites of endocytosis (Huckaba et al., 2004; Kaksonen et al., 2003). They are localized to regions of polarized growth, being initially clustered at the new bud tip but redistributing throughout the bud cortex as the bud grows (Moseley and Goode, 2006; Pruyne and Bretscher, 2000). Microscopical studies have shown that the mitochondrial tubular network and actin cables colocalize (Drubin et al., 1993), while time-lapse *in vivo* cell imaging of fluorescently labeled actin and mitochondria has revealed the movement of mitochondria alongside actin filaments (Fehrenbacher et al., 2004). Affecting the overall stability of actin with different drugs or by actin mutation results in abnormal mitochondrial distribution and motility (Boldogh et al., 2005; Boldogh and Pon, 2006; Drubin et al., 1993; Fehrenbacher et al., 2004).

There are two views of how mitochondrial motility is achieved. The first involves a protein complex called the mitochore formed by three mitochondrial outer membrane proteins, Mdm10p, Mdm12p and Mmm1p, that is thought to power the anterograde movement of mitochondria towards the bud by recruitment of the Arp2/3 complex and subsequent actin polymerization (Boldogh et al., 2003; Fehrenbacher et al., 2003). The second, more conventional view is that mitochondrial motility involves a motor protein. In higher eukaryotes, mitochondrial transport occurs on microtubules and is powered by kinesin and dynein motor proteins (Hollenbeck and Saxton, 2005). In yeast, several organelles use class V myosin motors for transport. These organelles include vacuoles, secretory vesicles, and Golgi structures whose transport to the bud is dependent on one of the class V myosins, Myo2p and Myo4p (Pashkova et al., 2005; Pruyne et al., 1998;

Rossanese et al., 2001; Schott et al., 1999). The inheritance of organelles has been impaired by specific mutations in the Myo2p tail, which affect the binding of adaptor proteins to the Myo2p molecule (Catlett et al., 2000; Ishikawa et al., 2003; Pashkova et al., 2006). Mitochondrial inheritance, specifically, is affected by a Myo2p allele, *myo2-573*, implicating Myo2p in mitochondrial transport (Altmann and Westermann, 2005; Itoh et al., 2002; Altmann et al., 2008). Interestingly, additional proteins, including Mmr1p, Ypt11p and Gem1p, have been shown to independently affect mitochondrial inheritance in relation to motor-based movement (Boldogh et al., 2004; Frederick et al., 2004, 2008; Frederick and Shaw, 2007; Itoh et al., 2002).

1.6.2 Vacuole inheritance

The yeast vacuole is analogous to the mammalian lysosome and the plant vacuole. These organelles function in the turnover of proteins, storage of metabolites and resistance to cellular stress (Weisman, 2003). Yeast cells have developed mechanisms to accurately partition their vacuoles between dividing cells. Similar to mitochondria, vacuoles undergo several distinctive cell cycle-coordinated stages. Just before bud formation, the vacuole prepares for cell division by aligning with the polarized actin cytoskeleton and positioning a segment of its body at the new bud site (Catlett et al., 2000; Hill et al., 1996). The appearance of the new bud is accompanied by the formation of one or more "segregation structures", described as either a long tubule or a sequence of small vesicles (Raymond et al., 1990; Weisman, 2006). The segregation structure elongates from the vacuole body in the mother cell and migrates to the new bud soon after its formation (Catlett et al., 2000; Hill et al., 1996; Weisman, 2003). Frequent fusion

and fission events affect the integrity of the segregation structure, thereby permitting the accumulation of a number of small vacuolar vesicles in the bud (Gomes de Mesquita et al., 1991). Dissolution of the segregation structure marks the end of vacuolar inheritance, while fusion of the recently transferred vesicles in the bud will form a new vacuole (Conradt et al., 1992; Wickner and Haas, 2000).

In *S. cerevisiae*, vacuoles are moved along the actin cytoskeleton by the motor Myo2p and the adaptor protein complex composed of Vac8p and Vac17p (Hill et al., 1996). Cells lacking Vac17p, a peripheral membrane protein, specifically display abnormal vacuolar inheritance. Vac17p was shown to interact directly with Myo2p, and the presence of Myo2p on vacuoles depends on Vac17p, as overproduction of Vac17p increases Myo2p recruitment to vacuoles (Ishikawa et al., 2003). Thus, Vac17p is the protein receptor for Myo2p on vacuoles. However, the localization of Vac17p on vacuoles is lost in the absence of Vac8p, with which it interacts directly (Tang et al., 2003; Wang et al., 1998). Furthermore, Vac8p shows interaction with the Myo2p cargo-binding tail only in the presence of Vac17p, suggesting the presence of a multiprotein complex of Myo2p-Vac17p-Vac8p on the vacuolar membrane that powers the movement of the vacuole along actin tracks (Tang et al., 2003).

1.7 Focus of this thesis

The focus of this thesis is to study the peroxisomal inheritance in the yeast *Saccharomyces cerevisiae*. The peroxisomal inheritance process, an ordered and closely regulated process, may be divided into three individual events: (1) the retention of a proportion of the peroxisomal population in the mother cell, (2) the ordered movement of

the remaining portion of the peroxisomes into the emerging bud and (3) the retention

of the transferred peroxisomes within the bud. The regulation of these events is essential

to the proper distribution of peroxisomes during cell division. The work presented in this

thesis describes the identification and characterization of two peroxisomal proteins, Inp1p

and Yjl185p, involved in peroxisomal inheritance.

CHAPTER TWO: MATERIALS AND METHODS

2.1 Materials

2.1.1 List of chemicals and reagents

2-(*N*-Morpholino)ethanesulfonic acid (MES)	Sigma
5-bromo-4-chloro-3-indolyl-β-D-galactoside (X-gal)	Rose Scientific
acetone	Fisher
acrylamide	Roche
agar	Difco
agarose, UltraPure	Invitrogen
albumin, bovine serum (BSA)	Roche
ammonium bicarbonate (NH_4HCO_3)	Sigma
ammonium chloride (NH_4Cl)	EM Science
ammonium persulfate	BDH
ammonium sulfate (($NH4$)$_2SO_4$)	BDH
ampicillin	Sigma
anhydrous ethyl alcohol	Commercial Alcohols
antipain	Roche
aprotinin	Roche
benzamidine hydrochloride	Sigma
boric acid	EM Science
Brij 35	EM Science
bromophenol blue	BDH
calcium pantothenate	Sigma
chloroform	Fisher
Complete Protease Inhibitor Cocktail	Roche
Complete Supplement Mixture (CSM)	BIO 101
Coomassie Brilliant Blue R-250	ICN
cytochrome *c*, horse heart	Sigma
D-(+)-glucose	EM Science
dithiothreitol (DTT)	Fisher
ethylenedinitrilo-tetraacetic acid (EDTA)	EM Science
formaldehyde, 37% (v/v)	Biochemicals
Geneticin	Invitrogen
glass beads	Sigma
glycerol	EM Science
glycine	Roche

isoamyl alcohol	Fisher
isopropyl β-D-thiogalactopyranoside (IPTG)	Roche
lanolin	Alfa Aesar
leupeptin	Roche
L-histidine	Sigma
lithium acetate	Sigma
L-leucine	Sigma
L-lysine	Sigma
magnesium sulfate (MgSO$_4$)	Sigma
maltose	Sigma
MitoTracker CMXRos	Molecular Probes
N,N,N',N'-tetramethylethylenediamine (TEMED)	EM Science
N,N'-dimethylformamide (DMF)	BDH
N,N'-methylenebisacrylamide	Sigma
N-propylgallate	Sigma
Nycodenz	BioLynx
oleic acid	Fisher
Paraffin	Fisher
Pefabloc SC	Roche
Pepstatin A	Sigma
Peptone	Difco
phenol, buffer saturated	Invitrogen
phenylmethylsulphonylfluoride (PMSF)	Roche
poly *L*-lysine	Sigma
polyethylene glycol, M.W. 3350 (PEG)	Sigma
Ponceau S	Sigma
potassium acetate	BDH
potassium chloride	BDH
potassium permanganate (KMnO$_4$)	BDH
potassium phosphate, dibasic (K$_2$HPO$_4$)	EM Science
potassium phosphate, monobasic (KH$_2$PO$_4$)	EM Science
salmon sperm DNA, sonicated	Sigma
Sephadex G25	Amersham
skim milk powder	Carnation
sodium acetate	EM Science
sodium cacodylate	Fisher

sodium carbonate (Na_2CO_3)	BDH
sodium chloride	EM Science
sodium dithionite ($Na_2S_2O_4$)	BDH
sodium dodecyl sulfate (SDS)	Bio-Rad
sodium fluoride (NaF)	Sigma
sodium phosphate, dibasic (Na_2HPO_4)	BDH
sodium sulphite (Na_2SO_3)	Sigma
sorbitol	EM Science
sucrose	EM Science
Thiamine-HCl	Sigma
trichloroacetic acid (TCA)	EM Science
tris(hydroxymethyl)aminomethane (Tris)	Roche
Triton X-100	VWR
tryptone	Difco
Tween 20	Sigma
Tween 40	Sigma
uracil	Sigma
vaseline	Vaseline
xylene cyanol FF	Sigma
yeast extract	Difco
yeast nitrogen base without amino acids (YNB)	Difco
2-mercaptoethanol	BioShop

2.1.2 List of enzymes

CIP (calf intestinal alkaline phosphatase)	NEB
Easy-A high-fidelity polymerase	Stratagene
Platinum *Pfx* DNA polymerase	Invitrogen
restriction endonucleases	NEB
Quick T4 DNA ligase	NEB
RNase A (ribonuclease A), bovine pancreas	Sigma
T4 DNA ligase	NEB
Zymolyase 20T	ICN
Zymolyase 100T	ICN

2.1.3 Molecular size standards

1 kb DNA ladder (500-10,000 bp)	NEB
1 kb DNA ladder (75-12,216 bp)	Invitrogen
100 bp DNA ladder (100-1,517 bp)	NEB
prestained protein marker, broad range (6-175 kDa)	NEB

2.1.4 Multicomponent systems

BigDye Terminator Cycle Sequencing Ready Reaction Kit	Applied Biosystems
Matchmaker Two-Hybrid System	Clontech
pGEM-T Vector System	Promega
pMAL Protein Fusion and Purification System	NEB
QIAprep Spin Miniprep Kit	Qiagen
QIAquick Gel Extraction Kit	Qiagen
QIAquick PCR Purification Kit	Qiagen
Ready-To-Go PCR Beads	Amersham Biosciences

2.1.5 Plasmids

pDsRed-SKL	Smith et al., 2002
pHis5-GFP+	Dr. Richard Wozniak, University of Alberta
pGEM-T	Promega
pMAL-c2	NEB
pRS315	NEB
YEp13	Broach et al.,1979
pGAD424	Clontech
pGBT9	Clontech

2.1.6 Antibodies

The antibodies used in this study are described in Tables 2-1 and 2-2.

Table 2-1. Primary antibodies

Antibody	Type	Code	Dilution	Reference
Anti-GFP [a]	rabbit		1:5000	Eitzen et al., 1996
Y. lipolytica thiolase	guinea pig	N-3°	1:10,000	Eitzen et al., 1996
Anti-TAP	rabbit	TAP	1:1000	Open Biosystems
S. cerevisiae G6PDH	rabbit	G6PDH	1:20,000	Sigma-Aldrich
Clb2	rabbit		1:2000	Santa Cruz Biotechnology
Gsp1	rabbit		1:2000	Santa Cruz Biotechnology
S. cerevisiae Sdh2p [b]	rabbit	Sdh2	1:5000	Dibov et al., 1998

[a]A gift of Dr. Gary Eitzen (University of Alberta, Edmonton, Canada).
[b]A gift of Dr. Bernard Lemire (University of Alberta, Edmonton, Canada).

Table 2-2. Secondary antibodies

Specificity	Type	Dilution	Source
horseradish peroxidase-conjugated anti-rabbit IgG	donkey	1:30,000	Amersham Biosciences
horseradish peroxidase-conjugated anti-guinea pig IgG	goat	1:30,000	Sigma-Aldrich

2.1.7 Oligonucleotides

The oligonucleotides used in this study were synthesized by Sigma-Genosys (Oakville, Ontario) and are described in Table 2-3.

Table 2-3. Oligonucleotides

Name	Sequence[a,b,c] 5' – 3'	Application
0235	TATCTGCAGGACAGGCATAGAAGATTTCAGA GGAGATCCATATCTGGTCTTGGCGACCTTGG TGAAGCTCAAAAACTTAAT	*INP1-GFP* construction
0236	TATCTGCAGGACAGGCATAGAAGATTTCAGA GGAGATCCATATCTGGTCTTGGCGACCTTGG TGAAGCTCAAAAACTTAAT	*INP1-GFP* construction
0256	GGAATAATGAGTCTTTGAGCGATAA	Check *INP1-GFP/PrA* tagging
0257	CTTGTCCTTACTTTCACAATGGTCT	Check *INP1-GFP/PrA* tagging
0367	TCTAGAC A AAAATGGTTTTATCAAGG GGA GAAA	Clone *INP1* into pTMBV4
0368	CCATGGAGGTCGCCAAGACCAGATAT	Clone *INP1* into pTMBV4
0543	ATT<u>GGATCC</u>TCAATTAATGTTAACCCATGTTT TT	Clone *INP1* into YEp13
0544	ATT<u>GGATCC</u>TGTAACGACTTCTCCCTCCAG	Clone *INP1* into YEp13
0861	ATT<u>AGATCT</u>TCAATTAATGTTAACCCATGTTT TT	Clone *INP1-GFP* into YEp13
0862	ATT<u>AGATCT</u>AGGGAGTGTTGTAAAGAGTACT	Clone *INP1-GFP* into YEp13
0423	ATT<u>GGATCC</u>ATGGTTTTATCAAGGGGAGAAA C	Clone *INP1* into pMal-c2X
0424	ATT<u>GTCGAC</u>TCAAAGGTCGCC AAGACCAGA	Clone *INP1* into pMal-c2X
0650	TAAAGAAACTTACAAATGCCCAAAG	Primer C *YJL185c*
0545	TCATGTTAATTATCTGGAGAGCACA	Primer D *YJL185c*
0637	TTGGAAAACACATCTTGGTTTGGCTGGACTT TACTTTCTAGGTTTTTGGACAGAGAATGGGG TGAAGCTCAAAAACTTAAT	*YJL185c-GFP* construction
0638	CCATCCGACCTTGTATAATATAATGTAGCAT ATATGTGCACGGATATATATACATCTTAGGC TGACGGTATCGATAAGCTT	*YJL185c-GFP* construction

1775	*AAGGTCTACATTTTTCGTCTGATAACTCTCAGGA AATTAAACAAAGTGGT*AGATTGTACTGAGAGT GCAC	*INP1* deletion
1776	*ATTTATATTCACATTGTATACTCCTTCACTTTGGT TTACACCTACATTCA*CTGTGCGGTATTTCACAC CG	*INP1* deletion
0652	ATT<u>GGATCC</u>AAATGGCATCTGTGAACAATTA CCA	Clone *YJL185c* into pGAD424 and pGBT9
0653	ATT<u>CTGCAG</u>CTACCATTCTCTGTCCAAAAAC C	Clone *YJL185c* into pGAD424 and pGBT9
0654	ATT<u>GGATCC</u>AAATGGTTTTATCAAGGGGAGA AACA	Clone *INP1* into pGAD424 and pGBT9
0655	ATT<u>GTCGAC</u>TCAAAGGTCGCCAAGACCAGAT	Clone *INP1* into pGAD424 and pGBT9
2101	ATT<u>GGATCC</u>ATCGCGTATTGG	Clone *YJL185c* into YEp13
2102	ATT<u>GGATCC</u>ATATGTGCACGG	Clone *YJL185c* into YEp13

[a]Restriction endonuclease recognition sites are underlined.
[b]Sequences for homologous recombination are italicized.

2.1.8 Standard buffers and solutions

The compositions of commonly used buffered solutions are given in Table 2-4.

Table 2-4. Common solutions

Solution	Composition	Reference
1 × PBS	137mM NaCl, 2.7 mM KCl, 8 mM Na_2HPO_4, 1.5 mM K_2HPO_4, pH 7.3	(Pringle et al., 1991)
1 × protease inhibitor (PIN) cocktail	1 μg/ml each of antipain, aprotinin, leupeptin, pepstatin, 0.5 mM benzamidine hydrochloride, 5 mM NaF, 1 mM PMSF or 0.5 mg Pefabloc SC/ml	(Smith, 2000)
1 × TBST	20 mM Tris-HCl, pH 7.5, 150 mM NaCl, 0.05% (w/v) Tween 20	(Huynh et al., 1985)

1 × transfer buffer	20 mM Tris, 150 mM glycine, 20% (v/v) methanol	Towbin et al., 1979
5 × SDS-PAGE running buffer	0.25 M Tris-HCl, pH 8.8, 2 M glycine, 0.5% SDS	Ausubel et al., 1989
10 × TBE	0.89 M Tris-borate, 0.89 M boric acid, 0.02 M EDTA	Maniatis et al., 1982
2× sample buffer	20% (v/v) glycerol, 167 mM Tris-HCl, pH 6.8, 2% SDS, 0.005% bromophenol blue	Ausubel et al., 1989
6 × DNA loading dye	0.25% bromophenol blue, 0.25% xylene cyanol, 30% (v/v) glycerol	Maniatis et al., 1982
Breakage buffer	2% (v/v) Triton X-100, 1% SDS, 100 mM NaCl, 10 mM Tris-HCl, pH 8.0, 1 mM EDTA, pH 8.0	Ausubel et al., 1989
Disruption buffer	20 mM Tris-HCl, pH 7.5, 0.1 mM EDTA, pH 7.5, 100 mM KCl, 10% (w/v) glycerol	Eitzen, 1997
Ponceau stain	0.1% Ponceau S, 1% TCA	Szilard, 2000
Solution B	100 mM KH_2PO_4, 100 mM K_2HPO_4, 1.2 M sorbitol	Pringle et al., 1991
TE	10 mM Tris-HCl, pH 7.0-8.0 (as needed), 1 mM EDTA	Maniatis et al., 1982

2.2 Microorganisms and culture conditions

2.2.1 Bacterial strains and culture conditions

Escherichia coli strains and culture media used in this study are described in Tables 2-5 and 2-6, respectively. Bacteria were grown at 37°C. Bacterial cultures of 5 ml or less were grown in culture tubes in a rotary shaker at 200 rpm. Bacterial cultures greater than 5 ml were grown in flasks in a rotary shaker at 250 rpm. On average, culture volumes were 20% of flask volumes.

Table 2-5. *E. coli* strains

Strain	Genotype	Source
DH5α	F⁻, Φ80d*lac*ZΔM15, Δ(*lac*ZYA-*arg*F), U169, *rec*A1, *end*A1, *hsd*R17(r$_k^-$, m$_k^+$), *pho*A, *sup*E44, λ⁻, *thi*-1, *gyr*A96, *rel*A1	Invitrogen
BL21-DE3	F⁻, *omp*T, *hsd*SB(r$_B^-$ m$_B^-$) *gal*, *dcm* (DE3)	Novagen

Table 2-6. Bacterial culture media

Medium	Composition	Reference
LB[a,b]	1% tryptone, 0.5% yeast extract, 1% NaCl	Maniatis et al., 1982
SOB	2% tryptone, 0.5% yeast extract, 10 mM NaCl, 2.5 mM KCl	Maniatis et al., 1982
TYP[a]	1.6% tryptone, 1.6% yeast extract, 0.5% NaCl, 0.25% K$_2$HPO$_4$	Promega Protocols and Applications Guide, 1989/1990

[a]Ampicillin was added to 100 μg/ml for plasmid selection when necessary.
[b]For solid media, agar was added to 1.5%.

2.2.2 Yeast strains and culture conditions

S. cerevisiae strains used in this study are listed in Tables 2-7. Culture media for yeast are described in Table 2-8. Yeast was grown at 30°C. Yeast cultures of 10 ml or less were grown in 16 mm × 150 mm glass tubes in a rotating wheel. Yeast cultures greater than 10 ml were grown in flasks in a rotary shaker at 250 rpm. On average, culture volumes were 20% of flask volumes.

Table 2-7. *S. cerevisiae* strains

Strain	Genotype	Reference
BY4741	*MATa, his3Δ1, leu2Δ0, met15Δ0, ura3Δ0*	(Giaever et al., 2002)
BY4742	*MATα, his3Δ1, leu2Δ0, lys2Δ0, ura3Δ0*	(Giaever et al., 2002)
inp1Δ	*MATα, his3Δ1, leu2Δ0, lys2Δ0, ura3Δ0, inp1::KanMX4*	(Giaever et al., 2002)
yjl165Δ	*MATα, his3Δ1, leu2Δ0, lys2Δ0, ura3Δ0, YJL185c::KanMX4*	(Giaever et al., 2002)
pex3Δ	*MATα, his3Δ1, leu2Δ0, lys2Δ0, ura3Δ0, PEX3::KanMX4*	(Giaever et al., 2002)
vps1Δ	*MATα, his3Δ1, leu2Δ0, lys2Δ0, ura3Δ0, VPS1::KanMX4*	(Giaever et al., 2002)
inp1Δ/POT1-GFP	*MATα, his3Δ1, leu2Δ0, lys2Δ0, ura3Δ0, inp1::KanMX4, pot1::POT1-GFP (HIS5)*	This study
yjl185Δ/POT1-GFP	*MATα, his3Δ1, leu2Δ0, lys2Δ0, ura3Δ0, YJL185c::KanMX4, pot1::POT1-GFP (HIS5)*	This study
yjl185Δinp1Δ/ POT1-GFP	*MATα, his3Δ1, leu2Δ0, lys2Δ0, ura3Δ0, YJL185c::KanMX4, INP1::KanMX4, pot1::POT1-GFP (HIS5)*	This study
BY4741/POT1-GFP	*MATa, his3Δ1, leu2Δ0, met15Δ0, ura3Δ0, pot1::POT1-GFP (HIS5)*	This study
BY4742/POT1-GFP	*MATα, his3Δ1, leu2Δ0, lys2Δ0, ura3Δ0, pot1::POT1-GFP (HIS5)*	This study
INP1-TAP	*MATa, his3Δ1, leu2Δ0, met15Δ0, ura3Δ0, inp1::INP1-TAP (HIS3)*	(Ghaemmaghami et al., 2003)
INP1-GFP	*MATa, his3Δ1, leu2Δ0, met15Δ0, ura3Δ0, inp1::INP1-GFP (HIS5)*	This study
INP1-prA	*MATα, his3Δ1, leu2Δ0, lys2Δ0, ura3Δ0, inp1::INP1-protA (HIS5)*	This study
PEX3-prA	*MATα, his3Δ1, leu2Δ0, lys2Δ0, ura3Δ0, pex3::PEX3-protA (HIS5)*	Vizeacoumar et al., 2003
PEX11-TAP	*MATa, his3Δ1, leu2Δ0, met15Δ0, ura3Δ0, pex11::PEX11-TAP (HIS3)*	(Ghaemmaghami et al., 2003)
PEX17-TAP	*MATa, his3Δ1, leu2Δ0, met15Δ0, ura3Δ0, pex17::PEX17-TAP (HIS3)*	(Ghaemmaghami et al., 2003)

PEX19-TAP	*MATa,*	*his3Δ1,*	*leu2Δ0,*	*met15Δ0,*	*ura3Δ0,* (Ghaemmaghami et
	pex19::PEX19-TAP (HIS3)				al., 2003)
PEX25-TAP	*MATa,*	*his3Δ1,*	*leu2Δ0,*	*met15Δ0,*	*ura3Δ0,* (Ghaemmaghami et
	pex25::PEX25-TAP (HIS3)				al., 2003)
PEX30-TAP	*MATa,*	*his3Δ1,*	*leu2Δ0,*	*met15Δ0,*	*ura3Δ0,* (Ghaemmaghami et
	pex30::PEX30-TAP (HIS3)				al., 2003)
VPS1-TAP	*MATa,*	*his3Δ1,*	*leu2Δ0,*	*met15Δ0,*	*ura3Δ0,* (Ghaemmaghami et
	vps1::VPS1-TAP (HIS3)				al., 2003)
YJL185c-GFP	*MATa,*	*his3Δ1,*	*leu2Δ0,*	*met15Δ0,*	*ura3Δ0,* This study
	yjl185c::YJL185c-GFP (HIS5)				
YJL185c-GFP/	*MATa,*	*his3Δ1,*	*leu2Δ0,*	*met15Δ0,*	*ura3Δ0,* This study
POT1-mRFP	*yjl185c::YJL185c-GFP (HIS5), pot1::POT1-mRFP*				
	(URA3)				
inp1Δ/YJL185cGFP/	*MATa,*	*his3Δ1,*	*leu2Δ0,*	*met15Δ0,*	*ura3Δ0,* This study
POT1-mRFP	*INP1::KanMX4,*	*yjl185c::YJL185c-GFP*		*(HIS5),*	
	pot1::POT1-mRFP (URA3)				
pex3Δ/YJL185cGFP/	*MATa,*	*his3Δ1,*	*leu2Δ0,*	*met15Δ0,*	*ura3Δ0,* This study
POT1-mRFP	*PEX3::KanMX4,*	*yjl185c::YJL185c-GFP*		*(HIS5),*	
	pot1::POT1-mRFP (URA3)				
SFY526	*MATa, ura3-52, his3-200, ade2-101, lys2-801, trp1-*				(Harper et al., 1993)
	901,	*leu2-3,*	*112,*	*gal4-542,*	*gal80-538,*
	LYS2::GAL1$_{UAS}$*-GAL1*$_{TATA}$*-lacZ, MEL1*				

Table 2-8. Yeast culture media

Medium	Composition[a,b]	Reference
Nonfluorescent medium	6.61 mM KH_2PO_4, 1.32 mM K_2HPO_4, 4.06 mM $MgSO_4 \cdot 7H_2O$, 26.64 mM $(NH_4)SO_4$, 1 × CSM, 0.5% (w/v) Tween 40, 0.1% glucose, 1% agarose, 2% galactose	This study
SCIM	0.67% YNB, 0.5% yeast extract, 0.5% peptone, 0.5% (w/v) Tween 40, 0.3% glucose, 0.3% (v/v) oleic acid, 1 × CSM	This study
Sporulation medium	1% potassium acetate, 0.1% yeast extract, 0.05% glucose	(Rose et al., 1988)
SM	0.67% YNB, 2% glucose, 1× CSM without leucine, uracil, or tryptophan, as required	This study

YEPA	1% yeast extract, 2% peptone, 2% sodium acetate	(Brade, 1992)
YEPD	1% yeast extract, 2% peptone, 2% glucose	(Rose et al., 1988)
YPBO	0.3% yeast extract, 0.5% peptone, 0.5% K_2HPO_4, 0.5% KH_2PO_4, 0.2% (w/v) Tween 40 or 1% (v/v) Brij 35, 1% (v/v) oleic acid	(Kamiryo et al., 1982)

[a]For solid media, agar was added to 2%.
[b]Glucose, galactose, oleic acid and geneticin were added after autoclaving.
[c]Supplemented with histidine, leucine, lysine or uracil, each at 50 µg/ml, as required.

2.2.3 Mating, sporulation and tetrad dissection of *S. cerevisiae*

S. cerevisiae strains were mated as described by Rose et al. (1988). Haploid strains of opposite mating type were streaked in single straight lines onto individual YEPD agar plates and incubated overnight. Strains were then replica plated onto fresh YEPD agar so that streaks of cells of opposite mating type were at right angles to each other and incubated overnight. These cells were then replica plated onto YND agar supplemented with the auxotrophic requirements of the diploid strain. Diploid cells emerged after overnight incubation.

Sporulation and tetrad dissection of *S. cerevisiae* strains were performed according to Rose et al. (1988), with modification. Each diploid strain was grown overnight in 5 ml of YND medium supplemented with the appropriate auxotrophic requirements. Cells were harvested by centrifugation and washed twice with 10 ml of water. Approximately 5 µl of the cell pellet was transferred to 3 ml of sporulation medium and incubated for 3 to 7 days. The appearance of tetrads was examined by light microscopy. When approximately 10% or more of cells formed tetrads, 1 ml of cells was transferred to a microcentrifuge tube and washed twice with water. The cell pellet was

resuspended in 1 ml of water. 10 μl of cells was transferred to 1 ml of water containing 3 to 5 μg of Zymolyase 20T and incubated at 30°C in a rotating wheel for 15 min. 20 μl of spheroplasted cells was spread in a single line near the edge of a thin YEPD plate. Tetrads were dissected using a Zeiss Axioskop 40 microscope equipped with a Tetrad Manipulator System (Carl Zeiss). The separated spores were incubated for 2 days at 30°C.

2.3 Introduction of DNA into microorganisms

2.3.1 Chemical transformation of *E. coli*

Plasmid DNA was introduced into Subcloning Efficiency, chemically competent *E. coli* DH5α cells, as described by the manufacturer (Invitrogen). Briefly, 1 to 2 μl of ligation reaction (Section 2.5.7) or 0.5 μl (0.25 μg) of plasmid DNA was added to 25 μl of cells. The resulting mixture was incubated on ice for 30 min, subjected to a 20 sec heat shock at 37°C, and chilled on ice for 2 min. 1 ml of LB medium was added, and the cells were incubated in a rotary shaker for 45 to 60 min at 37°C. Cells were spread onto LB agar plates containing ampicillin and incubated overnight at 37°C. When necessary, 100 μl of 2% X-gal in DMF and 50 μl of 100 mM IPTG were added to agar plates to allow for blue/white selection of colonies carrying recombinant plasmids.

2.3.2 Electroporation of *E. coli*

E. coli DH5α or BLR-DE3 cells were made electrocompetent as recommended by Invitrogen for high efficiency transformation with plasmid DNA. Cells were grown overnight in 10 ml of SOB medium. 0.5 ml of this overnight culture was transferred to

500 ml of SOB medium and incubated at 37°C until the culture reached an OD_{600} of

0.5. Cells were harvested by centrifugation at 2,600 × g for 15 min at 4°C, washed twice

with 500 ml of ice-cold 10% (v/v) glycerol, and resuspended in a minimal amount of

10% (v/v) glycerol. Cells were either used immediately or frozen as 100 μl aliquots by

immersion in a dry ice/ethanol bath and stored at -80°C. For transformation, 1 μl of

ligation reaction or 0.5 μl of plasmid DNA was added to 20 μl of cells. The mixture was

placed between the bosses of an ice-cold disposable microelectroporation chamber (width

~0.15 cm) (Whatman Biometra) and submitted to an electrical pulse of 395 V (amplified

to ~2.4 kV) at a capacitance of 2 μF and a resistance of 4 kΩ using a Cell-Porator

connected to a Voltage Booster (Whatman Biometra). Cells were then immediately

transferred to 1ml of LB, incubated in a rotary shaker at 37°C for 45 to 60 min, and

spread onto LB agar plates containing ampicillin.

2.3.3 Chemical transformation of yeast

Plasmid DNA was introduced into yeast as described by Gietz and Woods (2002).

Basically, 25 μl of cells was scraped from a fresh plate with a sterile toothpick and

resuspended in 1 ml of water. The cells were harvested by centrifugation, resuspended in

1 ml of 100 mM lithium acetate, and incubated at 30°C for 5 min. The cells were again

harvested by centrifugation, and the following components were added on top of the cell

pellet in order: 240 μl of 50% (w/v) PEG, 36 μl of 1 mM lithium acetate, 50 μl of sheared

salmon sperm DNA (2 mg/ml), 1 μl of plasmid DNA and 20 μl of water. The mixture

was vortexed strongly for 1 min and incubated at 42°C for 20 min. The cells were

harvested by centrifugation, resuspended gently in 200 μl of water and plated onto SM or

YND agar. Plates were incubated at 30°C for approximately 3 days to allow colony formation.

2.3.4 Electroporation of yeast

Yeast cells were made electrocompetent as recommended by Ausubel et al. (1989). Cells were grown overnight in 10 ml of YEPD. 5 ml of overnight culture was transferred to 45 ml of YEPD and incubated for 4 to 5 h or until the culture reached an OD_{600} of ~1.0. Cells were then harvested by centrifugation at 2,000 × g, resuspended in 50 ml TE 7.5 containing 100 mM lithium acetate, and incubated for 30 min at room temperature or 30°C with gentle agitation. DTT was added to a final concentration of 20 mM, and the incubation was continued for another 15 min. The cells were harvested by centrifugation at 2,000 × g, washed once with 50 ml each of room-temperature water, ice-cold water, and ice-cold 1 M sorbitol. Cells were resuspended in a minimal volume of ice-cold 1 M sorbitol. 20 μl of cells was mixed with 1 μl of plasmid DNA or 100 to 150 ng of purified DNA fragment, placed between the bosses of an ice-cold microelectroporation chamber (width ~0.15 cm), submitted to an electrical pulse of 250 V (amplified to ~1.6 kV) at a capacitance of 2 μF and a resistance of 4 kΩ; the Cell-Porator was connected to a Voltage Booster. Cells were then resuspended in 100 μl of ice-cold 1 M sorbitol and plated onto SM or YND agar plates. Plates were incubated at 30°C for 3 to 5 days for colony formation.

2.4 Isolation of DNA from microorganisms

2.4.1 Isolation of plasmid DNA from bacteria

Single bacterial colonies were inoculated into 2 ml of LB containing ampicillin and incubated overnight at 37°C. Cells were harvested by centrifugation in a microcentrifuge tube, and plasmid DNA was isolated by using a QIAprep Spin Miniprep Kit following the manufacturer's instructions (Qiagen). The method is based on the alkaline lysis of bacterial cells, the adsorption of DNA onto silica in the presence of high salt, and the elution of DNA in low salt buffer. Plasmid DNA was eluted in 50 µl of the supplied elution buffer.

2.4.2 Isolation of chromosomal DNA from yeast

Yeast genomic DNA was prepared as described by Ausubel et al. (1989). Cells were grown overnight in 10 ml of YEPD, harvested by centrifugation for 5 min at 2,000 × g, washed twice in 10 ml of water, and transferred to a 2.0 ml microcentrifuge tube. 200 µl each of breakage buffer (Table 2-4), glass beads and phenol/chloroform/isoamyl alcohol (25:24:1) was added to the cells. The mixture was vortexed for 3 to 5 min at 4°C to simultaneously break yeast cells and separate nucleic acids from proteins. 200 µl of TE 8.0 was added, and the mixture was vortexed briefly. The organic and aqueous phases were separated by centrifugation at 16,000 × g for 5 min at room temperature. The aqueous phase was extracted once against an equal volume of phenol/chloroform/isoamyl alcohol (25:24:1). DNA was precipitated by the addition of 2.5 volumes of absolute ethanol and centrifugation at 16,000 × g for 5 min at room temperature. The pellet was washed once with 1 ml 70% (v/v) ethanol, dried in a rotary vacuum desiccator and

dissolved in 50 μl of TE 8.0 containing 100 μg RNase A/ml. DNA was incubated at 37°C for 1 to 2 h to allow for digestion of RNA.

2.5 DNA manipulation and analysis

Reactions were generally carried out in 1.5 ml microcentrifuge tubes, and microcentrifugation was performed in an Eppendorf microcentrifuge at $16,000 \times g$.

2.5.1 Amplification of DNA by the polymerase chain reaction (PCR)

PCR was used to amplify specific DNA sequences. Primers, reaction components and cycling conditions were designed using standard protocols (Innis and Gelfand, 1990; Saiki, 1990). A reaction usually contained 0.1 to 0.5 μg of yeast genomic DNA or 100 to 200 ng of plasmid DNA, 20 pmol of each primer, 0.25 mM of each dNTP, 1 mM Mg_2SO_4, and 1.25 U of Platinum *Pfx* DNA polymerase (Invitrogen) in 50 μl of the supplied reaction buffer. Reactions were performed in 0.6-ml microcentrifuge tubes in a Robocycler 40 with a Hot Top attachment (Stratagene). Alternatively, Ready-to-Go PCR Beads were used as recommended by the manufacturer (Amersham Biosciences).

2.5.2 Digestion of DNA by restriction endonucleases

Usually, 1 to 2 μg of plasmid DNA or purified DNA was digested by restriction endonucleases for 1 h to 1.5 h as described in the manufacturer's protocol. Digestion was immediately terminated by agarose gel electrophoresis of the DNA fragments, except for plasmid DNA, which required dephosphorylation.

2.5.3 Dephosphorylation of 5'-ends

Plasmid DNA linearized by one restriction endonuclease was subjected to dephosphorylation at its 5'-ends to prevent intramolecular ligations. After digestion of plasmids, reactions were mixed with 10 U of CIP and incubated at 37°C for 30 min. Dephosphorylation was terminated by agarose gel electrophoresis of the DNA fragments.

2.5.4 Separation of DNA fragments by agarose gel electrophoresis

DNA fragments in solution were mixed with 0.2 volume of 6 × DNA loading dye and separated by electrophoresis in 1% agarose gels in 1 × TBE containing 0.5 μg of ethidium bromide/ml. Gels were subjected to electrophoresis at 10 V/cm in 1 × TBE, and DNA fragments were subsequently visualized on an ultraviolet transilluminator (Photodyne, Model 3-3006).

2.5.5 Purification of DNA fragments from agarose gel

A DNA fragment of interest was excised from agarose gel with a razor blade, and the DNA was extracted from the agarose slice using the QIAquick Gel Extraction Kit according to the manufacturer's instructions (Qiagen). This method is based on the dissolution of agarose gel and adsorption of DNA to a silica-membrane in the presence of a high concentration of chaotropic salts, followed by washing and elution of DNA in the presence of low salts. DNA was usually eluted in 30 to 50 μl of the supplied elution buffer.

2.5.6 Purification of DNA from solution

Contaminants (small oligonucleotides, salts, enzymes, etc.) were removed from DNA solutions by using the QIAquick PCR Purification Kit according to the manufacturer's instructions (Qiagen). This method uses the same principle as that of the QIAquick Gel Extraction Kit (Section 2.5.5), except that no dissolution of agarose gel was involved. DNA was generally eluted in 30 to 50 µl of the supplied elution buffer.

2.5.7 Ligation of DNA fragments

Fragments of DNA treated with restriction endonucleases (Section 2.5.2) and purified as described in Section 2.5.6 were ligated using 1 µl of T4 DNA ligase in buffer supplied by the manufacturer (NEB). The reaction was run usually in a volume of 10 µl, with the molar ratio of plasmid to insert being between 1:3 and 1:10 and incubation overnight at 16°C. Alternatively, 1 µl of Quick T4 DNA ligase (NEB) in 1 × Quick Ligation Buffer was used in a reaction volume of 20 µl. The reaction was incubated at room temperature for 10 min.

PCR products after purification by agarose gel electrophoresis (Section 2.5.5) were sometimes ligated with the vector pGEM-T using the pGEM-T Vector System according to the manufacturer's instructions (Promega).

2.5.8 DNA sequencing

Sequencing of DNA was performed using the BigDye Terminator v1.1/3.1 Cycle Sequencing Ready Reaction Kit as described by the manufacturer (Applied Biosystems). This method is based on the method as described (Sanger et al., 1977) and involves the

random incorporation of fluorescent dideoxy terminators during the elongation of DNA sequences with a modified version of *Taq* DNA polymerase. Essentially, a reaction contained 1 µl of plasmid DNA, 3.2 pmol of primer, 3 µl of Terminator Ready Reaction Mix, and 2.5 µl of the supplied 5 × buffer in a total volume of 20 µl. The reaction was subjected to cycle sequencing using the Robocycler 40 with a Hot Top attachment under the following conditions: 1 cycle at 96°C for 2 min; 25 cycles at 96°C for 46 sec, 50°C for 51 sec and 60°C for 4 min 10 sec; 1 cycle at 6°C to hold. Reaction products were precipitated by addition of 80 µl of 75% isopropanol for 20 min at room temperature, collected by microcentrifugation at 16,000 × g for 20 min, washed twice with 250 µl of 75% isopropanol, dried in a rotary vacuum dessicator, dissolved in 15 µl of Template Suppression Reagent, heated at 95°C for 2 min and immediately cooled on ice. Reaction products were then separated by capillary electrophoresis, and fluorescence was detected and recorded by an ABI 310 Genetic Analyzer (Applied Biosystems).

2.6 Protein manipulation and analysis

2.6.1 Preparation of yeast whole cell lysates

Yeast lysates were prepared by disruption of yeast with glass beads using a modification of a procedure as described (Needleman and Tzagoloff, 1975). Cells were harvested by centrifugation at 2,000 × g for 5 min, washed twice with 10 ml of water, and resuspended in an equal volume of ice-cold Disruption Buffer (Table 2-4) containing 1 × PIN (Table 2-4) and 1 mM DTT. Ice-cold glass beads were added until they reached the meniscus of the cell suspension. The mixture was vortexed for 5 min at 4°C, and glass

beads were pelleted by microcentrifugation for 20 sec at 4°C. The supernatant was recovered and clarified by microcentrifugation for 20 min at 4°C.

Yeast lysates were also prepared by denaturation with alkali and a reducing agent. Cells were harvested by centrifugation at 2,000 × g for 5 min, transferred to a microcentrifuge tube, and resuspended in 240 to 500 µl of 1.85 M NaOH, 7.4% 2-mercaptoethanol. The cell suspension was incubated on ice for 5 min and mixed with an equal volume of 50% TCA by vortexing. The mixture was further incubated on ice for 5 min and subjected to microcentrifugation at 16,000 × g for 10 min at 4°C. The pellet was washed once with water and resuspended first in 50 to 150 µl of Magic A (1 M unbuffered Tris, 13% SDS) and then in an equal volume of Magic B (30% (v/v) glycerol, 200 mM DTT, 0.25% bromophenol blue). The mixture was boiled for 10 min and then subjected to microcentrifugation at 16,000 × g for 1 min. The supernatant was collected.

2.6.2 Precipitation of proteins

Proteins were precipitated from solution by adding TCA to a final concentration of 10% and incubation on ice for 30 min to overnight. Precipitates were collected by microcentrifugation at 16,000 × g for 30 min at 4°C, and the resultant pellet was washed twice with 1 ml of ice-cold acetone, dried in a rotary vacuum dessicator and dissolved in 2 × sample buffer (Table 2-4).

2.6.3 Determination of protein concentration

The protein concentration of a sample was determined by the method of Bradford (Bradford, 1976). A standard curve was prepared by adding 1 ml of Bio-Rad Protein

Assay Dye to 100 µl aliquots of water containing 2 µg, 4 µg, 6 µg, 8 µg, 10 µg, 12 µg, 14 µg, 16 µg, 18 µg and 20 µg of BSA. Samples were incubated for 5 min at room temperature, and absorbance was measured at 595 nm using a Beckman DU640 spectrophotometer. Absorbance values were plotted against the BSA concentrations to generate a standard curve. Absorbance of a protein sample was measured in the same way as for BSA standards, and the protein concentration was estimated by comparing the absorbance value with the standard curve.

2.6.4 Separation of proteins by electrophoresis

Proteins were separated by sodium dodecyl sulfate-polyacrylamide gel electrophoresis (SDS-PAGE) as described by Ausubel et al. (1989). Protein samples were mixed with an equal volume of 2 × sample buffer containing 10 mM DTT, denatured by boiling for 5 min, and separated by electrophoresis on discontinuous slab gels. Stacking gels contained 3% acrylamide (30:0.8 acylamide:N,N'-methylene-bis-acrylamide), 60 mM Tris-HCl, pH 6.8, 0.1% SDS, 0.1% (v/v) TEMED, and 0.1% ammonium persulfate. Resolving gels contained 10% acrylamide (30:0.8 acylamide:N,N'-methylene-bis-acrylamide), 370 mM Tris-HCl, pH 8.8, 0.1% SDS, 0.1% (v/v) TEMED, and 0.043% ammonium persulfate. Electrophoresis was conducted in 1 × SDS-PAGE running buffer (Table 2-4) at 50-200 V using a Bio-Rad Mini Protean II vertical gel system.

2.6.5 Detection of proteins by staining

Proteins in polyacrylamide gels were visualized by staining with 0.1% Coomassie Brilliant Blue R-250, 10% (v/v) acetic acid, 35% (v/v) methanol for 1 h with gentle

agitation. Unbound dye was removed by multiple washes in 10% (v/v) acetic acid, 35% (v/v) methanol. Gels were dried for 1 h at 80°C on a Bio-Rad Model 583 gel drier.

2.6.6 Detection of proteins by immunoblotting

Proteins separated by SDS-PAGE were transferred to nitrocellulose membrane (Bio-Rad) in 1 × transfer buffer (Table 2-4) at 100 mA for 16 h at room temperature using a Trans-Blot tank transfer system with plate electrodes (Bio-Rad). Proteins transferred to nitrocellulose were visualized by staining in Ponceau stain (Table 2-4) for several minutes and destaining in water. The nitrocellulose was incubated in blocking solution (1% skim milk powder, 1 × TBST (Table 2-4)) with gentle agitation to prevent nonspecific binding of antibodies. Specific proteins on nitrocellulose were detected by incubation with primary antibody in blocking solution for 1 h at room temperature with gentle agitation. The nitrocellulose was then incubated with appropriate HRP-labeled secondary antibody in blocking solution for 1 h. After each antibody incubation, unbound antibodies were removed by washing the nitrocellulose three times with 1 × TBST for 10 min each. Antigen-antibody complexes were detected using an ECL Western Blotting Detection Kit according to the manufacturer's instructions (Amersham Biosciences) and exposing the nitrocellulose to X-Omat BT film (Kodak).

Nitrocellulose could be reblotted using a Re-Blot Western Blot Recycling Kit according to the manufacturer's instructions (Chemicon). The nitrocellulose was incubated with 1 × Antibody Stripping Solution at room temperature for 15 to 30 min with gentle agitation, rinsed with 1 × TBST, and blotted as described above.

2.7 Subcellular fractionation of S. *cerevisiae* cells

2.7.1 Peroxisome isolation from *S. cerevisiae* cells

Peroxisomes were isolated from *S. cerevisiae* cells as described by Smith et al. (2002). Cells grown in oleic acid-containing medium were harvested by centrifugation at 800 × *g* in a Beckman JA10 rotor at room temperature and washed twice with water. Cells were resuspended in 10 mM DTT, 100 mM Tris-HCl, pH 9.4, at a concentration of 10 ml per g of wet cells and incubated at 30°C for 35 min with gentle agitation. Cells were collected by centrifugation at 2,500 × *g* in a Beckman JS13.1 rotor for 10 min at 4°C and washed once with Zymolyase buffer (50 mM potassium phosphate, pH 7.5, 1.2 M sorbitol, 1 mM EDTA). Cells were resuspended in Zymolyase buffer containing 0.125 mg of Zymolyase 100T/ml at a concentration of 8 ml per g of wet cells and incubated at 30°C for 45 min to 1 h with gentle agitation to convert cells to spheroplasts. Spheroplasts were harvested by centrifugation at 2,200 × *g* in a Beckman JS13.1 rotor for 8 min at 4°C and washed once with 1.2 M sorbitol, 2.5 mM MES, pH 6.0, 1 mM EDTA. Spheroplasts were then resuspended in buffer H (0.6 M sorbitol, 2.5 mM MES, pH 6.0, 1 mM EDTA, 1 × complete protease inhibitor cocktail (Roche)) at a concentration of 2 ml per g of wet cells. Resuspended spheroplasts were transferred to a homogenization mortar and disrupted by 10 strokes of a Teflon pestle driven at 1,000 rpm by a stirrer motor (Model 4376-00, Cole-Parmer). Cell debris, unbroken cells and nuclei were pelleted by centrifugation at 1,000 × *g* in a Beckman JS13.1 rotor for 8 min at 4°C. The postnuclear supernatant (PNS) was subjected to four additional centrifugations at 1,000 × *g* in a Beckman JS13.1 rotor for 8 min at 4°C. The PNS was fractionated by centrifugation at 20,000 × *g* in a Beckman JS13.1 rotor for 30 min at 4°C into pellet (20KgP) and

supernatant (20KgS) fractions. The 20KgS fraction could be further subfractionated by ultracentrifugation at 250,000 × g in a Beckman TLA120.2 rotor for 1 h at 4°C into a pellet (250KgP) fraction enriched for high-speed pelletable organelles and a supernatant (250KgS) fraction enriched for cytosol. The 20KgP was resuspended in 11% (w/v) Nycodenz in buffer H and loaded onto the top of a discontinuous Nycodenz gradient (6.6 ml of 17%, 16.5 ml of 25%, 4.5 ml of 35% and 3 ml of 50% (w/v) Nycodenz in buffer H). Organelles were separated by ultracentrifugation at 100,000 × g for 80 min at 4°C in a Beckman VTi50 rotor. 18 fractions of 2 ml each were collected from the bottom of the gradient.

2.7.2 Extraction and subfractionation of peroxisomes

Extraction and subfractionation of peroxisomes were performed according to Smith et al. (2000) with modifications. Basically, organelles in the 20KgP fraction (containing ~50 µg of protein) were lysed by incubation in 10 volumes of ice-cold Ti8 buffer (10 mM Tris-HCl, pH 8.0) containing 2 × complete protease inhibitor cocktail on ice for 1 h with occasional vortexing and separated by ultracentrifugation at 200,000 × g for 1 h at 4°C in a TLA120.2 rotor into a membrane fraction (Ti8P) and a soluble fraction (Ti8S). The Ti8P fraction was resuspended in ice-cold Ti8 to a final protein concentration of 0.5 mg/ml and mixed with 10 volumes of ice-cold 0.1 M Na_2CO_3, pH 11.3. The mixture was incubated on ice for 45 min with occasional vortexing and subjected to ultracentrifugation at 200,000 × g for 1 h at 4°C in a TLA120.2 rotor to yield a fraction enriched for integral membrane proteins (CO_3P) and a fraction enriched for peripheral membrane proteins (CO_3S).

2.8 Microscopy

2.8.1 Confocal 4D video microscopy

Cells were grown in YEPD medium and then incubated in SCIM for 16 h. Slides were prepared according to (Adames et al., 2001) with modifications. 200 µl of hot 1% agarose in nonfluorescent medium (Table 2-8) was used to prepare a thin agarose pad on a slide with two 18 mm square wells (Cel-line Brand). 1 to 2 µl of culture was placed onto the slide, covered with a cover slip and sealed with Valap (1:1:1 mixture of vaseline, lanolin and paraffin). Cells were incubated at room temperature for image capture. Images were captured as described (Hammond and Glick, 2000) using a modified LSM 510 META confocal microscope equipped with a 63× 1.4 NA Plan-Apo objective (Carl Zeiss). A piezoelectric actuator was used to drive continuous objective movement, allowing for the rapid collection of z-stacks. The sides of each pixel represented 0.085 µm of the sample. Stacks of 14 optical sections spaced 0.4 µm apart were captured at each time point. The interval between time points is indicated for each movie. GFP was excited using a 488-nm laser, and its emission was collected using a 505-nm long-pass filter. The resulting images were filtered three times using a 3×3 hybrid median filter to reduce shot noise. Fluorescence images from each stack were projected using an average intensity algorithm that involved multiplication of each pixel value by an appropriate enhancement factor for better contrast. Correction for exponential photobleaching of GFP was performed by exponentially increasing the enhancement factor with each projection. The transmitted light images from each stack were projected using a maximum intensity algorithm. The resulting projections were smoothened by means of a blurring algorithm. These operations were performed using

NIH Image (http://rsb.info.nih.gov/nih-image/). Adobe Photoshop (Adobe Systems) was used to merge the fluorescent and transmitted light projections. Processed projections were assembled into movies using Apple QuickTime Pro 6.5.2 at a rate of 10 frames per second. Postprocessing operations such as the tracking of peroxisomes and 3D reconstruction were performed using Imaris 4.1 (Bitplane, Zurich, Switzerland). Peroxisome velocity was measured as the frame-to-frame displacement of peroxisomes over the time interval between each two consecutive frames using MetaMorph software (Universal Imaging). Only movements within mother cells were measured. For each peroxisome, maximal velocity achieved is presented. Velocities may be underestimates, since movements perpendicular to the focal plane were not considered.

2.8.2 Quantification of rates of peroxisome inheritance

Peroxisome inheritance was quantified as described (Rossanese et al., 2001; Fagarasanu et al., 2005). Cells synthesizing a genomically encoded chimera between GFP and the peroxisomal matrix enzyme 3-ketoacyl-CoA thiolase (Pot1p-GFP) were grown in YEPD medium for 16 h, transferred to SCIM and incubated in SCIM for 16 h to achieve an OD_{600} of 0.5. Peroxisomes were visualized by direct fluorescence confocal microscopy. For each randomly chosen field, three optical sections of 5 μm thickness were collected at a z-axis spacing of 1.6 μm using a high detector gain to ensure the capture of weak fluorescent signals. Optical sections were then projected onto a single image. All visibly budded cells were considered for analysis, and buds were assigned to four categories of bud volume, expressed as a percentage of mother cell volume (Category I, 0-12%; Category II, 12-24%; Category III, 24-36%; Category IV, 36-48%). Since cell volume is not directly

accessible, bud area was first measured using Zeiss LSM 5 Image Browser software and grouped into four "area" categories (that superimpose on the aforementioned "volume" categories if a spherical geometry is assumed for all cells) according to bud cross-sectional area expressed as a percentage of mother cell cross-sectional area: Category I, 0-24%; Category II, 24-39%; Category III, 39-50%; Category IV, 50-61%. Buds were then scored using an all-or-none criterion for the presence or absence of peroxisomal fluorescence. In the case of cells overproducing Inp1p, mother cells were scored in the same manner. Quantification was always performed on at least 25 budded cells from each category of bud size.

2.9 Yeast two-hybrid analysis

Yeast two-hybrid analysis was performed using the Matchmaker Two-Hybrid System according to the manufacturer's instructions (Clontech) with modifications.

2.9.1 Construction of chimeric genes

Chimeric genes were made by amplifying the ORFs of *INP1* and *YJL185c* by PCR and ligating them in-frame and downstream of sequences encoding the activation domain (AD) and DNA-binding domain (DB) of the *GAL4* transcriptional activator in plasmids pGAD424 and pGBT9, respectively. To construct pGAD424-*INP1* and pGBT9-*INP1*, the *INP1* ORF was amplified by PCR using primers 0654 and 0655. To construct pGAD424-*YJL185c* and pGBT9-*YJL185c*, the *YJL185c* ORF was amplified by PCR using primers 0652 and 0653. All PCR products were digested and ligated into pGAD424 and pGBT9.

2.9.2 Assays for two-hybrid interactions

Plasmid pairs encoding AD and DB fusion proteins were transformed into *S. cerevisiae* strain *SFY526* as described in Section 2.3.3. Transformants were grown in SM medium (Table 2-8). Possible interactions between AD and DB fusion proteins were detected by testing for activation of the integrated *LacZ* construct using the β-galactosidase filter assay according to the instructions of the manufacturer (Clontech). For filter assays, cells were streaked directly onto filter paper placed on solid media and broken by 4 freeze-thaw cycles at -80°C.

2.10 Assay for direct protein binding

The glutathione-S-transferase (GST) fusion protein of Inp1p was constructed using pGEX4T-1 (Amersham Biosciences). Recombinant expression and isolation of GST and GST-Inp1p were done according to the manufacturer's instructions.

250 μg of purified GST-Inp1p or GST protein immobilized on glutathione resin were incubated with 250 μg of yeast lysates expressing TAP-tagged peroxins or Vps1p in H-buffer (20 mM HEPES, pH 7.5, 60 mM NaCl, 1 mM DTT, 0.5% Triton X-100, 1 μg leupeptin/ml, 1 μg pepstatin/ml, 1 μg aprotinin/ml, 1 mM phenanthroline, 1 mM PMSF) for 2 h at 4°C on a rocking platform. The immobilized fractions were allowed to settle and were then washed three times with H-buffer prior to protein elution in sample buffer (50 mM Tris-HCl, pH 6.8, 2% SDS, 5% glycerol, 0.001% bromophenol blue, 5% 2-mercaptoethanol). The eluted proteins were subjected to SDS-PAGE. Immunoblotting with rabbit antibodies to TAP (Open Biosystems) was used to detect protein interactions

in the assay. HRP-conjugated donkey anti-rabbit IgG secondary antibodies were used to detect primary antibodies in immunoblot analysis. Antigen-antibody complexes in immunoblots were detected by ECL (Amersham Biosciences).

2.11 Rhodamine phalloidin staining of actin

Cells were grown to low log in SCIM for 16 h and then fixed in the medium by addition of formaldehyde to a final concentration of 4% for 5 min. The cells were collected by centrifugation, resuspended in PBS containing 4% final formaldehyde and kept for 30 min at room temperature with mixing. The cells were washed twice in PBS and resuspended in 500 μl of PBS. 10 μl of rhodamine-conjugated phalloidin (Molecular Probes) dissolved in methanol according to the manufacturer's instructions was then added to 100 μl of cell suspension, and the mixture was incubated for 30 min in the dark. The cells were washed 5 times with 1 ml of PBS and analyzed by microscopy.

CHAPTER THREE: THE ROLE OF INP1 PROTEIN IN PEROXISOME

PARTITIONING

3.1 Overview

This chapter reports the identification of Inp1p, a peripheral membrane protein of peroxisomes of *S. cerevisiae*, that affects both the morphology of peroxisomes and their partitioning during cell division. *In vivo* 4-dimensional (4D) video microscopy showed an inability of mother cells to retain a subset of peroxisomes in dividing cells lacking the *INP1* gene, whereas cells overexpressing *INP1* exhibited immobilized peroxisomes that failed to be partitioned to the bud. Overproduced Inp1p localized to both peroxisomes and the cell cortex, supporting an interaction of Inp1p with specific structures lining the cell periphery. The levels of Inp1p vary with the cell cycle. Pull-down experiments showed the ability of Inp1p to bind Pex25p, Pex30p and Vps1p, which have been implicated in regulating peroxisome division. In summary, Inp1p acts as a factor that retains peroxisomes in cells and controls peroxisome division. Inp1p is the first peroxisomal protein directly implicated in peroxisome inheritance.

3.2 Inp1p is a peripheral membrane protein of peroxisomes

A global analysis of protein localization in *S. cerevisiae* identified Ymr204p, a protein of unknown function encoded by the *S. cerevisiae* genome, as a heretofore unknown peroxisomal protein (Huh et al., 2003). Since Ymr204p was shown to be the first peroxisomal protein directly implicated in peroxisome inheritance (see below), we renamed it Inp1p for Inheritance of peroxisomes protein 1. The demonstration of a peroxisomal localization for Inp1p in the study conducted by Huh and coworkers remained tentative because this global analysis of protein localization was done in *S. cerevisiae* strains grown in glucose-containing medium, and peroxisomes are dispensable

for growth of yeast in glucose. We therefore set about to determine the subcellular localization of Inp1p in cells incubated in oleic acid-containing medium, the metabolism of which requires peroxisomes and leads to increased numbers of peroxisomes per cell.

A genomically encoded fluorescent chimera of Inp1p and GFP, Inp1p-GFP, was localized in oleic acid-incubated cells by confocal microscopy. Inp1p-GFP colocalized with a fluorescent chimera of monomeric red fluorescent protein (mRFP) and the peroxisome targeting signal 1 (PTS1) Ser-Lys-Leu (mRFP-PTS1) to punctate structures characteristic of peroxisomes (Figure 3-1 A).

Subcellular fractionation was also used to establish that Inp1p is peroxisomal. A genomically encoded protein A (prA) chimera of Inp1p, Inp1p-prA, like the peroxisomal matrix protein thiolase, localized preferentially to the 20KgP fraction enriched for peroxisomes and mitochondria (Figure 3-1 B). Isopycnic density gradient centrifugation of the 20KgP fraction showed that Inp1p cofractionated with thiolase but not with the mitochondrial protein, Sdh2p (Figure 3-1 C). Therefore, both confocal microscopy and subcellular fractionation showed Inp1p to be peroxisomal.

Organelle extraction was used to determine the subperoxisomal location of Inp1p. Peroxisomes were subjected to hypotonic lysis in dilute alkali Tris buffer, followed by ultracentrifugation to yield a supernatant (Ti8S) fraction enriched for matrix proteins and a pellet (Ti8P) fraction enriched for membrane proteins (Figure 3-1 D). Inp1p-prA cofractionated with a protein A chimera of the integral membrane protein Pex3p to the Ti8P fraction. The soluble peroxisomal matrix protein thiolase was found almost exclusively in the Ti8S fraction. The Ti8P fraction was then extracted with alkali Na_2CO_3 and subjected to ultracentrifugation. This treatment releases proteins associated with, but

Figure 3-1. Inp1p is a peripheral membrane protein of peroxisomes. (A) Inp1p-GFP colocalizes with mRFP-PTS1 to punctate structures characteristic of peroxisomes by direct confocal microscopy. The panel at right presents the merged image of the left and middle panels in which colocalization of Inp1p-GFP and mRFP-PTS1 is shown in yellow. Bar, 1 μm. (B) Inp1p-pA localizes to the 20KgP subcellular fraction enriched for peroxisomes. Immunoblot analysis of equivalent portions the 20KgS and 20KgP subcellular fractions from cells expressing Inp1p-pA was performed with antibodies to the peroxisomal matrix enzyme, thiolase. (C) Inp1p-pA cofractionates with peroxisomes. Organelles in the 20KgP fraction were separated by isopycnic centrifugation on a discontinuous Nycodenz gradient. Fractions were collected from the bottom of the gradient, and equal portions of each fraction were analyzed by immunoblotting. Fractions enriched for peroxisomes and mitochondria were identified by immunodetection of thiolase and Sdh2p, respectively. (D) Purified peroxisomes were ruptured by treatment with Ti8 buffer and subjected to ultracentrifugation to obtain a supernatant fraction, Ti8S, enriched for matrix proteins and a pellet fraction, Ti8P, enriched for membrane proteins. The Ti8P fraction was treated further with alkali Na_2CO_3 and separated by ultracentrifugation into a supernatant fraction (CO_3S) enriched for peripherally associated membrane proteins and a pellet fraction (CO_3P) enriched for integral membrane proteins. Equivalent portions of each fraction were analyzed by immunoblotting. Immunodetection of thiolase and Pex3p-pA marked the fractionation profiles of a peroxisomal matrix and integral membrane protein, respectively. (E) The synthesis of Inp1p-pA is constant during incubation of *S. cerevisiae* in oleic acid medium. Cells grown for 16 h in YPD medium were transferred to, and incubated in, YPBO medium. Aliquots of cells were removed from the YPBO medium at the indicated times, and total cell lysates were prepared. Equal amounts of protein from the lysates were separated by SDS-PAGE, and Inp1p-pA, thiolase and glucose-6-phosphate dehydrogenase (G6PDH) were detected by immunoblot analysis. Antibodies against G6PDH were used to confirm the loading of equal amounts of protein in each lane. (F) *inp1*Δ cells are retarded in their growth on oleic acid medium. Cells of the wild-type strain *BY4742*, the deletion strain *inp1*Δ and the peroxisome assembly mutant strain *pex3*Δ were grown on YPD agar and then streaked onto YPBO agar (Streak 1). Following 3 d of incubation, cells were sampled from Streak 1 and restreaked onto the same YPBO agar (Streak 2). Incubation was continued for a further 3 d.

A Inp1p-GFP   mRFP-PTS1   Merge   B

                                    20KgS 20KgP

Inp1p-pA

Thiolase

C Fraction 1 2 3 4 5 6 7 8 9 10 11 12 13 14 15

Inp1p-pA

Thiolase

Sdh2p

D   Ti8S Ti8P CO3S CO3P

Inp1p-pA

Thiolase

Pex3p-pA

F   Streak 1   Streak 2
           (6 d)   (3 d)

BY4742

inp1Δ

pex3Δ

E Time (h) 0 1 2 4 6 8

Inp1p-pA

Thiolase

G6PDH
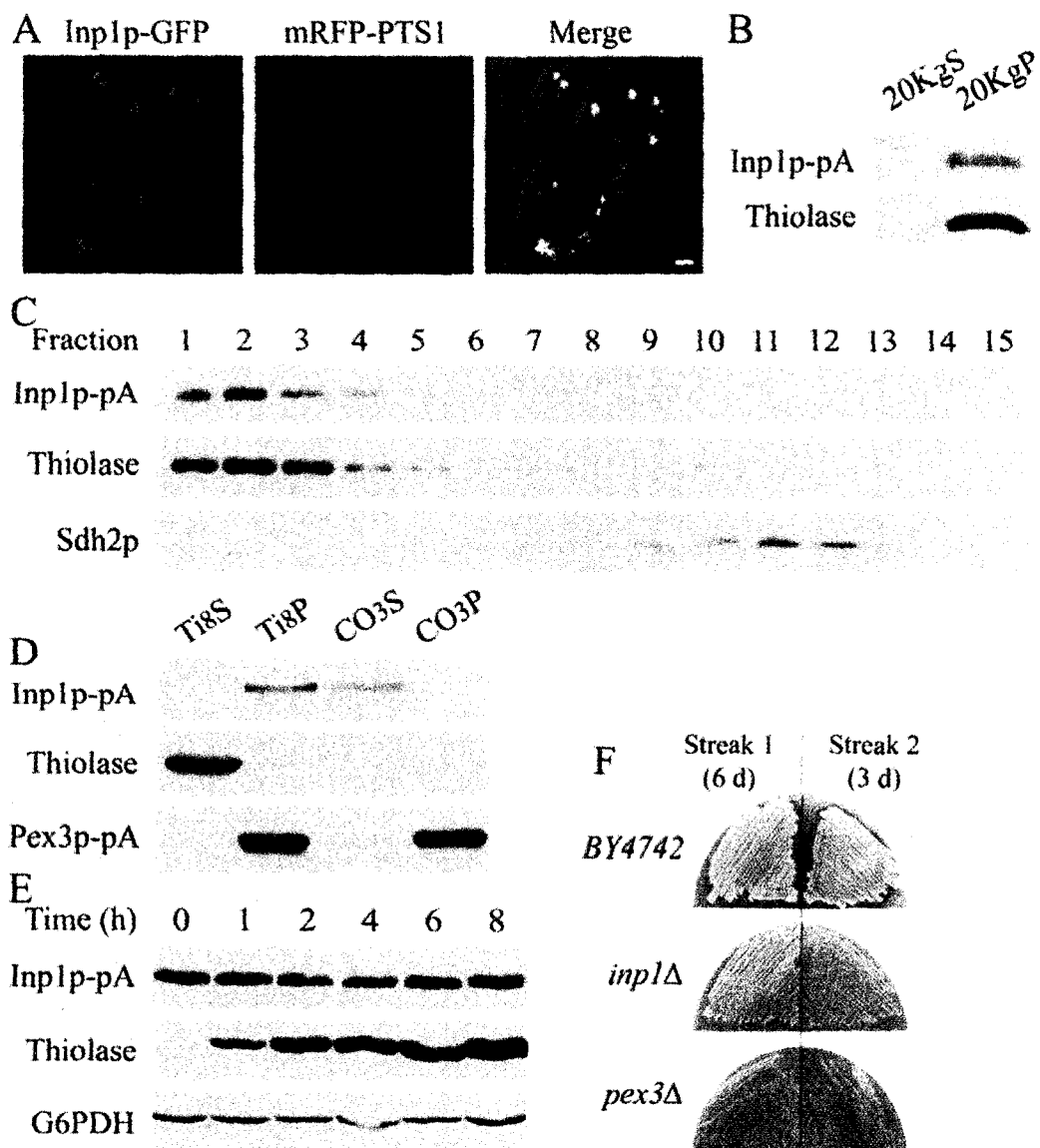
not integral to, membranes (Fujiki et al., 1982). Inp1p-prA fractionated to the supernatant (CO₃S) enriched for peripheral membrane proteins and did not cofractionate with Pex3p-prA to the pellet (CO₃P) enriched for integral membrane proteins. These results are consistent with Inp1p being a peripheral membrane protein of peroxisomes.

The synthesis of many peroxisomal proteins is induced by incubating yeast cells in oleic acid-containing medium. The genomically encoded protein A chimera of Inp1p was analyzed to monitor the expression of *INP1* under the control of its endogenous promoter. Cells synthesizing Inp1p-prA were grown in glucose-containing YPD medium and transferred to oleic acid-containing YPBO medium. Aliquots of cells were removed at the different times after the transfer to YPBO medium, and their lysates were subjected to SDS-PAGE and immunoblotting (Figure 3-1 E). Inp1p-prA was detected in cells grown in YPD medium at the time of transfer, and its level remained essentially unchanged during incubation in YPBO. Under the same conditions, the level of the peroxisomal matrix enzyme thiolase increased considerably from an undetectable level with time of incubation in YPBO, while the level of the cytosolic enzyme G6PDH remained constant and acted as a control for protein loading onto the gel.

Yeast strains that are compromised in peroxisome biogenesis and/or function often exhibit a growth defect in medium containing oleic acid as the sole carbon source, the metabolism of which requires the activity of normal, functioning peroxisomes. Cells deleted for the *INP1* gene were compromised in their growth on oleic acid-containing YPBO agar plates as compared to wild-type cells (Figure 3-1 F), consistent with a defect in some aspect of peroxisome biogenesis and/or function in *inp1Δ* cells.

3.3 Cells deleted for or overexpressing *INP1* exhibit abnormal peroxisomes

Wild-type and *inp1Δ* cells expressing a genomically integrated chimeric gene, *POT1-GFP*, encoding peroxisomal thiolase tagged at its carboxyl terminus with GFP, Pot1p-GFP, were incubated in YPBO medium and observed at different times of incubation by direct fluorescence confocal microscopy (Figure 3-2 A). Peroxisomes dramatically increased in size during the time of incubation in YPBO medium and were noticeably larger than peroxisomes of wild-type cells, particularly at longer times of incubation. There was also a dramatic decrease in the numbers of peroxisomes in *inp1Δ* cells with time of incubation as compared to wild-type cells. However, there was heterogeneity in the peroxisome phenotype of *inp1Δ* cells, with some cells exhibiting decreased numbers of enlarged peroxisomes and others exhibiting peroxisomes similar in size and number to peroxisomes of wild-type cells (e.g. Figure 3-2 A, 2 h image). EM (Figure 3-2 B) and morphometric analysis (Figure 3-2 C and Table 3-1) confirmed an overall increase in the size and decrease in the number of peroxisomes in *inp1Δ* cells with time of incubation in oleic acid-containing medium.

The multicopy plasmid YEp13 containing the *INP1* gene was introduced into wild-type cells synthesizing Pot1p-GFP to determine the effects of *INP1* overexpression on the peroxisome phenotype. Overexpression of *INP1* in cells incubated in oleic acid-containing medium led to a dramatic increase in the number of peroxisomes in most cells (Figure 3-3). In addition, overexpression of *INP1* led to an apparent irregularity in the distribution of peroxisomes between mother cells and buds, with a significant number of buds not containing any readily evident fluorescent peroxisomes (Figure 3-3).

Figure 3-2. Cells deleted for *INP1* exhibit an abnormal peroxisome phenotype. (A) The wild-type strain *BY4742* and the deletion strain *inp1*Δ expressing genomically integrated *POT1-GFP* encoding peroxisomal thiolase tagged at its carboxyl terminus with GFP (Pot1p-GFP) were grown for 16 h in glucose-containing YPD medium and then transferred to oleic acid-containing YPBO medium. Fluorescent images of cells at different times of incubation in YPBO medium were captured by confocal microscopy. Bar, 1 μm. (B) Ultrastructure of *BY4742* and *inp1*Δ cells at different times of incubation in oleic acid medium. Cells were cultured as in (A) and then fixed and processed for EM. (C) Morphometric analysis. P, peroxisome; M, mitochondrion; N, nucleus; V, vacuole; L, lipid droplet. Bar, 1 μm.

A Time (h)   0   2   4   6   8   24

BY4742

inp1Δ

B Time (h)   0   8   24

BY4742

inp1Δ

C

8 h

- ■ BY4742
- ⊠ inp1Δ

y-axis: % of total peroxisomes

x-axis: area of peroxisomes (μm^2)

24 h

- ■ BY4742
- ⊠ inp1Δ

y-axis: % of total peroxisomes

x-axis: area of peroxisomes (μm^2)
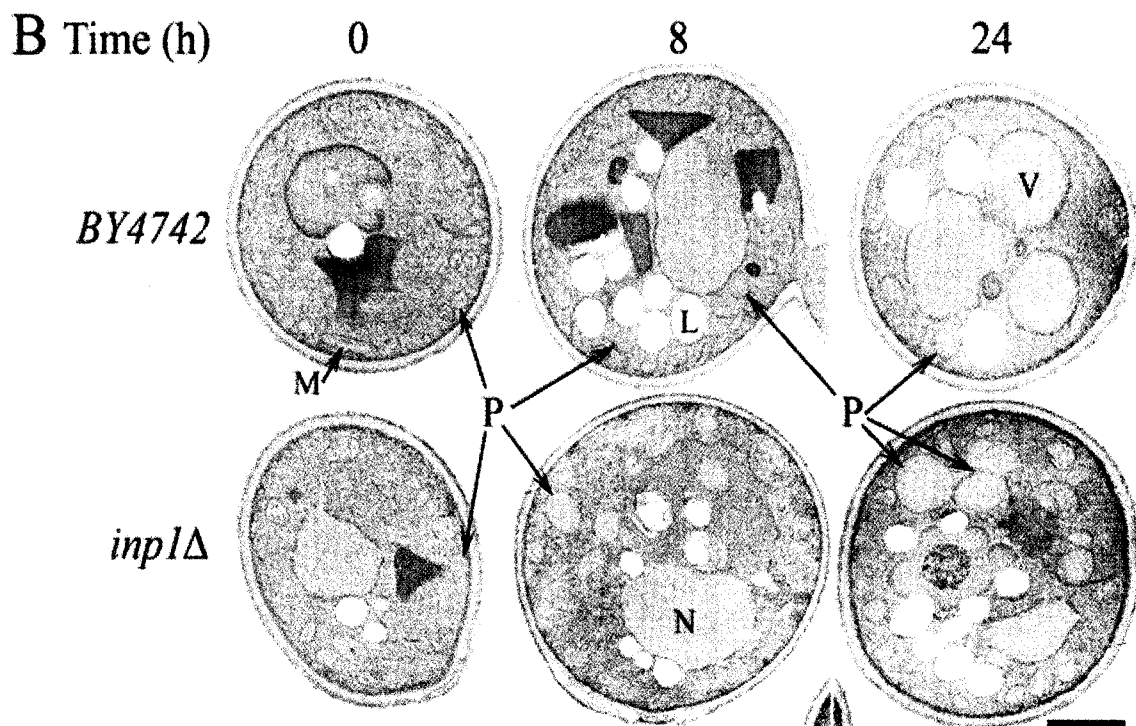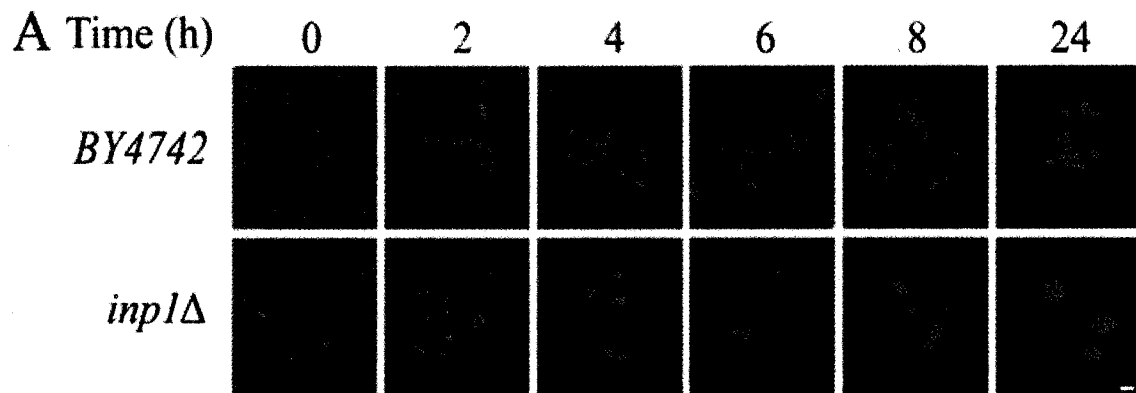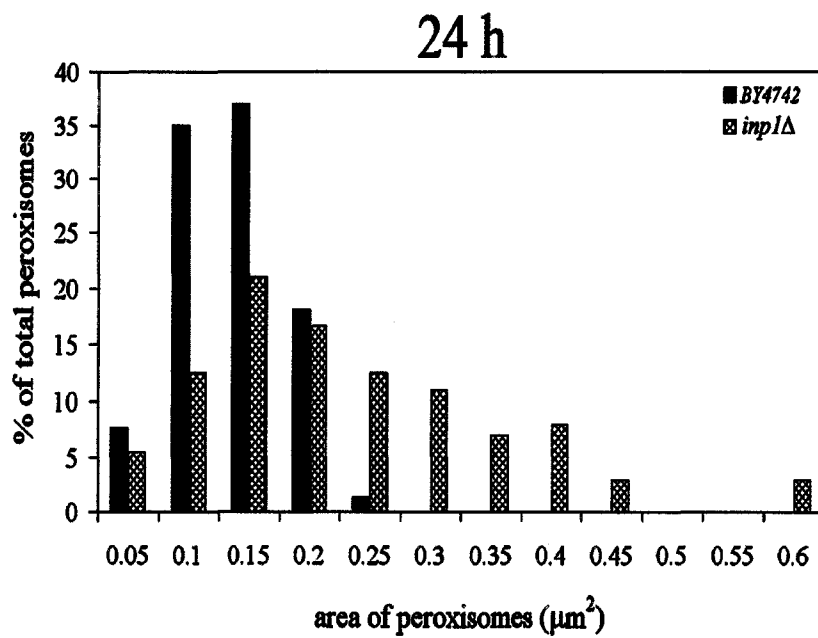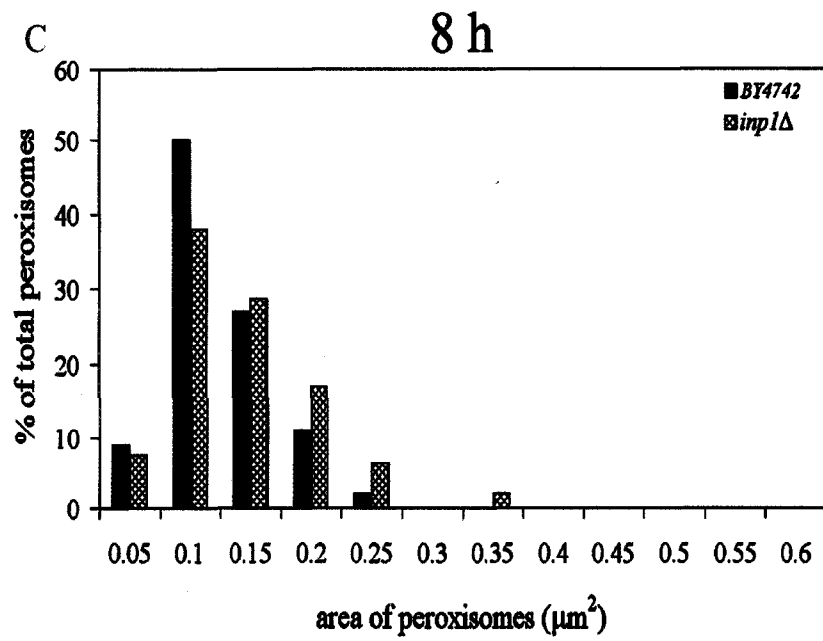
Table 3-1. Average area and numerical density of peroxisomes in wild-type and *inp1Δ*cells

Strain	Timeof incubation in YPBO (h)	Cell area assayed (μm^2)	Peroxisome count[a]	Numerical density of peroxisomes[b]	Average area of peroxisomes[c] (μm^2)
BY4742	8	526	0.21	0.86	0.07
inp1Δ	8	452	0.18	0.56	0.12
BY4742	24	369	0.24	0.78	0.11
inp1Δ	24	480	0.15	0.35	0.21

[a]No. of peroxisomes counted per μm^2 of cell area on micrographs.
[b]No. of peroxisomes per μm^3 of cell volume.
[c]Average area on micrographs.

YEp13   YEp13-*INP1*
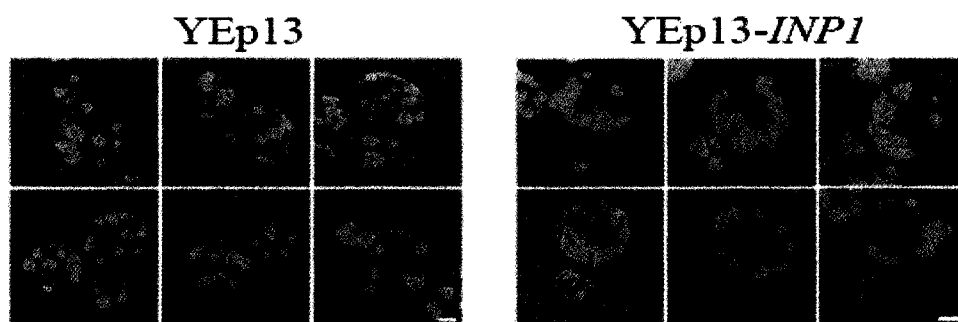
Figure 3-3. Cells deleted for *INP1* exhibit an abnormal peroxisome phenotype. Effects of *INP1* overexpression on the peroxisome phenotype. The strain *BY4742/POT1-GFP* was transformed with the empty multicopy plasmid YEp13 (panels at left) or with YEp13 containing the *INP1* gene (panels at right) for overexpression of *INP1*. Cells grown in SM medium for 16 h were transferred to and incubated in oleic acid-containing YNO medium for 8 h. Images were captured with a LSM510 META laser scanning microscope.

3.4 Deletion of *INP1* leads to increased numbers of mother cells without

peroxisomes

The uneven distribution of peroxisomes between mother cells and buds when Inp1p was either absent or overproduced suggested an involvement of Inp1p in partitioning peroxisomes between mother cell and bud during cell division. To investigate this possibility, wild-type and *inp1Δ* cells synthesizing Pot1p-GFP to fluorescently label peroxisomes were incubated in SCIM medium containing glucose and oleic acid, which permits both growth and division of cells and the proliferation of peroxisomes, and analyzed by direct fluorescence confocal microscopy. Fluorescent images were collected as a stack, and all optical slices were analyzed for each field. In wild-type cells, peroxisomes were observed in essentially all mother cells and buds, notwithstanding the size of the bud (Figure 3-4 A), as has been observed previously (Hoepfner et al., 2001). In contrast, a significant percentage of the budded cells of the *inp1Δ* strain lacked readily identifiable peroxisomes in the mother cell (Figure 3-4 A). Quantitation showed that *inp1Δ* cells exhibited an increase in the percentage of mother cells without peroxisomes with increasing bud size, with 29% of mother cells with the smallest buds (Category I) and 79% of mother cells with the largest bud (Category IV) lacking peroxisomes (Figure 3-4 A). These data suggest that the *inp1Δ* strain is defective in retaining peroxisomes in the mother cell during cell division.

Figure 3-4. Deletion or overexpression of *INP1* leads to defects in partitioning peroxisomes between mother cell and bud. (A) Wild-type and *inp1Δ* cells expressing *POT1-GFP* to fluorescently label peroxisomes were incubated for 16 h in SCIM containing glucose and oleic acid to allow for cell division and proliferation of peroxisomes. Fluorescent images of budded cells were acquired by confocal microscopy. Mother cells were scored for the presence or absence of fluorescent peroxisomes. Buds were sized according to four categories relative to the volume of the mother cell, expressed as a percentage of the mother cell volume (Category I, 0-12%; Category II, 12-24%; Category III, 24-36%; Category IV, 36-48%; see Materials and methods). Quantification was performed on at least 20 budded cells from each category. (B) Wild-type and *INP1*-overexpressing cells synthesizing Pot1p-GFP to label peroxisomes were incubated in SCIM and examined by confocal microscopy as described in (A). Buds were scored for the presence or absence of fluorescent peroxisomes, sized and categorized, and quantification was performed, as defined in (A). Bar, 1 μm.

A

B
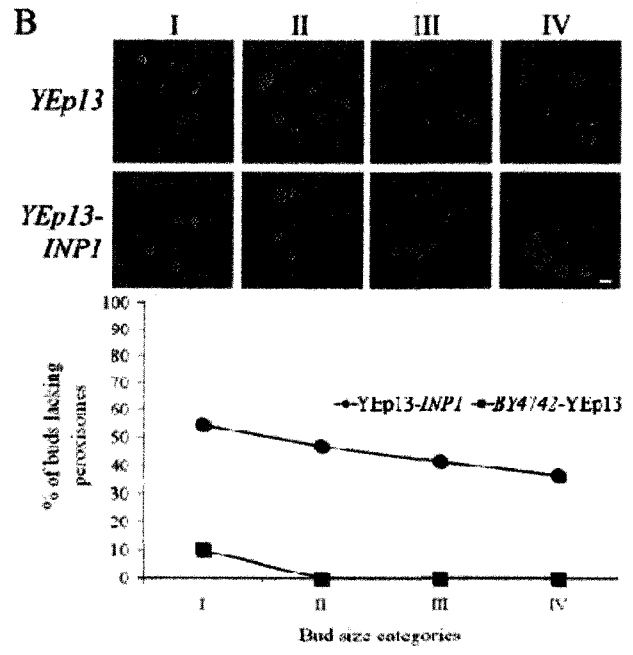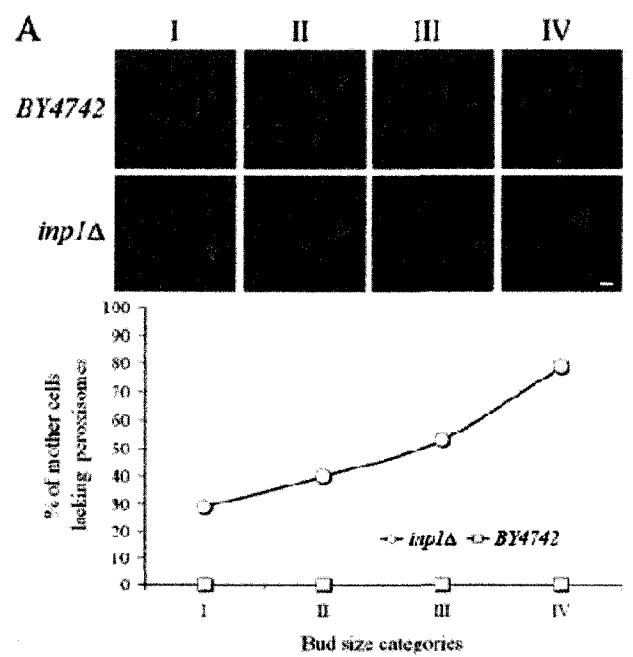
3.5 Overexpression of *INP1* leads to increased numbers of buds without peroxisomes

Overexpression of the *INP1* gene in cells led to increased numbers of buds without peroxisomes as compared to wild-type cells (Figure 3-4 B). Approximately 40% to 55% of buds of all size categories lacked peroxisomes (Figure 3-4 B). Only the smallest buds of wild-type cells lacked peroxisomes, and the percentage of the smallest buds (10%) lacking peroxisomes in the wild-type strain was much less than the percentage of smallest buds (55%) of the *inp1Δ* strain lacking peroxisomes. These data suggest that overproduction of Inp1p leads to retention of peroxisomes in the mother cell.

3.6 Impaired peroxisome inheritance in cells lacking or overexpressing *INP1*

The movement of peroxisomes between mother cell and bud was visualized by 4D *in vivo* video microscopy of both wild-type and *inp1Δ* cells expressing *POT1-GFP* to fluorescently label peroxisomes. In wild-type cells, peroxisomes moved in a directed manner from mother cell to bud (Figure 3-5 A see also http://www.jcb.org/cgi/content/full/jcb.200503083/DC1/3). Peroxisomes remained in the bud after their movement to the bud, while there was concomitant maintenance of the peroxisome population within the mother cell. In *inp1Δ* cells, peroxisome movement during cell division was compromised, resulting in an unbalanced distribution of peroxisomes between mother cell and bud. Frequently, all peroxisomes present in the mother cell before bud emergence were transported to the bud, resulting in a mother cell totally devoid of readily detectable fluorescent peroxisomes (Figure 3-5 B and see also

http://www.jcb.org/cgi/content/full/jcb.200503083/DC1/4). Occasionally, peroxisomes were observed to travel back and forth multiple times between the bud and the mother cell within an area restricted to around the bud neck (Figure 3-5 C and see also http://www.jcb.org/cgi/content/full/jcb.200503083/DC1/5). Peroxisomes that traveled from the bud to the center of the mother cell far beyond the region of the bud neck were also observed (Figure 3-5 D and see also http://www.jcb.org/cgi/content/full/jcb.200503083/DC1/6). This phenomenon was never observed in wild-type cells. Due to the larger size of many peroxisomes in *inp1Δ* cells, a delay was often observed in the passage of a peroxisome into the bud, indirectly affecting peroxisome partitioning (Figure 3-5 E and see also http://www.jcb.org/cgi/content/full/jcb.200503083/DC1/7). In cells overexpressing *INP1*, peroxisomes appeared to remain stationary at cortical locations within the mother cell and did not passage into the bud (Figure 3-5 F and see also http://www.jcb.org/cgi/content/full/jcb.200503083/DC1/8). Therefore, the data from 4D *in vivo* video microscopy are consistent with a role for Inp1p acting as a positive factor in the retention of peroxisomes within cells. When cells overexpressing Inp1p were subjected to latrunculin A treatment the localization of peroxisomes did not change indication that the actin cytoskeleton is not directly involved in anchoring peroxisomes at the cell cortex (Figure 3-5 H).

Figure 3-5. Peroxisome movement during cell division as visualized by 4D *in vivo* video microscopy. Peroxisomes were fluorescently labeled with genomically encoded Pot1p-GFP. Cells grown in SCIM for 16 h were placed onto a slide covered with a thin agarose pad containing SCIM. Cells were visualized at room temperature on a LSM 510 META confocal microscope specially modified for 4D *in vivo* video microscopy (see Materials and methods). Representative frames from videos show the specific movement patterns of peroxisomes within each strain. (A) Wild-type *BY4742* cells. Some peroxisomes move directionally from mother cell to bud. A population of peroxisomes remains within the mother cell (see also http://www.jcb.org/cgi/content/full/jcb.200503083/DC1/3). (B-E) *inp1*Δ cells. (B) The peroxisomes present in the mother cell before bud emergence (0') gather at the presumptive bud site (30'). Subsequently, all peroxisomes are transported into the growing bud (30'-170'). Inside the bud, peroxisomes localize to sites of active growth, being initially clustered at the bud tip and then relocated to the bud neck region prior to cytokinesis (see also http://www.jcb.org/cgi/content/full/jcb.200503083/DC1/4). (C) Peroxisomes present in the mother cell (3') move into the bud (31'). One peroxisome then returns to the mother cell from the bud (72') (see also http://www.jcb.org/cgi/content/full/jcb.200503083/DC1/5). (D) Initially, peroxisomes perform saltatory movements (10'-30') and are then inserted into the growing bud (57'-107') (see also http://www.jcb.org/cgi/content/full/jcb.200503083/DC1/6). (E) All peroxisomes present in mother cells before bud emergence move into the buds (72') (see also http://www.jcb.org/cgi/content/full/jcb.200503083/DC1/7). In the topmost cell, a peroxisome passes with difficulty into the bud due to its large size (0'-36'). In the cell at bottom, left, peroxisomes gather at the bud site (0'-3') and eventually enter the forming bud. At 92', one peroxisome returns to the mother cell. Some peroxisomes remain in the mother cell and display chaotic movements. In the cell at bottom, right, peroxisomes display chaotic movements (0'-18') and then gather at the new bud site. Eventually all peroxisomes move into the bud (184') (see also http://www.jcb.org/cgi/content/full/jcb.200503083/DC1/7). (F, G, H) Wild-type *BY4742* cells overexpressing *INP1*. (F) Peroxisomes appear immobile (0'-145'). Analysis of individual optical sections from the 4D data showed the peroxisomes to be located at the cell cortex. Both first and second generation buds lack peroxisomes (see also http://www.jcb.org/cgi/content/full/jcb.200503083/DC1/8). (G) Peroxisomes retain fixed cortical positions in mother cells. One peroxisome reaches the bud, keeps its mobility for a defined period of time (until 100') but eventually becomes immobile (see also http://www.jcb.org/cgi/content/full/jcb.200503083/DC1/9). (H) When Inp1p is overexpressed and actin is depolymerised with latrunculin A peroxisomes maintain fixed cortical positions in mother cells. Bar, 1 μm.

A *BY4742*

B *inp1Δ*

C

D

E
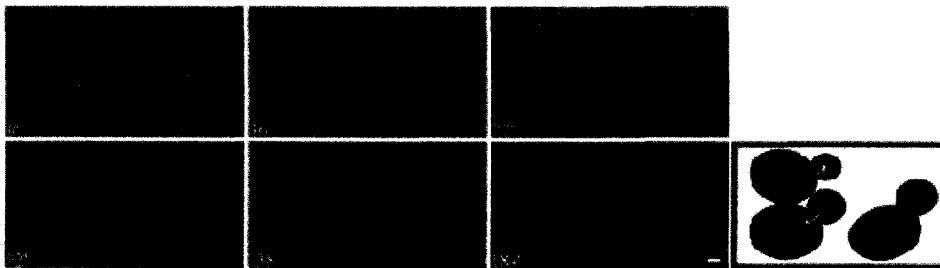
F *YEp13-INP1*

G
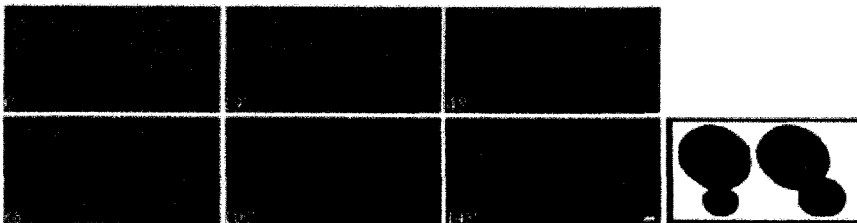
H *YEp13-INP1* + Lat A

3.7 Peroxisomes associate with actin cables in wild-type and *inp1Δ* cells but not in cells overexpressing *INP1*

The partitioning of peroxisomes at cell division depends on the movement of peroxisomes on polarized actin cables from mother cell to bud. Since we observed defects in the movement of peroxisomes from mother cell to bud in cells either deleted for or overexpressing the *INP1* gene, we analyzed the organization of actin, and its relationship to peroxisomes, in wild-type cells and cells lacking or overexpressing *INP1*. Actin was detected with rhodamine-phalloidin, and peroxisomes by fluorescence of Pot1p-GFP (Figure 3-6). In cells of all strains, actin showed normal polarized structures, with patches at sites of growth and distinct actin cables. A significant number of peroxisomes colocalized with actin cables in wild-type cells (Figure 3-6, top panels) and *inp1Δ* cells (Figure 3-6, middle panels). In contrast, in cells overexpressing *INP1* (Figure 3-6, bottom panels), most peroxisomes localized preferentially to the cell cortex and showed no clear association with actin cables.

3.8 Overproduced Inp1p localizes to peroxisomes and to the cell cortex

If Inp1p acts to secure peroxisomes to the cell cortex during cell division, overproduced Inp1p should also associate with the cell periphery in glucose-grown cells that have few peroxisomes. To test this, Inp1p-GFP was overproduced in wild-type *BY4742/POT1-RFP* cells grown in glucose-containing medium. Inp1p-GFP showed both peroxisomal and cortical localizations, supportive of Inp1p being the link between peroxisomes and an anchoring cortical structure (Figure 3-7).

	F-actin	Thiolase	Merge
BY4742/ POT1-GFP			
inp1Δ/ POT1-GFP			
YEp13- INP1/ POT1-GFP			
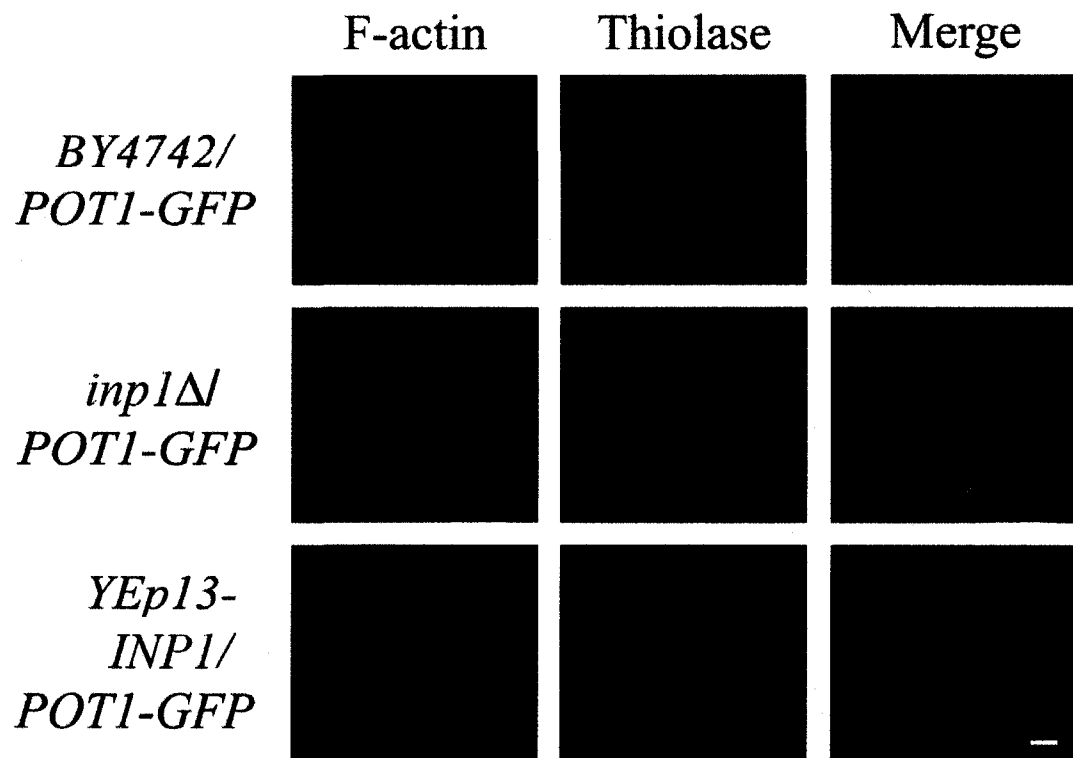
Figure 3-6. Microscopic colocalization analysis of peroxisomes and actin. Cells were incubated for 16 h in SCIM medium containing glucose and oleic acid. Filamentous actin (F-actin) was detected by staining with rhodamine-phalloidin. Peroxisomes were detected by fluorescence of Pot1p-GFP (Thiolase). The panels at right show the merge of rhodamine and GFP signals. Bar, 1 μm.
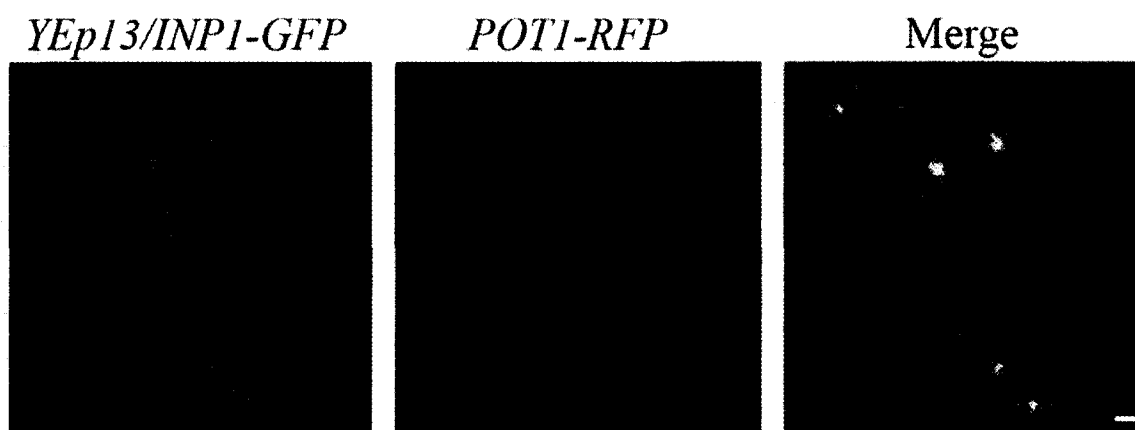
Figure 3-7. Overproduced Inp1p is localized to peroxisomes and the cell cortex. The strain *BY4742/POT1-RFP* transformed with a multicopy YEp13 plasmid construct overexpressing *INP1-GFP* were grown to mid-log phase in glucose-containing SM medium and examined by confocal microscopy. Overproduced Inp1p-GFP is localized to both peroxisomes and the cell cortex. Bar, 1 μm.

3.9 Peroxisomes are actively retained in the mother cell

Our data show a role for Inp1p in retaining peroxisomes in mother cells. Conceptually, the distribution of peroxisomes between mother cell and bud could be a time-dependent process controlled indirectly by cytokinesis or a process in which peroxisomes are actively retained in the mother cell independently of cell cycle duration. To choose between these views, wild-type *BY4742/POT1-GFP* cells were treated with hydroxyurea to arrest cells in S phase, which leads to a protracted opening of the bud neck. This approach has been used to demonstrate an active retention mechanism for mitochondria in cells (Yang et al., 1999). After treating cells with hydroxyurea, peroxisomes remained equally distributed between the mother cell and the now hyperelongated bud (Figure 3-8). In addition, the peroxisomes in the mother cell were cortically localized. These results show that peroxisomes are actively retained in the mother cell.

3.10 The levels of Inp1p vary with the cell cycle

The accurate partitioning of peroxisomes between mother cell and bud is an ordered process that progresses in distinct steps through the cell cycle. Accordingly, it might be expected that Inp1p would be subject to some form of cell cycle-dependent regulation. To test this, cells were subjected to and released from α factor-induced G1-arrest. The levels of Inp1p varied with the cell cycle (Figure 3-9), peaking 60 min after α factor release.

3.11 Inp1p binds Pex25p, Pex30p and Vps1p

In vitro binding assays were performed to begin identifying interacting partners of Inp1p. Bacterially produced GST fused to Inp1p (GST-Inp1p) and GST alone were immobilized on glutathione resin and incubated with yeast lysates expressing TAP-tagged Pex11p, Pex17p, Pex19p, Pex25p, Pex30p and Vps1p. Inp1p was observed to interact with Pex25p, Pex30p and Vps1p (Figure 3-10), all of which have been implicated in controlling peroxisome size and number.

BY4742/POT1-GFP + hydroxyurea

bottom   middle   top
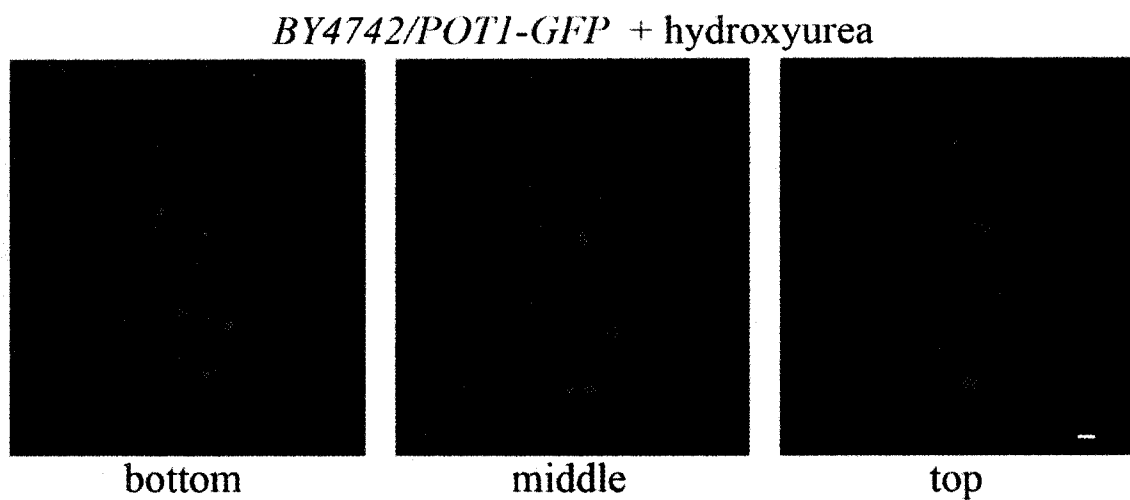
Figure 3-8. Peroxisomes are actively retained in the mother cell. Wild-type *BY4742/POT1-GFP* cells grown to mid-log phase in YPD medium were arrested in S-phase by the addition of 200mM hydroxyurea for 6 h. Fluorescent images of arrested cells were captured as a *z*-stack (bottom, middle, top) by confocal microscopy. The lower cell is the mother cell, and the upper cell is the hyperelongated bud. Bar, 1 μm.
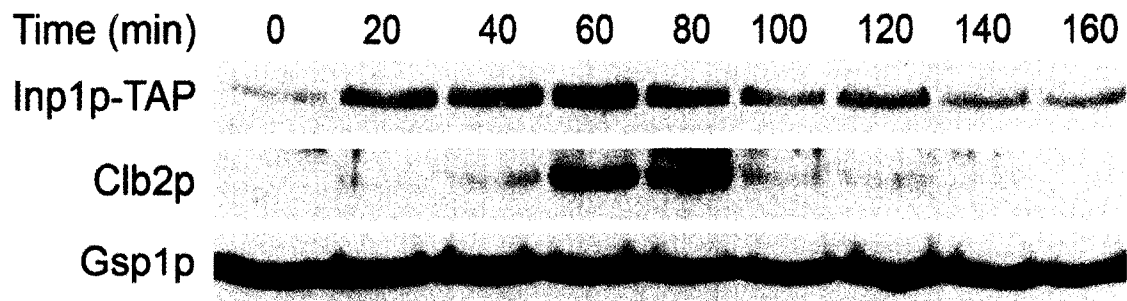
Figure 3-9. The levels of Inp1p vary with the cell cycle. Cells expressing TAP-tagged Inp1p were grown for 16 h in YPD and synchronized in G1 by addition of α factor (0 min). After removal of α factor, cells were incubated in YPD at 23°C. Samples were removed at the indicated times, and total cell lysates were prepared, separated by SDS-PAGE, transferred to nitrocellulose and analyzed by immunoblotting with antibodies directed against the TAP tag, the cyclin Clb2p or Gsp1p (Ran). Gsp1p serves as a control for protein loading.
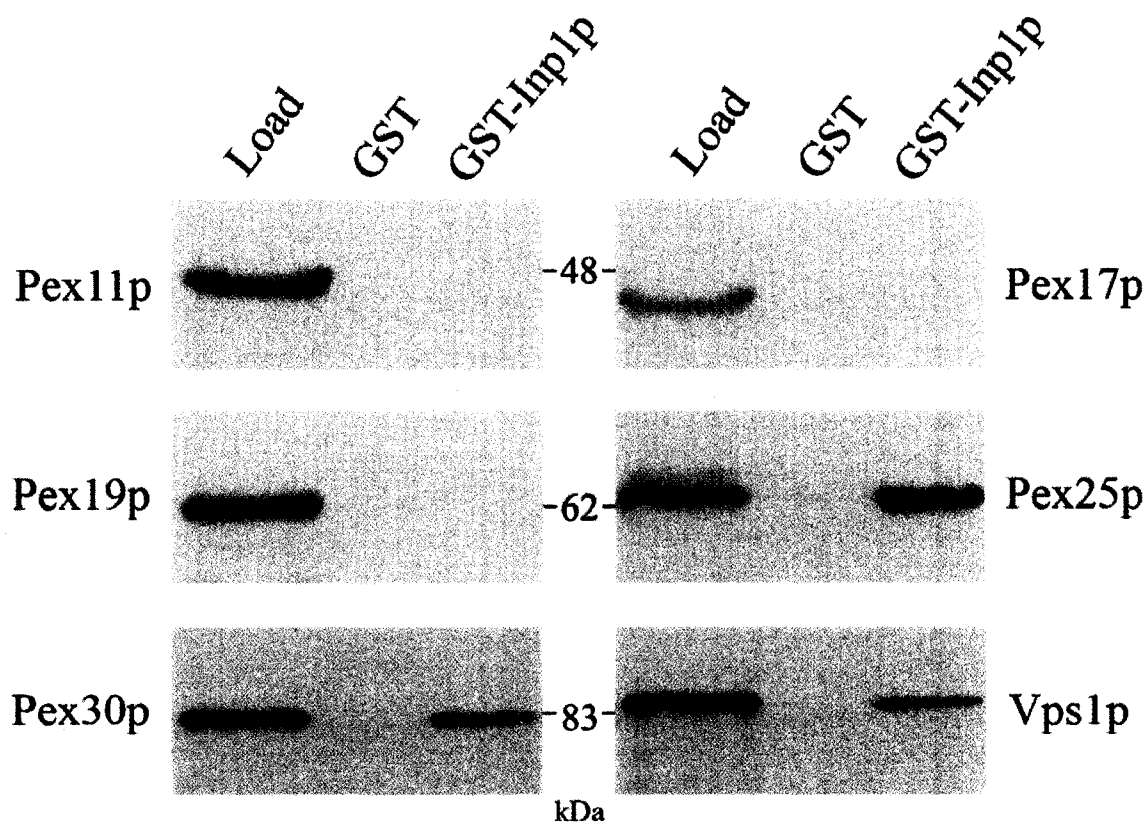
Figure 3-10. Inp1p binds Pex25p, Pex30p and Vps1p. GST-Inp1p and GST alone were immobilized on glutathione-Sepharose and incubated with whole cell lysates containing TAP-tagged peroxins or Vps1p. Lysates and bound fractions were resolved by SDS-PAGE, and TAP chimeras were detected by immunoblotting with anti-TAP antibody. Inp1p interacts with Pex25p, Pex30p and Vps1p but not with Pex11p, Pex17p, Pex19p or GST alone. Load represents 10% of the quantity of lysate applied to glutathione-Sepharose for pull-downs.

3.12 Discussion

3.12.1 Inheritance of organelles in budding yeast

Eukaryotic cells partition each of their organelle populations during cell division. In budding yeasts such as *S. cerevisiae*, organelles must be delivered to the emerging bud. A polarized actin cytsoskeletal system is required both for the formation of the bud itself and for the faithful delivery of every organelle type to the emerging bud. Organelles are duplicated or fragmented in the mother cell prior to their delivery using molecular motors along actin tracks to the bud. In comparison to what is known about the molecular players and mechanisms controlling the inheritance of the vacuole, Golgi apparatus, ER and mitochondria, relatively little is known about how peroxisomes are inherited.

3.12.2 The discovery of Inp1p

Here we report that Inp1p, a protein of unknown function encoded by the *S. cerevisiae* genome, is required for peroxisome inheritance. Inp1p is the first peroxisomal protein to be directly implicated in the inheritance of peroxisomes. Inp1p had tentatively been identified as a peroxisomal protein in a large-scale screen of protein localization in *S. cerevisiae* (Huh et al., 2003). We confirmed the localization of Inp1p to peroxisomes by microscopic analysis and subcellular fractionation under conditions of peroxisome proliferation in oleic acid-containing medium and demonstrated that Inp1p is a peripheral membrane protein of peroxisomes. Inp1p is not required for peroxisome assembly per se, since cells harboring a deletion of the *INP1* gene contain readily identifiable peroxisomes by microscopic analysis.

When incubated in oleic acid-containing medium, cells deleted for the *INP1* gene showed a progressive decrease in the average number of peroxisomes with time. Concomitant with this decrease in peroxisome number over time was an increase in the overall sizes of individual peroxisomes. However, there was heterogeneity in the peroxisome populations of individual cells deleted for the *INP1* gene, with some cells containing a few enlarged peroxisomes and other cells containing a population of peroxisomes similar in size and number to wild-type cells. This heterogenous peroxisome phenotype of *inp1Δ* cells is distinct from the peroxisome phenotype of cells deleted for one or more of the peroxin-encoding genes *PEX11*, *PEX25* and *PEX27*, where all cells contain fewer and enlarged peroxisomes in comparison to wild-type cells (Erdmann and Blobel, 1995; Marshall et al., 1995; Rottensteiner et al., 2003; Smith et al., 2002; Tam et al., 2003). Moreover, in the *inp1Δ* strain, there was a large increase in the number of mother cells lacking readily identifiable peroxisomes, and the overall proportion of mother cells without peroxisomes increased with increasing bud size. These observations, combined with the fact that overexpression of the *INP1* gene led conversely to large numbers of buds without readily identifiable peroxisomes and the relocation of peroxisomes to the cortical regions of cells, including mother cells, strongly suggested a role for Inp1p in peroxisome inheritance.

3.12.3 Retention mechanisms

The inheritance of organelles in budding yeast consists of two complimentary processes: the retention of a subset population of an organelle in the mother cell and the ordered movement of the remaining portion of the organelle population to the forming

bud. The close control of both processes is crucial to the successful distribution of the organelle from mother cell to bud. A retention mechanism within the mother cell has been described for mitochondria (Yang et al., 1999). Retained mitochondria accumulate at the tip of the mother cell distal to the site of bud emergence (the so called "retention zone"), a process that likely involves the actin cytoskeleton. Retention mechanisms also operate in the bud. After being delivered to the bud, both organelles and individual types of molecules have been shown to remain anchored to the bud cell cortex at discrete locations, as demonstrated for mitochondria (Simon et al., 1997), *ASH1* mRNA (Long et al., 1997; Takizawa et al., 1997) and the protein chitin synthase 3 (DeMarini et al., 1997). Recently, the Rab-like protein Ypt11p was shown to be required for the retention of newly inherited mitochondria within buds of *S. cerevisiae* (Boldogh et al., 2004).

3.12.4 The role of Inp1p in peroxisome retention

We performed 4D *in vivo* video microscopical imaging to get initial mechanistic insight into the role for Inp1p in peroxisome inheritance. 4D *in vivo* video microscopy showed that in wild-type cells, a subset of peroxisomes partitioned to the emerging bud, while the remaining peroxisomes in the mother cell retained fixed cortical positions. The movements of peroxisomes into the bud correlated with the actin cytoskeleton, which undergoes a defined sequence of cell-cycle regulated rearrangements (Moseley and Goode, 2006). In their directed movement to the bud, peroxisomes always concentrated at the sites of active growth, being initially clustered at the bud tip and later spread over the entire bud cortex. We and others (Hoepfner et al., 2001) observed that prior to cytokinesis, subsets of peroxisomes from both the mother cell and the bud redistribute to

the neck region, while the remaining peroxisomes remain anchored to the cortices of the mother cell and bud.

Peroxisomes moved from mother cells to buds in *inp1Δ* cells at velocities comparable to those in the wild-type cells. Moreover, in *inp1Δ* cells, there was also no delay in the passage of peroxisomes to the emerging bud, except in those cells containing greatly enlarged peroxisomes. In this case, because peroxisomes were much too large to pass into the bud at the incipient bud stage, they had to undergo division to smaller peroxisomes before moving into the growing bud. Since the absence of Inp1p does not affect the velocity of peroxisome movement during cell division or the time taken for a peroxisome to enter the bud, Inp1p apparently is not directly involved in the movement of peroxisomes between mother cell and bud, presumably along actin tracks. In addition, actin as a whole is apparently normal in *inp1Δ* cells, as no defect in cell polarity was observed in these cells. Therefore, a major reorganization of the actin cytoskeletal system in cells lacking Inp1p cannot explain why these cells exhibit defects in peroxisome inheritance. How then might Inp1p function in peroxisome inheritance? Frequently, peroxisomes were observed moving between the bud and mother cell within a restricted area near the neck. A similar kind of bidirectional movement has been reported for late Golgi elements in the *cdc1-304* temperature-sensitive strain of *S. cerevisiae* (Rossanese et al., 2001). On occasion, peroxisomes, after having passaged to the bud, returned deep into the interior of the mother cell, a phenomenon we never observed in wild-type cells. One could explain the movements of peroxisomes from buds to mother cells by proposing that peroxisomes delivered to the bud in *inp1Δ* cells have a decreased affinity for a structure that retains peroxisomes within the bud, with the possibility that some

peroxisomes actually elude the anchoring mechanism completely. In their random free movement, peroxisomes that re-entered the mother cell from the bud were reloaded onto polarized actin tracks and thus reinserted into the bud. Accordingly, peroxisomes fail to be actively retained in either the mother cell or the bud, resulting in the disruption of the ordered vectorial process of peroxisome segregation during cell division. The fact that overproduction of Inp1p retains peroxisomes in the mother cell at fixed cortical positions and prevents the distribution of a subset of peroxisomes to the growing bud implicates Inp1p directly in tethering peroxisomes to anchoring structures in both the mother cell and bud.

3.12.5 Proposed model for Inp1p's role in peroxisome retention

A proposed model for the function of Inp1p in partitioning peroxisomes between mother cell and bud is presented in Fig. 3-11. A subset of peroxisomes is transported to the bud by a process dependent on Myo2p (Hoepfner et al., 2001), while the remaining peroxisomes are retained within the mother cell on a cortical anchor. The peroxisomal peripheral membrane protein Inp1p would link the peroxisome to the cortical anchor. It is noteworthy that overproduction of Inp1p led to a distinctly enhanced cortical distribution of peroxisomes in cells. Whether a given peroxisome will be delivered to the bud or retained in the mother may depend on a tug-of-war between Inp1p and Myo2p.
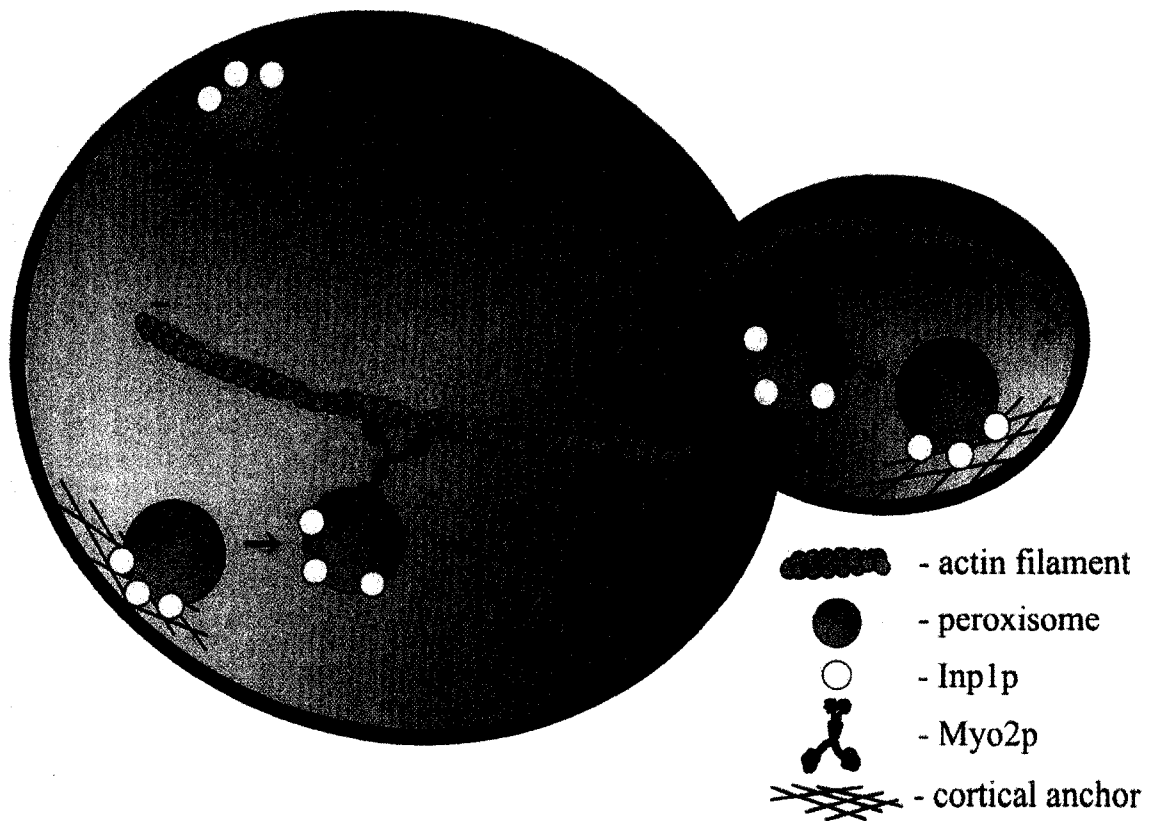
Figure 3-11. A model for Inp1p function in peroxisome retention. Peroxisomes move along polarized actin cables in a Myo2p-dependent manner from mother cell to bud. Concomitantly, a subset of peroxisomes is retained within the mother cell. Inp1p acts to link peroxisomes to a cortical anchor and retain peroxisomes in the mother cell and bud.

Accordingly, both under- and overproduction of Inp1p would lead to impairment of the normal inheritance of peroxisomes. Once peroxisomes are delivered to the bud, they are prevented from returning to the mother cell. Inp1p also appears to play a role also in retaining peroxisomes within the bud, probably by attaching peroxisomes to anchoring structures present in the bud.

Thus, Inp1p seems to have a dual role in the division and the inheritance of peroxisomes in *S. cerevisiae*. How might these two functions be related? Other proteins are known to influence both the morphology of organelles and their distribution. Mdm10p, Mdm12p and Mmm1p are mitochondrial outer membrane proteins that affect mitochondrial shape and segregation (Boldogh et al., 2003). Mutation of any one of these proteins results in the presence of giant, spherical mitochondria that exhibit defects in partitioning at cell division. As mentioned in Chapter 1, there are studies (Boldogh et al., 2003) indicating that these proteins form a complex that connects the minimum heritable unit of mitochondria (mtDNA and mitochondrial membranes) to actin, therefore functioning as a mitochondrial counterpart to the kinetochore or the "mitochore". These proteins affect the retention of mitochondria within the mother cell (Yang et al., 1999) and also Myo2p-independent mitochondrial movement (Boldogh et al., 2001).

3.12.6 Concluding remarks

In closing, I have presented evidence demonstrating that the peroxisomal peripheral membrane protein, Inp1p, is directly implicated in the inheritance of peroxisomes in *S. cerevisiae*. Inp1p is the first peroxisomal protein shown to be involved

in the inheritance of peroxisomes. Inp1p acts as a peroxisome-retention factor, tethering peroxisomes to anchoring structures within the mother cell and bud.

CHAPTER FOUR: THE PEROXISOMAL PROTEIN ENCODED BY *YJL185C*

BINDS INP1 PROTEIN AND IS REQUIRED FOR PEROXISOME RETENTION

4.1 Overview

This chapter reports the identification of Yjl185p, a new peroxisomal protein of *S. cerevisiae*, which affects the morphology of peroxisomes as well as their partitioning during cell division. Yjl185p is a new binding partner of Inp1p as shown by yeast two-hybrid assays. Microscopy studies revealed a defect in the morphology and distribution of peroxisomes in cells lacking or overexpressing the *YJL185c* gene when compared to wild-type cells. Interestingly, *yjl185Δ* cells retain fewer peroxisomes in the distal portion of the mother cells as compared to wild-type. The deletion strain *yjl185Δ* grows slower on oleic-acid containing plates, indicating a biogenesis defect in the peroxisomes of these cells. Double mutant *yjl185Δvps1Δ* cells present abnormal peroxisomes partitioning between the mother and daughter cells. The retention of peroxisomes on the cell cortex is not directly connected to the proliferation of peroxisomes, as shown by the ability of peroxisomes to divide in a strain with minimal retention. In summary, Yjl185p is a new peroxisomal protein that interacts with Inp1p and functions in the retention of peroxisomes on the distal portion of the mother cells.

4.2 Inp1p interacts with Yjl185p by the two-hybrid assay

A large scale protein interaction study identified a new binding partner of Inp1p, a protein of an unknown function encoded by the open reading frame *YJL185c* (Ito et al., 2001). To investigate whether Inp1p interacts with Yjl185p we performed a two-hybrid assay (Figure 4-1). Initially, we constructed fusion proteins of Inp1p and Yjl185p with each of the domains of the transcription factor Gal4: the activating domain (AD) and the binding domain (BD). As shown in Figure 4-1, different combinations of these constructs

Figure 4-1. Inp1p interacts with Yjl185p by the two-hybrid assay. We constructed fusion proteins of Inp1p and Yjl185p with each of the domains of the transcription factor Gal4: the activating domain (AD) and the binding domain (BD). Different combinations of these constructs were further introduced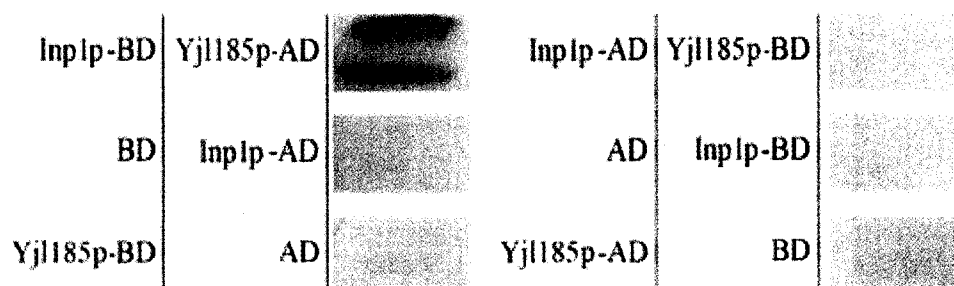 in the *S. cerevisiae* SFY526 strain and the cells expressing the fusion proteins were subjected to the β-galactosidase filter detection assay. The assay shows a strong interaction in cells expressing the fusion proteins Inp1p-BD and Yjl185p-AD.

were further introduced into the *S. cerevisiae* SFY526 strain and the cells expressing the fusion proteins were subjected to a β-galactosidase filter detection assay. The emergence of the blue color on the filter paper signals that a positive interaction between the tested candidate proteins has occured. The controls confirmed a lack of auto-activation in our individual constructs and also a comparison for known positive and negative interactions (not shown). The assay shows a strong interaction in cells expressing the fusion proteins Inp1p-BD and Yjl185p-AD the blue color appearing faster and at a higher intensity than the positive control. Interestingly, when the proteins are fused with the opposite domains, Yjl185p-BD and Inp1p-AD, the assay shows no interaction. It appears that this interaction is highly specific being dependent on distinct conformational shapes that are only acquired when Inp1p-BD is in close proximity toYjl185p-AD.

4.3 The phenotype of *yjl185Δ* cells display abnormal peroxisomal distribution

The interaction between Yjl185p and Inp1p led us to speculate on their possible involvement in a common pathway. To investigate this idea further, wild-type *BY4742* and *yjl185Δ* yeast cells expressing the peroxisomal marker protein thiolase (Pot1p) tagged with GFP were used to analyze peroxisomal distribution and morphology. The cells were grown in SCIM media for 16 h and then analyzed by direct fluorescence confocal microscopy. Wild-type cells contain on average 9-11 peroxisomes, which are distributed throughout the cytoplasm (Figure 4-2 A). In contrast, the peroxisomes in *yjl185Δ* cells preferentially localized near the bud neck region, leaving the distal part of the mother cell devoid of peroxisomes. Moreover, the size and number of peroxisomes

appear to be affected in this mutant possibly because of the clustering of peroxisomes to within a smaller volume of the cell. Close examination of a cell displaying this phenotype by acquiring optical slices of increased resolution (Figure 4-2 B) revealed a slight increase in the size of peroxisomes as well as a decreased number of these organelles. However, these results will need to be further verified by electron microscopy. To better understand to which degree Yjl185p participates in the distribution of peroxisomes we quantified the above described phenotype. Budded cells were separated into 4 categories depending on different bud sizes from the smallest to the largest (Figure 4-2 C). Next, at least 30 cells were counted for each category with the results showing a clear difference between *yjl185Δ* and wild-type control cells (Figure 4-2 D).

Wild-type *BY4742*, *yjl185Δ*, *inp1Δ* and *yjl185Δinp1Δ* yeast cells were grown in SCIM media and then processed for electron microscopy analysis (Figure 4-3). The *yjl185Δ* mutant cells showed an increase in peroxisomal size when compared with wild-type, while both *inp1Δ* and *yjl185Δinp1Δ* yeast cells show a larger size of peroxisomes. Thus, Yjl185p is a protein that is required for the proper partitioning of peroxisomes and also for the regulation of their size and number.

4.4 Overexpression studies in different deletion strains

We examined the consequence of overproducing Yjl185p on peroxisomes as well as the interplay between Yjl185p and Inp1p. Wild-type yeast cells expressing Pot1p-GFP as well as containing the empty multicopy plasmid YEp13 as a control were grown in SCIM for 16 h and then analyzed by confocal microscopy. The morphology and

Figure 4-2. *yjl185Δ* **cells show an abnormal peroxisomal distribution.** (A) Wild-type *BY4742* and *yjl185Δ* yeast cells expressing POT1-GFP were used to analyze the peroxisomal distribution and morphology. The cells were grown in SCIM media for 16 h and then analyzed by direct fluorescence confocal microscopy. Wild-type cells contain peroxisomes fairly distributed throughout the cytoplasm. The peroxisomes in *yjl185Δ* cells show a preferential localization near the bud neck region. (B) Optical slices of increased magnification. (C) Buds were sized according to four categories relative to the volume of the mother cell, expressed as a percentage of the mother cell volume (Category I, 0-12%; Category II, 12-24%; Category III, 24-36%; Category IV, 36-48%). (D) The mother cells were scored for the absence of peroxisomes in the distal region and quantification was performed on at least 30 budded cells from each category. Bar, 1 μm.

A BY4742/POT1-GFP   yjl185Δ/POT1-GFP

B

C

D

Percentage of mother cells without distal peroxisomes

Bud size categories
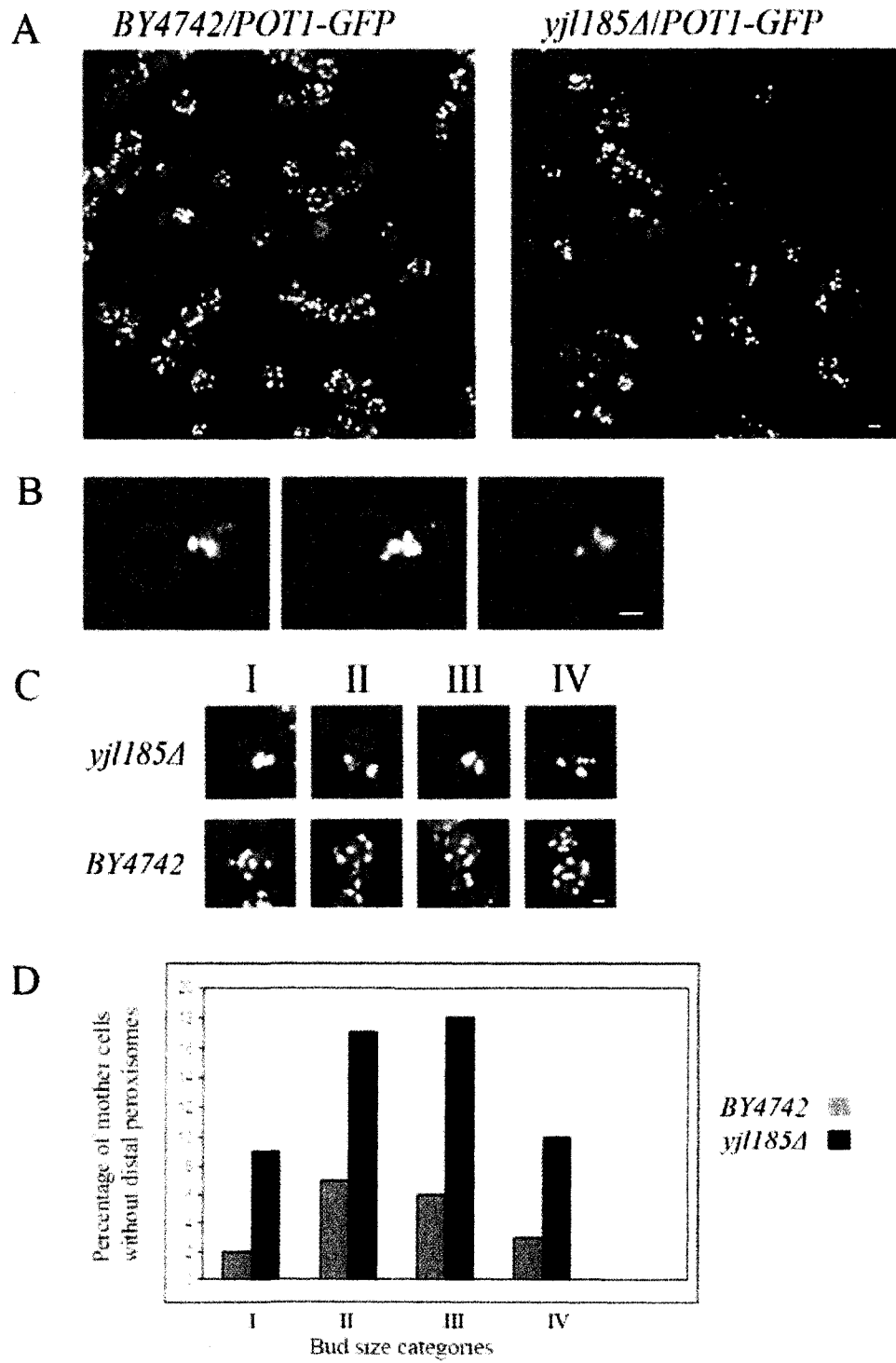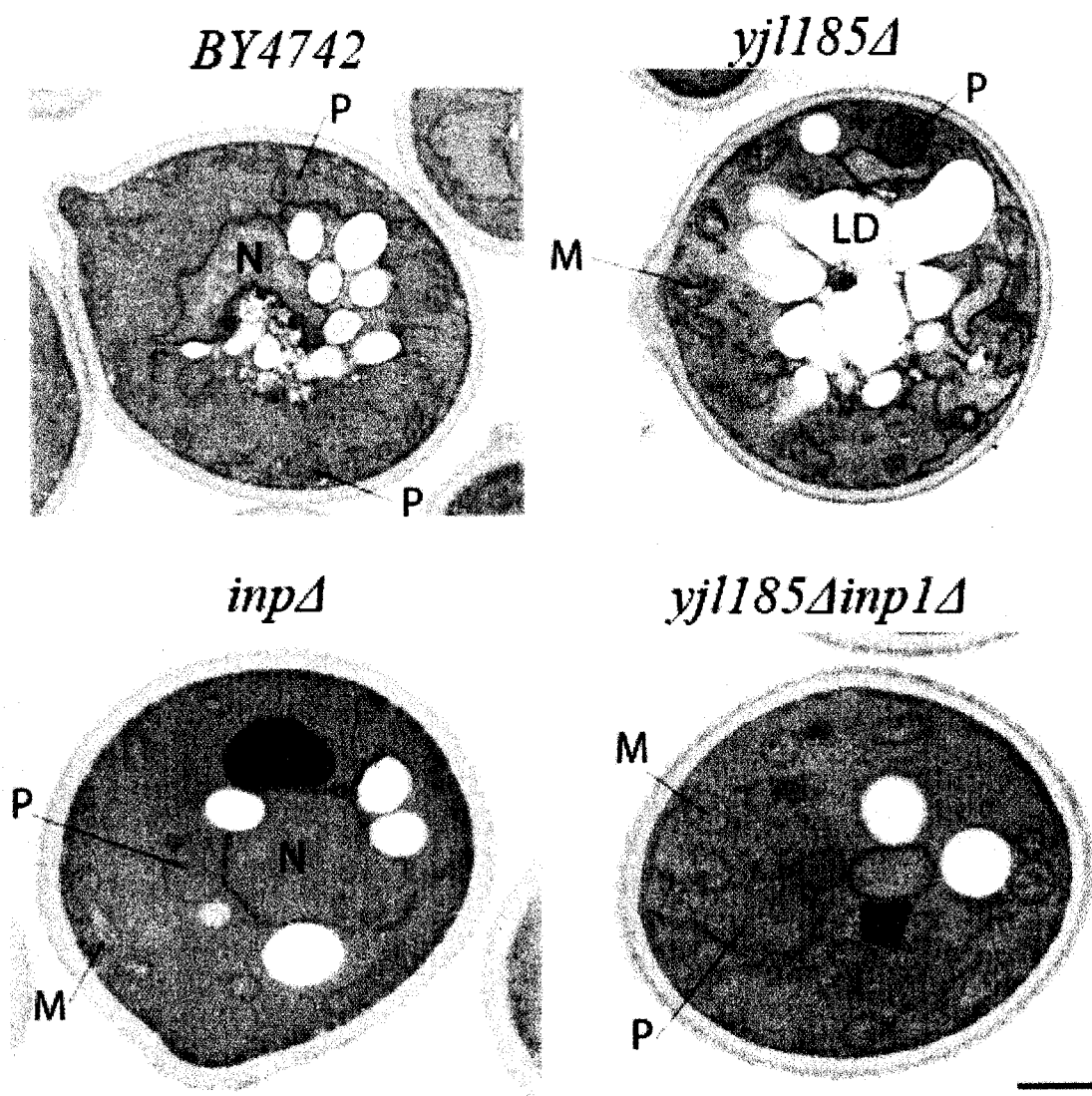
BY4742
yjl185Δ

Figure 4-3. *yjl185Δ* cells show peroxisomes of abnormal size. *BY4742, yjl185Δ, inp1Δ* and *yjl185Δinp1Δ* yeast cells were grown in SCIM media and then processed for electron microscopy analysis. *yjl185Δ* cells show an increase in the size of peroxisomes when compared with *BY4742*; *inp1Δ* and *yjl185Δinp1Δ* cells show even larger peroxisomes. P – peroxisomes, M – mitochondria, N – nucleus, LD – lipid droplet. Bar, 2 μm.
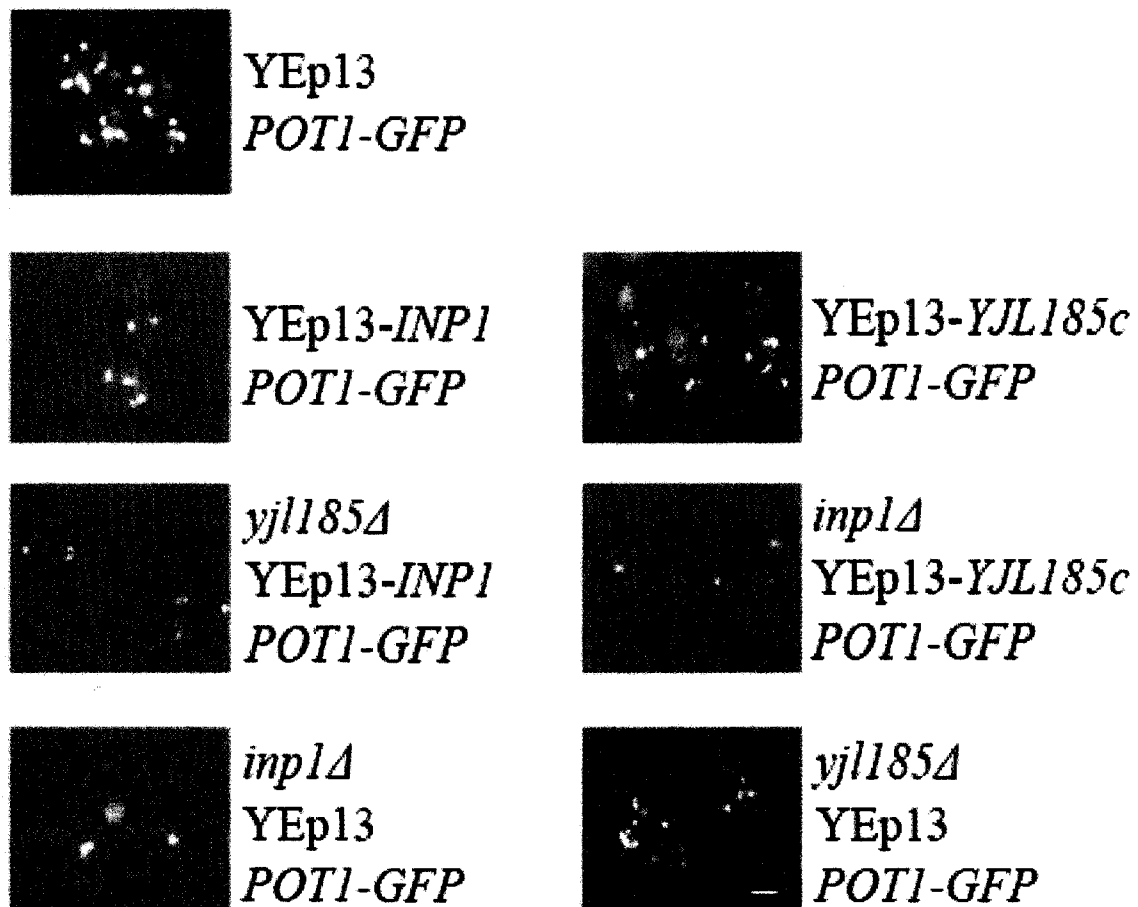
Figure 4-4. Effects of overexpression of *YJL185c* and *INP1* on peroxisome morphology and distribution. Wild-type yeast cells expressing Pot1p-GFP as well as containing the empty multicopy plasmid YEp13 as a control were grown in SCIM for 16 h and then analyzed by confocal microscopy. *INP1* overexpression increases the retention of peroxisomes on the mother cell cortex. The deletion of *yjl185Δ* decreased the percentage of cells with exclusive mother cell localization of peroxisomes. The overproduction of Yjl185p leads to impaired peroxisomal morphology having a decreased number as well as some tubular peroxisomes. This phenotype was no longer seen when the plasmid YEp13 containing *YJL185c* was transformed into cells deleted for *inp1Δ*. Bar, 1μm.

distribution of peroxisomes is normal making it a good control for our subsequent analysis (Figure 4-4). *INP1* overexpression interrupts the equal distribution of peroxisomes between the mother cell and the bud by increasing the retention of peroxisomes on the mother cell cortex. The deletion of *yjl185Δ* in this strain decreased the percentage of cells with exclusive mother cell localization of peroxisomes. The overproduction of Yjl185p leads to impaired peroxisomal morphology having a decreased number as well as some tubular peroxisomes. This phenotype was no longer manifested when the plasmid containing *YJL185c* was transformed into cells deleted for *inp1Δ*.

4.5 Yjl185p shows peroxisomal localization

To determine the cellular localization of Yjl185p we constructed a genomically encoded fluorescent chimera of Yjl185p and GFP (Yjl185p-GFP) and co-expressed it with the peroxisomal marker Pot1p-mRFP (Figure 4-5). Following 16 h of growth in SCIM media, of cells expressing both Yjl185p-GFP and Pot1p-RFP, the confocal microscopy analysis showed colocalization of Yjl185p with peroxisomes. Interestingly, we could also detect a weak cortical localization of Yjl185p-GFP. Furthermore, we examined the localization of these two fluorescent fusion proteins in the deletion mutants *inp1Δ* and *pex3Δ*. In cells lacking Inp1p, the peroxisomal localization of Yjl185p was preserved while the cortical signal was present even in the characteristic mother cells devoid of peroxisomes. The deletion of PEX3 results in the expected mislocalization of Pot1-mRFP to the cytoplasm while the punctate signal of Yjl185p disappeared.
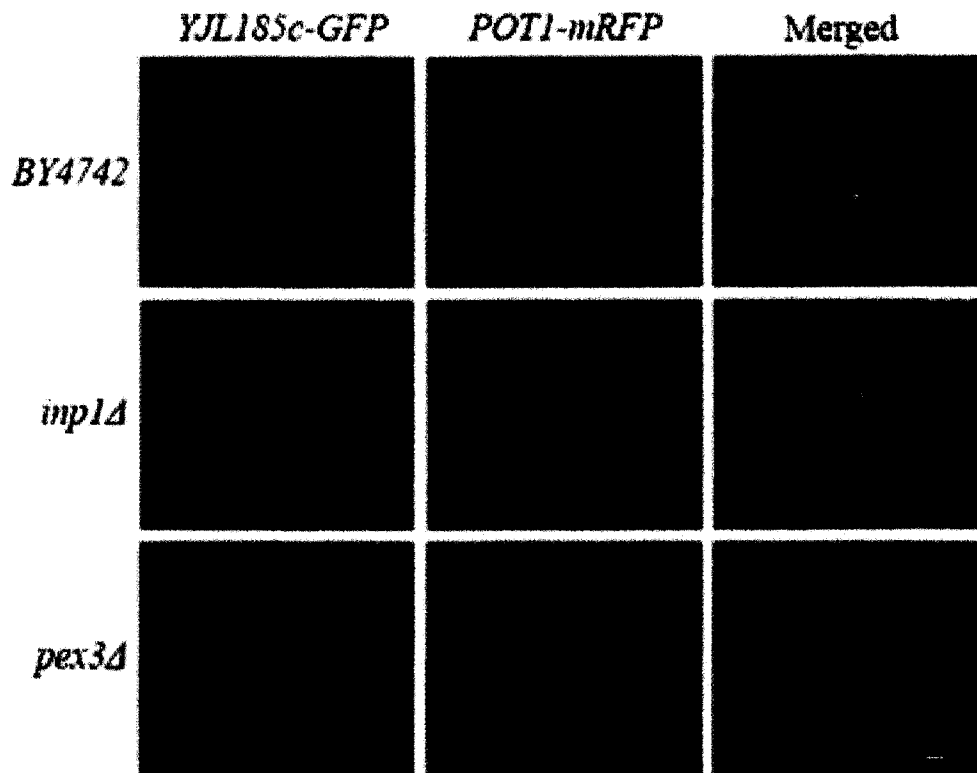
Figure 4-5. Yjl185p is a peroxisomal protein. Following 16 h of growth in SCIM, cells expressing both Yjl185p-GFP and Pot1p-mRFP showed colocalization of Yjl185p with peroxisomes by confocal microscopy. Yjl185p-GFP shows a weak cortical localization. In cells lacking Inp1p, the peroxisomal localization of Yjl185p was preserved, while the cortical signal was present even in characteristic mother cells devoid of peroxisomes. The deletion of Pex3p caused the expected mislocalization of thiolase to the cytosol while the punctate signal of Yjl185p was undetectable. Bar, 1 μm.

4.6 *yjl185Δ* cells exhibit slower growth on YPBO

A basic method for testing the functionality of peroxisomes in specific yeast strains is to grow the cells on oleic acid-containing media (YPBO). Wild-type cells together with *yjl185Δ*, *inp1Δ* and *pex3Δ* deletion strains were grown in glucose-containing media YEPD and then plated on YPBO plates in progressively decreasing serial dilutions (Figure 4-6). The *yjl185Δ* cells grew at a slower rate than wild-type cells but faster than *inp1Δ* cells. The negative control, *pex3Δ*, which has no peroxisomes, did not grow.

4.7 The phenotype of *yjl185Δvps1Δ* cells presents abnormal peroxisomal partitioning

The cortical protein Num1p colocalizes on mitochondria with the dynamin-related protein Dnm1p. Additionally, the single mutant *num1Δ* cells show aberrant mitochondrial morphology while the double mutant *num1Δdnm1Δ* cells show perturbed mitochondrial distribution. Using this analogy to mitochondria we examined the effects on peroxisomes of deleting *YJL195c* as well as the corresponding dynamin-related protein for peroxisomes, Vps1p. Wild-type *BY4742* as well as the mutant cells *yjl185Δ*, *vps1Δ*, and *yjl185Δvps1Δ* synthesizing Pot1p-GFP to fluorescently label peroxisomes were incubated in SCIM media for 16 h and then analyzed by fluorescence confocal microscopy (Figure 4-7). The wild-type peroxisomes have the characteristic morphology and distribution. In the *yjl185Δ* cells we can observe the preferential localization of peroxisomes in the proximal region of the cell. The *vps1Δ* mutant cells contain a single large peroxisome that usually divides by sending a tubular section in the bud. In *yjl185Δvps1Δ* cells
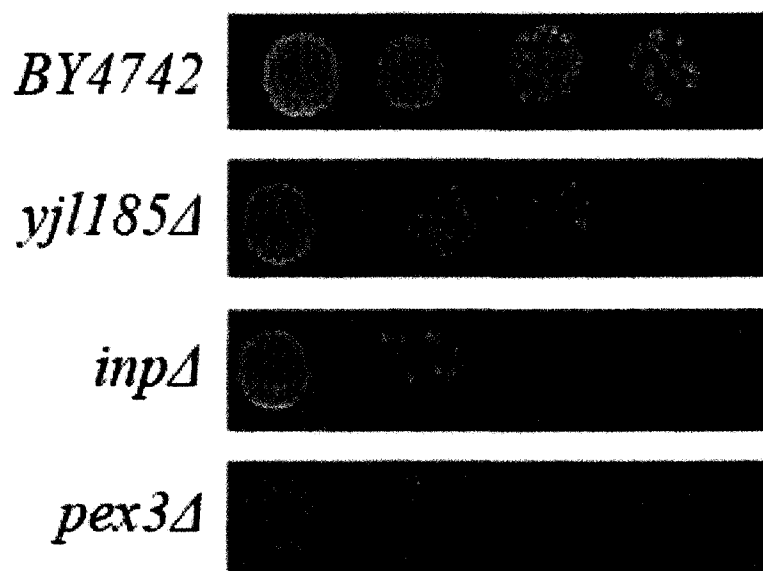
Figure 4-6. *yjl185Δ* **cells exhibit slower growth on YPBO.** *BY4742, yjl185Δ, inp1Δ* and *pex3Δ* cells were streaked on YPBO plates in progressively decreasing serial dilutions. The *yjl185Δ* cells grew more slowly than *BY4742* cells, while *inp1Δ* cells showed an even less growth. The *pex3Δ* cells show no growth.
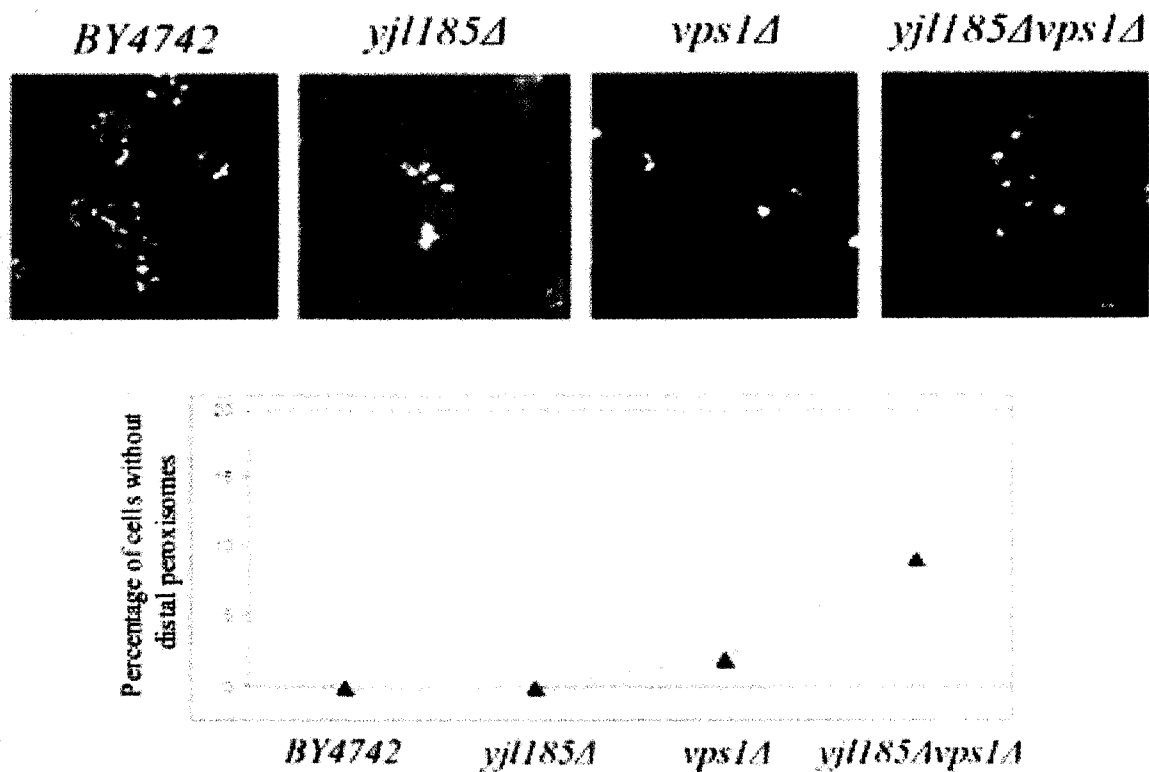
Figure 4-7. *yjl185Δvps1Δ* **cells present an abnormal distribution of peroxisomes.** Wild-type *BY4742* as well as the mutant cells *yjl185Δ*, *vps1Δ*, and *yjl185Δvps1Δ* synthesizing Pot1p-GFP were incubated in SCIM for 16 h and then analyzed by fluorescence confocal microscopy. The preferential localization of peroxisomes to the proximal region of the cell can be observed in *yjl185Δ* cells. *vps1Δ* mutant cells contain a single large peroxisome that usually divides by sending a tubular projection to the bud. In *yjl185Δvps1Δ* cells, the morphology as well as the distribution of peroxisomes is abnormal, with mother cells containing no peroxisomes.

the morphology as well as the distribution of peroxisomes is abnormal with mother cells containing no peroxisomes. This suggests the requirement of both Yjl185p and Vps1p for the proper retention to occur. The graph shows the quantification of cells that have abnormal retention as a percentage out of the whole cell population.

4.8 *In vivo* video microscopy analysis of wild-type and *yjl185Δ* cells

Theoretically, the phenotype in *yjl185Δ* cells could be determined by the random movement of highly mobile peroxisomes from one side of the cell to the other. Alternatively, the peroxisomes found close to the bud neck could be immobilized at that region. In order to distinguish between these two possibilities, we performed *in vivo* video microscopy analysis. Wild-type *BY4742* and *yjl185Δ* cells containing genomically integrated *POT1-GFP* to fluorescently label peroxisomes, were prepared for *in vivo* acquisition of movies by incubation in SCIM media for 16 h (Figure 4-8). Images were acquired every 20 sec for 14 min for the wild-type cells and for 28 min for the *yjl185Δ* cells. As expected, in the wild-type cells we notice mobile as well as static peroxisomes. The peroxisomes in the *yjl185Δ* cells show some oscillatory movements but they appear to stay in the same region over time.

4.9 Retention deficits do not prevent the division of peroxisomes

There is an apparent connection between division of peroxisomes and their retention seen not only in the deletion phenotype of Yjl185p, but also in the Inp1p
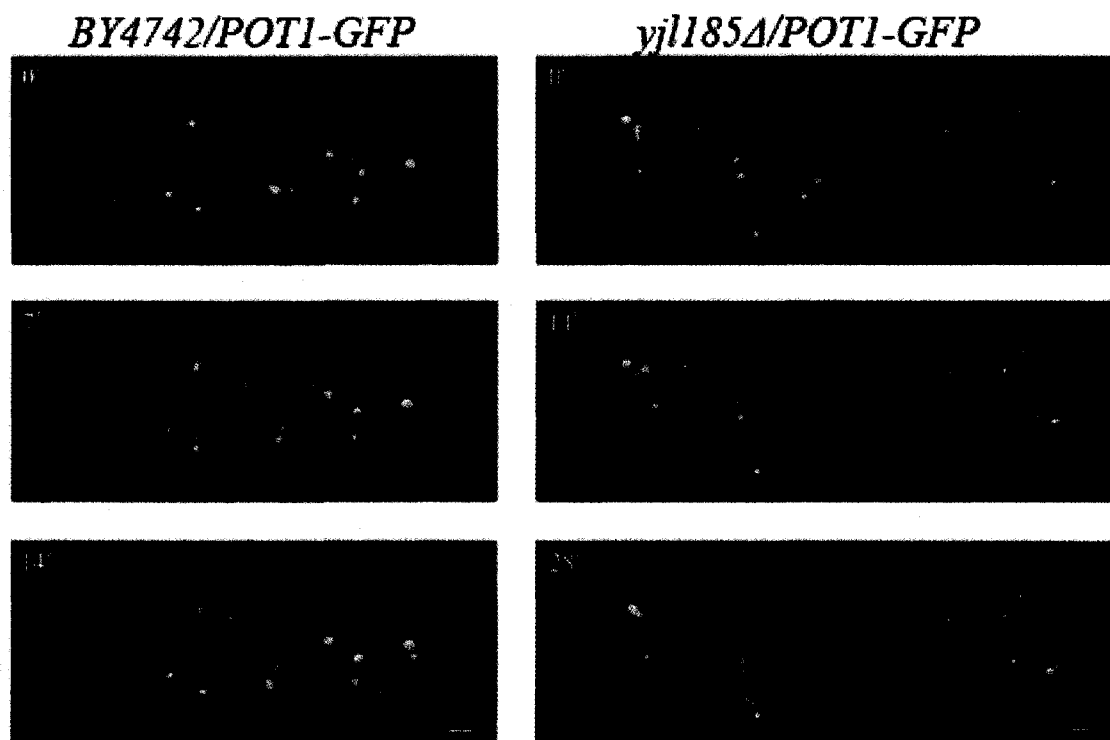
Figure 4-8. *In vivo* **video microscopy of wild-type** *BY4742* **and** *yjl185Δ* **cells.** Wild-type *BY4742* and *yjl185Δ* cells containing genomically integrated *POT1-GFP* were prepared for the *in vivo* acquisition of movies by incubation in SCIM for 16 h. Images were acquired every 20 sec for 14 min for *BY4742* cells and for 28 min for *yjl185Δ* cells. Wild-type cells have mobile as well as static peroxisomes. The peroxisomes in the *yjl185Δ* cells show some oscillatory movements but appear to stay in the same region over time. Bar, 1 μm.

deletion strain. The cells lacking any of these proteins have morphological changes in their peroxisomes and also abnormal distribution patterns. We investigated the link between the two processes by observing the ability of peroxisomes to divide in a background with greatly decreased retention. For an even more noticeable effect we induced the proliferation of peroxisomes with the multicopy plasmid YEp13 carrying and overproducing Pex11p (YEp13-*PEX11*). We used as a background *inp1ΔPOT1-GFP* cells which have decreased retention of peroxisomes and wild-type as a control. These cells were transformed with the peroxisomes-proliferating construct YEp13-*PEX11*, grown for 16 h in SCIM and then analyzed by fluorescence microscopy (Figure 4-9). The wild-type cells overexpressing *PEX11* present three morphological distinct peroxisomal populations, as described (Li and Gould, 2002): peroxisomes of regular size; long elongated peroxisomes and small peroxisomes in increased numbers. Interestingly, the minimal retention in the *inp1Δ* strain does not prevent peroxisomal proliferation and thus the peroxisomes are still able to divide and exhibit similar morphologies as in the above described wild-type cells. One can often observe a tubular peroxisome in the process of being transferred from the mother cell to the bud and obviously the characteristic mother cells lacking peroxisomes.

4.10 Discussion

4.10.1 Peroxisomal retention

Even though the existence of an anchoring mechanism of organelles has been postulated for a long time, the identification of the factors implicated or the general principles applied by these remained unknown. However, in the peroxisomal retention

BY4742/POT1-GFP
YEp13-*PEX11*

inp∆/POT1-GFP
YEp13-*PEX11*

Figure 4-9. Deficits in peroxisome retention do not prevent peroxisome division. The peroxisome-proliferating plasmid YEp13-*PEX11* was transformed into the *inp1∆* cells, a background with greatly decreased retention. The minimal retention in the *inp1∆* strain does not prevent peroxisomal proliferation to occur, and thus the peroxisomes are still able to divide and exhibit similar morphologies as in wild-type cells. Bar, 1 µm.

process we have recently made significant progress by the characterization of Inp1p,

a protein required for the retention of peroxisomes on the cell cortex. Since Inp1p was the

first identified protein directly involved in actively retaining peroxisomes we continued

our analysis by examining its binding partners.

4.10.2 Identification of Yjl185p

A very promising candidate was a protein of an unknown function encoded by the

open reading frame *YJL185c* which was shown to interact with Inp1p by the yeast two-

hybrid method (Ito et al., 2001). As we have also shown, the interaction between the two

fusion proteins appears to be highly specific because the assay shows a strong positive

interaction only when Inp1p-BD is co-expressed with Yjl185p-AD. The distribution of

fluorescently labeled peroxisomes in the deletion strain *yjl185Δ* showed an accumulation

of peroxisomes near the bud neck area of the mother cell. In addition, *in vivo* video

microscopy showed the relative immobility of these peroxisomes at the proximal region

of the mother cell. The cells having this distribution pattern with the distal region of

mother cells depleted of peroxisomes is somewhat similar to the phenotype of *inp1Δ*

cells. However, in the case of *yjl185Δ* cells the retention of peroxisomes is only

regionally affected. Specifically, Inp1p appears to be responsible for tethering

peroxisomes indiscriminately to the cell cortex whereas Yjl185p may be responsible for

distal retention of peroxisomes. Peroxisomal partitioning occurs in stages that are

synchronized with the cell division cycle and area-specific factors could modulate the

retention of peroxisomes accordingly. The release of peroxisomes from different areas of

the cell cortex for their subsequent transport to the bud might be controlled by the time-

dependent downregulation of these area-specific factors. This suggestion is supported

by the fact that *YJL185c* is a cell cycle-regulated genes in *Saccharomyces cerevisiae* as

reported recently (de Lichtenberg et al., 2005). Previous data established that proteins

directly involved in peroxisomal inheritance, Inp1p and Inp2p, are also regulated

according to different cell cycle stages peaking in G2-M. The expression of *YJL185c* also

varies in the cell cycle reaching a maximal expression in G2 which would fit the

previously observed expression pattern of Inp1p and Inp2p (de Lichtenberg et al., 2005).

Interestingly, the deletion of Yjl185p in cells overexpressing *INP1* causes a

decreased retention in the mother cell. This suggests not only that Yjl185p contributes to

the cortical immobilization of peroxisomes in the *INP1* overexpression phenotype, but

also the existence of some other retention factors that act through Inp1p.

The subcellular localization of Yjl185p is mainly peroxisomal as determined by

microscopy studies. Apparently, the amount of Yjl185p varies on peroxisomes as there

are some peroxisomes that have a very strong matching Yjl195p-GFP signal and others

that have not. Moreover, Yjl195p-GFP was also seen at the cell periphery. This was not

surprising since Yjl185p is a phosphoinositide-binding protein (Zhu et al., 2001).

Phosphoinositides are key structural and functional components of cellular membranes,

although they are present in minute amounts and often only transiently. Acting as second

messengers they regulate different biological processes, which include cellular growth,

cytoskeletal rearrangements and membrane trafficking, among others. Yjl185p binds PI-

(3, 4)/P2 which may explain the localization at the cell cortex. Another protein that binds

PI-(3, 4)/P2 is Myo4p, a type V myosin, which is required for *ASH1* mRNA anchoring at

the cell cortex (Gonsalvez et al., 2004). We next observed the localization of Yjl185p in

the deletion mutant *inp1Δ* which contain mother cells lacking peroxisomes. The peroxisomes in this strain show the typical preference for the newly formed bud and contain Yjl185p. This shows that Yjl185p is not dependent on Inp1p for its peroxisomal localization. Interestingly, the cortical localization of Yjl185p-GFP was preserved even in cells without peroxisomes.

Yeast cells require functional peroxisomes to grow in a medium containing oleic acid. To test whether the deletion strain *yjl185Δ* contains functional peroxisomes we grew these cells together with the appropriate controls on YPBO plates. The cells deleted for *YJL185c* grew much slower that the wild-type cells which suggests a degree of impairment in the biogenesis and/or function of peroxisomes in this strain.

The cortical Num1 protein, which was previously known as a nuclear migration factor, was recently showen to be involved in both mitochondrial division and segregation (Cerveny et al., 2007). The Num1 protein colocalizes on mitochondria in punctate structures with the dynamin-related Dnm1 protein. Moreover, when the mitochondrial morphology was analyzed in the single mutant *num1Δ* cells it showed striking similarities with the mitochondrial phenotype of the *dnm1Δ* cells. In these mutants the mitochondria form long tubules connected with each other that create a large mitochondrial network in the cells. The report further illustrates the effect of deleting both these genes, *NUM1* and *DNM1,* from the cells and the consequence of these deletions on mitochondria. Apart from the above described impaired mitochondrial morphology, there was a partitioning defect of mitochondria with the transfer of the mitochondrial network to the bud (Cerveny et al., 2007). The Num1 protein shares several similarities with the Yjl185 protein: it localizes to the cell cortex, it binds lipids at

the plasma membrane and its levels of expression vary in the cell cycle. Peroxisomes are also divided by a corresponding dynamin-like protein named Vps1, which resembles mitochondria. Thus, we next investigated whether double deletion of *YJL195c* and *VPS1* would have a similar effect. The peroxisomes of the mutant *yjl185Δvps1Δ* cells have abnormal morphology as well as impaired distribution between the mother cell and the bud, with all the peroxisome being transferred to the bud. Thus, the retention of peroxisomes needs the presence of both Yjl185p and Vps1p to function properly. One possible interpretation would be that the peroxisomal phenotype of *vps1Δ* and mitochondrial phenotype of *dnm1Δ* cells facilitates the otherwise subtle effect of deleting Yjl185p and Num1p, respectively.

4.10.3 The proliferation of peroxisomes does not depend on their anchoring on the cell cortex

There is increasing evidence of a connection between the division of peroxisomes and their retention. The deletion of both Inp1p and Yjl185p influences the size and number as well as the retention of peroxisomes. Furthermore, this is not an isolated case for peroxisomes, as there are proteins with a similar functional impact on other organelles. For mitochondria, these are the cortical Num1 protein and the mitochondrial outer membrane proteins (Boldogh et al., 2003; Cerveny et al., 2007). We investigated the correlation between peroxisomal division and retention by observing the ability of peroxisomes to proliferate in a background with decreased retention. Proliferation of peroxisomes was induced by overproducing Pex11p (Li and Gould, 2002), a well-known protein involved in peroxisomal division, in yeast cells deleted for Inp1p, the retention

factor for peroxisomes. Interestingly, peroxisomal proliferation with its characteristic multiple small and long tubular peroxisomes was still observed in a minimal retention background suggesting the existence of other division mechanisms not relying on the cortical anchoring of peroxisomes.

4.10.4 Concluding remarks

In conclusion, my studies present the identification of Yjl185p as a novel peroxisomal protein involved in inheritance of peroxisomes in *S. cerevisiae*. Yjl185p is a new binding partner of Inp1p and acts as an additional retention factor in the distal region of the mother cell.

CHAPTER FIVE: DISCUSSION AND SYNOPSIS

5.1 What have we added to what is known of peroxisome inheritance?

Eukaryotic cells have developed different strategies to distribute their organelles between mother cell and daughter cell so as to preserve the number of organelles in each cell after multiple rounds of cell division. Mammalian cells, which divide by fission, may ensure the accurate partitioning of their organelles by adopting a probabilistic strategy wherein organelles are dispersed more or less indiscriminately in the cytoplasm. The division of the cell into two equally sized daughter cells by the cytokinetic machinery divides organelles more or less equitably to the resultant cells. In this setting, the greater the number of a particular organelle in the cell cytoplasm, the greater the probability of its inheritance (Warren and Wickner, 1996). Nevertheless, even though the distribution of several organelles in the cytoplasm is apparently stochastic, cells rigorously regulate the dynamics and localization of all their organelles.

Mammalian cells have large numbers of peroxisomes that are uniformly distributed in the cytoplasm, which contrasts with other organelles such as the Golgi complex that are few in number or unique in the cell (Schrader et al., 2003). Observations on the regulation of peroxisome motility and distribution in mammalian cells (Schrader et al., 2003) showed that peroxisomes colocalize with the microtubule cytoskeleton (Rapp et al., 1996; Schrader et al., 2003; Wiemer et al., 1997). Furthermore, peroxisomes associate with microtubules both *in vivo* (Rapp et al., 1996; Wiemer et al., 1997; Schrader et al., 1996, 2000) and *in vitro* (Schrader et al., 1996, 2000). The use of microtubule-depolymerizing drugs in mammalian cells led to a disruption of peroxisomal motility and also to a loss of the uniform distribution of peroxisomes in the cytoplasm (Schrader et al., 2003). This suggests that a cell regulates the transport of peroxisomes to disperse them,

which is important both for the proper segregation of peroxisomes upon cell division and for their metabolic efficiency. *In vivo* time-lapse microscopy revealed that the majority of peroxisomes in mammalian cells (85-90%) display a slow local oscillatory movement. Interestingly, these peroxisomes were observed to bind to microtubules. The remaining peroxisomes (10-15%) show rapid directional movements that are dependent on the integrity of the microtubule cytoskeleton. These peroxisomes that undergo mainly unidirectional movements are able to move long distances before oscillating again (Rapp et al., 1996; Wiemer et al., 1997; Schrader et al., 2000, 2003). Apparently, the observed uniform distribution of peroxisomes in mammalian cells is preserved by local anchoring mechanisms that immobilize peroxisomes in specific areas throughout the cell. The less dynamic and thus more predictable nature of these stationary peroxisomes would ultimately ensure the accurate inheritance of these organelles.

In contrast to mammalian cells, the yeast *S. cerevisiae* divides by budding and thus has to actively and vectorially deliver its organelles to the bud. The polarized nature of cell division in *S. cerevisiae* has facilitated the analysis of organelle dynamics during cell division and has proven central to the identification of the initial molecular pathways underlying peroxisome dynamics and inheritance. Time-lapse microscopy showed that yeast peroxisomes have a characteristic dynamic behavior. Throughout the cell division cycle, peroxisomes move in several ordered stages that follow the polarity of the actin cytoskeleton. A subset of peroxisomes localizes to the presumptive bud site and is then transported to the nascent bud. Although peroxisomes in the mother cell retain fixed cortical positions, the dynamics of newly inherited peroxisomes correlate with the polarity of the actin cytoskeleton in the bud. Thus, peroxisomes cluster at the bud tip

during apical growth and are distributed over the entire bud cortex during the isotropic phase. At cytokinesis, peroxisomes localize to the mother-bud junction, consistent with a reorientation of the actin cytoskeleton for septum assembly at this stage of the cell cycle (Hoepfner et al., 2001). Peroxisome movement is dependent on the actin cytoskeleton and independent of microtubules (Hoepfner et al., 2001). Also, the dynamics of peroxisomes during the cell cycle are dependent on the actin-specific motor protein, Myo2p, because cells of a temperature-sensitive mutant strain of *MYO2* display a delay in the insertion of peroxisomes into the bud at the restrictive temperature (Hoepfner et al., 2001). This was the extent of knowledge of peroxisome dynamics and partitioning until the discovery of Inp1p.

The main feature exhibited by cells lacking Inp1p is an abnormal distribution of peroxisomes along the mother-bud axis. A large proportion of mother cells is devoid of peroxisomes, with the entire peroxisome population concentrated in the buds. Moreover, *in vivo* video microscopy of *inp1Δ* cells showed that all peroxisomes in the mother cell, displayed chaotic movements, and no peroxisomes maintained a fixed cortical position for a prolonged period of time, as was observed in wild-type cells. This lack of anchoring of peroxisomes resulted in their complete transfer to the newly formed bud, a situation never observed in wild-type cells. These results strongly suggested a role for Inp1p in the retention of peroxisomes at the cell periphery. Consistent with this role, overproduction of Inp1p caused all peroxisomes in the mother cell to maintain fixed cortical positions, thereby preventing their normal transfer to the daughter cell. Moreover, in glucose-grown cells, a condition in which cells have few peroxisomes, overproduced Inp1p-GFP, in addition to being localized to peroxisomes where it normally resides as a peripheral

membrane protein, also localized to the cell cortex. This observation showed that the peroxisomal protein Inp1p has an intrinsic affinity for structures lining the cell periphery. It is therefore likely that Inp1p attaches peroxisomes to an as of yet unidentified cortical anchor. In wild-type cells, the immobilization of peroxisomes at the cell cortex is also observed in the bud before cytokinesis occurs. This process probably prepares the bud for the ensuing cell cycle, when again about half of the peroxisomes need to be retained. Inp1p most probably plays a role in this process, as judged by the high frequency of peroxisomes that aberrantly return to the mother cell in cells lacking Inp1p. To summarize, Inp1p acts as a peroxisome-retention factor, tethering peroxisomes to anchoring structures within the mother cell and bud.

The screening of a yeast haploid deletion library to identify strains compromised in peroxisome inheritance led to the identification of Inp2p, the receptor for Myo2p on peroxisomes (Fagarasanu et al., 2006a). Inp2p is a peroxisomal membrane protein that interacts with the globular tail of Myo2p, as shown by both yeast two-hybrid analysis and *in vitro* binding. Thus, Inp2p directly binds to the Myo2p cargo binding domain. Peroxisomes in cells lacking Inp2p fail to be correctly partitioned to daughter cells, often resulting in mother cells retaining the entire complement of peroxisomes. Also, the overall velocities of peroxisomes in cells lacking Inp2p are decreased, and the movements displayed by peroxisomes are chaotic, as opposed to the fast, bud-directed vectorial movements of peroxisomes observed in wild-type cells. The levels of Inp2p oscillate with the cell cycle in a pattern that parallels the peroxisome dynamics observed in wild-type cells. Inp2p is not present in equal amounts on all peroxisomes but is found preferentially enriched in those peroxisomes that display Myo2p-dependent targeting, *i.e.*

peroxisomes that are present at sites of polarized growth. Moreover, upon overproduction of Inp2p, the entire peroxisome population accumulates at the sites of polarized growth, thereby depleting mother cells of peroxisomes. The specificity of Inp2p for peroxisome inheritance was shown by the observation that other organelles are segregated normally in cells either lacking or overproducing Inp2p. This showed that lack of Inp2p does not perturb peroxisome inheritance by grossly affecting cell polarity or disrupting the acto-myosin system. Thus, Inp2p is the peroxisomal receptor for Myo2p that binds peroxisomes to the transport machinery to ensure their proper transport to the growing bud.

Recent studies in the dimorphic yeast *Y. lipolytica* showed that peroxisome motility is dependent on the actin cytoskeleton in this organism and shows a strong similarity to peroxisome movement in *S. cerevisiae* (Chang et al., 2007). In nondividing *Y. lipolytica* cells, most peroxisomes maintain stable positions at the cell cortex. As the cells divide, approximately half of these static peroxisomes are removed from their previous positions and transferred to the emerging bud. Although the number of peroxisomes in *Y. lipolytica* is much greater than that observed in *S. cerevisiae*, peroxisomes in *Y. lipolytica* still undergo the characteristic cell cycle-dependent movements of peroxisomes seen in *S. cerevisiae*. Screening a database of all encoded *Y. lipolytica* proteins led to the identification of a protein encoded by the open reading frame YALI0F31229g that showed a significant sequence similarity to Inp1p. The involvement of this protein in peroxisome inheritance further justified its designation as *Yl*Inp1p (*Y. lipolytica* Inp1p). Mother cells lacking *Yl*Inp1p retain a small fraction of the peroxisome population, with most peroxisomes being transferred to the new bud. In contrast, mother

cells overexpressing *Yl*Inp1p are filled with peroxisomes, while the buds are empty.

Taken together, these data demonstrate that *Yl*Inp1p functions in peroxisome retention, similarly to Inp1p in *S. cerevisiae*. Furthermore, Inp1p seems to be conserved in numerous other fungi, including *Kluyveromyces lactis, Candida glabrata* and *Eremothecium gossypii*. It remains to be determined whether these potential Inp1 proteins play a similar role in peroxisome retention in these organisms.

Two-hybrid analysis revealed a new interaction partner of Inp1p, namely the protein encoded by the open reading frame *YJL185c*. Cells deleted for *YJL185c* showed a gathering of peroxisomes near the bud neck region, leaving the distal region of mother cells devoid of peroxisomes. While the distribution of the peroxisomes in *yjl185Δ* cells is somewhat similar to the distribution of peroxisomes in *inp1Δ* cells, the extent of the defect in peroxisome retention is different in the two deletion strains. The lack of Yjl185p affects the distribution of peroxisomes at the distal part of the mother cell, while the lack of Inp1p affects peroxisome retention along the entire cell cortex. Microscopy studies showed Yjl185p to be mostly peroxisomal, with small amounts at the cell periphery. The lipid-binding properties of Yjl185p may explain its localization at the cell cortex. Interestingly, deletion of Yjl185p affects the distribution, as well as the morphology, of peroxisomes, similarly to the deletion of *INP1*. These observations led to the speculation of a possible connection between peroxisome division and retention. We followed this idea by observing the ability of peroxisomes to proliferate in a background of cells exhibiting decreased retention of peroxisomes. We observed that peroxisomes are still able to proliferate in a background of decreased peroxisome retention, indicating the presence in the cytoplasm of division factors that function independently of cortically

anchored peroxisomes. In conclusion, Yjl185p is a novel peroxisomal protein involved in the inheritance of peroxisomes in *S. cerevisiae* that binds Inp1p and acts as an additional factor in the retention of peroxisomes in the mother cell at a region distal to the site of bud emergence.

Our current views of peroxisome inheritance in *S. cerevisiae* and the proteins involved in this process are shown in Figure 5-1. Because of its predicted role in peroxisome inheritance we suggest renaming the protein Yjl185p as Inp3p.

Peroxisome inheritance in *S. cerevisiae* is a well ordered and tightly regulated process consisting of three individual events that overlap in part in time: (1) the retention of a subset of peroxisomes by the mother cell, (2) the ordered movement of the remaining peroxisomes to the forming bud and (3) the retention of the transferred peroxisomes within the bud. Precise control of these three events is crucial to the proper distribution of peroxisomes to a budded cell. A stochastic segregation of peroxisomes in a cell that divides by budding would be a very ineffective process. That this would be the case can be seen from cells deleted for both *INP1* and *INP2*, in which peroxisomes are left without any means of anchoring to the cell cortex or any possibility of attaching to the translocation machinery, resulting in a random distribution of peroxisomes between mother cell and bud. As expected, *inp1Δ/inp2Δ* cells exhibit a significant number of buds devoid of peroxisomes (Fagarasanu et al., 2006a).
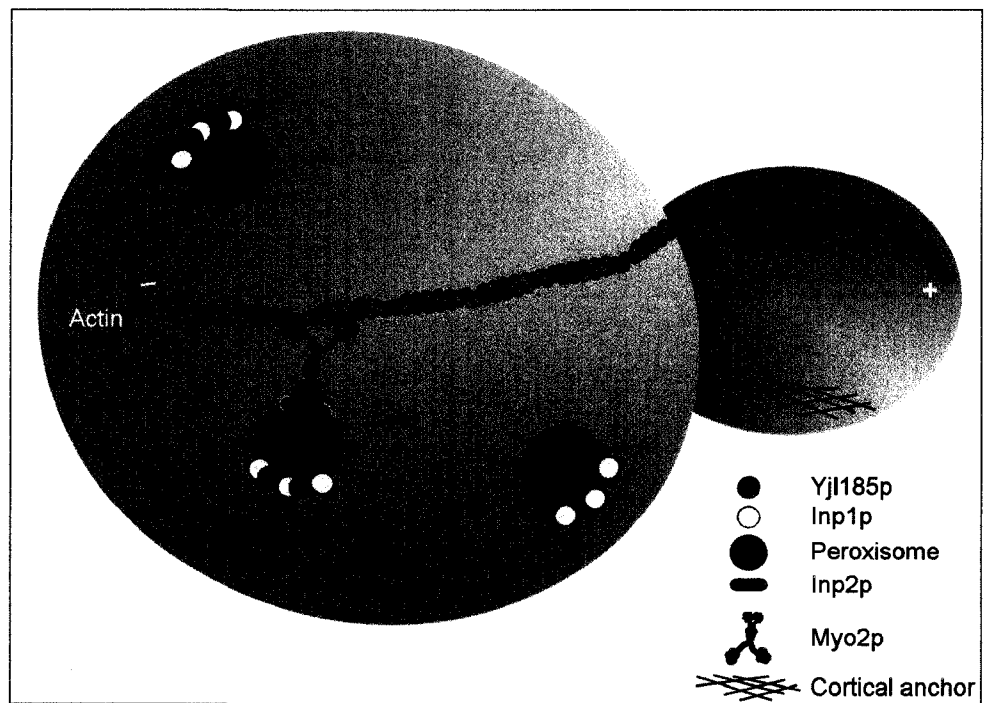
Figure 5-1. A view of peroxisome inheritance in the budding yeast *Saccharomyces cerevisiae.*

5.2 Future directions

Several important questions regarding peroxisome inheritance and dynamics in *S. cerevisiae* remain to be answered, including:

1. What is the nature of the cortical anchor to which peroxisomes attach? Is the cortically localized fraction of Inp3p a part of this anchor?

2. Does Inp1p or Inp3p associate with different protein complexes to function in the division and retention of peroxisomes?

3. Organelle inheritance and cell cycle events need to be coordinated. How is this coordination established and maintained? What is the nature of the interplay between Inp1p and Inp3p? What advantage is the oscillation of Inp1p during the cell cycle? What is the degradation machinery responsible for the turnover of Inp1p and Inp2p, and how is it regulated? Is the degradation of Inp1p and Inp2p linked to progression through the cell cycle, or is it regulated by partitioning peroxisomes between mother cell and bud? Is Inp1p loaded evenly onto different peroxisomes? Are the functions of Inp1p and Inp3p regulated by posttranslational processes like phosphorylation, or do their synthesis and turnover alone regulate their activities?

Research into peroxisome inheritance has experienced significant progress in the last few years by the identification and characterization of three peroxisomal proteins, Inp1p, Inp2p and Inp3p, involved in peroxisome inheritance. However, we have only observed the tip of the molecular iceberg of peroxisome inheritance, and the future holds the prospect of the identification of a number of additional cellular factors and processes that combine to produce the molecular symphony that is peroxisome inheritance.

CHAPTER SIX: REFERENCES

Adames, N. R., J. R. Oberle, and J. A. Cooper. 2001. The surveillance mechanism of the spindle position checkpoint in yeast. *J. Cell Biol.* 153:159-168.

Altmann, K., M. Frank, D. Neumann, S. Jakobs, and B. Westermann. 2008. The class V myosin motor protein, Myo2, plays a major role in mitochondrial motility in *Saccharomyces cerevisiae. J. Cell Biol.* 181:119-130.

Altmann, K., and B. Westermann. 2005. Role of essential genes in mitochondrial morphogenesis in *Saccharomyces cerevisiae. Mol. Biol. Cell* 16:5410-5417.

Ausubel, F. J., R. Brent, R. E. Kingston, D. D. Moore, J. G. Seidman, J. A. Smith, and K. Struhl. 1989. Current Protocols in Molecular Biology. Greene Publishing Associates, New York, NY.

Boldogh, I. R., K. L. Fehrenbacher, H. C. Yang, and L. A. Pon. 2005. Mitochondrial movement and inheritance in budding yeast. *Gene* 354:28-36.

Boldogh, I. R., D. W. Nowakowski, H. C. Yang, H. Chung, S. Karmon, P. Royes, and L.A. Pon. 2003. A protein complex containing Mdm10p, Mdm12p, and Mmm1p links mitochondrial membranes and DNA to the cytoskeleton-based segregation machinery. *Mol. Biol. Cell* 14:4618-4627.

Boldogh, I. R., and L. A. Pon. 2006. Interactions of mitochondria with the actin cytoskeleton. *Biochim. Biophys. Acta* 1763:450-462.

Boldogh, I. R., S. L. Ramcharan, H. C. Yang, and L. A. Pon. 2004. A type V myosin (Myo2p) and a Rab-like G-protein (Ypt11p) are required for retention of newly inherited mitochondria in yeast cells during cell division. *Mol. Biol. Cell* 15:3994-4002.

Boldogh, I. R., H. C. Yang, and L. A. Pon. 2001. Mitochondrial inheritance in budding yeast. *Traffic* 2:368-374.

Brade, A. M. Peroxisome Assembly in *Yarrowia lipolytica*. 1992. M.Sc. Thesis, McMaster University, Hamilton, Ontario, Canada.

Bradford, M. M. 1976. A rapid and sensitive method for the quantitation of microgram quantities of protein utilizing the principle of protein-dye binding. *Anal. Biochem.* 72:248-254.

Catlett, N. L., J. E. Duex, F. Tang, and L. S. Weisman. 2000. Two distinct regions in a yeast myosin-V tail domain are required for the movement of different cargoes. *J. Cell Biol.* 150:513-526.

Cerveny, K. L., S. L. Studer, R. E. Jensen, and H. Sesaki. 2007a. Yeast mitochondrial division and distribution require the cortical Num1 protein. *Dev. Cell* 12:363-375.

Chang, J., A. Fagarasanu, and R. A. Rachubinski. 2007. Peroxisomal peripheral membrane protein Yllnp1p is required for peroxisome inheritance and influences the dimorphic transition in the yeast *Yarrowia lipolytica. Eukaryot. Cell* 6:1528-1537.

Conradt, B., J.Shaw, T.Vida, S.Emr, and W.Wickner. 1992. In vitro reactions of vacuole inheritance in *Saccharomyces cerevisiae. J. Cell Biol.* 119:1469-1479.

de Lichtenberg, U., R. Wernersson, T. S. Jensen, H. B. Nielsen, A. Fausboll, P. Schmidt, F. B. Hansen, S. Knudsen, and S. Brunak. 2005. New weakly expressed cell cycle-regulated genes in yeast. *Yeast* 22:1191-1201.

DeMarini, D. J., A. E. Adams, H. Fares, V. C. De, G. Valle, J. S. Chuang, and J. R. Pringle. 1997. A septin-based hierarchy of proteins required for localized deposition of chitin in the *Saccharomyces cerevisiae* cell wall. *J. Cell Biol.* 139:75-93.

Drubin, D. G., H. D. Jones, and K. F. Wertman. 1993. Actin structure and function: roles in mitochondrial organization and morphogenesis in budding yeast and identification of the phalloidin-binding site. *Mol. Biol. Cell* 4:1277-1294.

Eitzen, G. A., R. K. Szilard, and R. A. Rachubinki. 1997. Enlarged peroxisomes are present in oleic acid-grown *Yarrowia lipolytica* overexpressing the *PEX16* gene

encoding an intraperoxisomal peripheral membrane peroxin. *J. Cell Biol.* 137:1265-1278.

Erdmann, R., and G. Blobel. 1995a. Giant peroxisomes in oleic acid-induced *Saccharomyces cerevisiae* lacking the peroxisomal membrane protein Pmp27p. *J. Cell Biol.* 128:509-523.

Faber, K. N., J. A. Heyman, and S. Subramani. 1998. Two AAA family peroxins, PpPex1p and PpPex6p, interact with each other in an ATP-dependent manner and are associated with different subcellular membranous structures distinct from peroxisomes. *Mol. Cell Biol.* 18:936-943.

Fagarasanu, A., M. Fagarasanu, G. A. Eitzen, J. D. Aitchison, and R. A. Rachubinski. 2006a. The peroxisomal membrane protein Inp2p is the peroxisome-specific receptor for the myosin V motor Myo2p of *Saccharomyces cerevisiae. Dev. Cell* 10:587-600.

Fagarasanu, A., M. Fagarasanu, and R. A. Rachubinski. 2007. Maintaining peroxisome populations: a story of division and inheritance. *Annu. Rev. Cell Dev. Biol.* 23:321-344.

Fagarasanu, A., and R. A. Rachubinski. 2007. Orchestrating organelle inheritance in *Saccharomyces cerevisiae. Curr. Opin. Microbiol.* 10:528-538.

Fagarasanu, M., A. Fagarasanu, Y. Y. C. Tam, J. D. Aitchison, and R. A. Rachubinski. 2005. Inp1p is a peroxisomal membrane protein required for peroxisome inheritance in *Saccharomyces cerevisiae. J. Cell Biol.* 169:765-775.

Fagarasanu, M., A. Fagarasanu and R. A. Rachubinski. 2006b. Sharing the wealth: Peroxisome inheritance in budding yeast. *Biochim. Biophys. Acta* 1763:1669–77.

Fehrenbacher, K. L., I. R. Boldogh, and L. A. Pon. 2003. Taking the A-train: actin-based force generators and organelle targeting. *Trends Cell Biol.* 13:472-477.

Fehrenbacher, K. L., H. C. Yang, A. C. Gay, T. M. Huckaba, and L. A. Pon. 2004. Live cell imaging of mitochondrial movement along actin cables in budding yeast. *Curr. Biol.* 14:1996-2004.

Frederick, R. L., J. M. McCaffery, K. W. Cunningham, K. Okamoto, and J. M. Shaw. 2004. Yeast Miro GTPase, Gem1p, regulates mitochondrial morphology via a novel pathway. *J. Cell Biol.* 167:87-98.

Frederick, R. L., K. Okamoto, and J. M. Shaw. 2008. Multiple pathways influence mitochondrial inheritance in budding yeast. *Genetics* 178:825-837.

Frederick, R. L., and J. M. Shaw. 2007. Moving mitochondria: establishing distribution of an essential organelle. *Traffic.* 8:1668-1675.

Fujiki, Y., A. L. Hubbard, S. Fowler, and P. B. Lazarow. 1982. Isolation of intracellular membranes by means of sodium carbonate treatment: application to endoplasmic reticulum. *J. Cell Biol.* 93:97-102.

Geuze, H. J., J. L. Murk, A. K. Stroobants, J. M. Griffith, M. J. Kleijmeer, A. J. Koster, A. J. Verkleij, B. Distel, and H. F. Tabak. 2003. Involvement of the endoplasmic reticulum in peroxisome formation. *Mol. Biol. Cell* 14:2900-2907.

Ghaemmaghami, S., W. K. Huh, K. Bower, R. W. Howson, A. Belle, N. Dephoure, E. K. O'Shea, and J. S. Weissman. 2003. Global analysis of protein expression in yeast. *Nature* 425:737-741.

Giaever, G., A. M. Chu, L. Ni, C. Connelly, L. Riles, S. Veronneau, S. Dow, A. Lucau-Danila, K. Anderson, B. Andre, A. P. Arkin, A. Astromoff, M. El-Bakkoury, R. Bangham, R. Benito, S. Brachat, S. Campanaro, M. Curtiss, K. Davis, A. Deutschbauer, K. D. Entian, P. Flaherty, F. Foury, D. J. Garfinkel, M. Gerstein, D. Gotte, U. Güldener, J. H. Hegemann, S. Hempel, Z. Herman, D. F. Jaramillo, D. E. Kelly, S. L. Kelly, P. Kotter, D. LaBonte, D. C. Lamb, N. Lan, H. Liang, H. Liao, L. Liu, C. Luo, M. Lussier, R. Mao, P. Menard, S. L. Ooi, J. L. Revuelta, C. J. Roberts, M. Rose, P. Ross-Macdonald, B. Scherens, G. Schimmack, B. Shafer, D. D. Shoemaker, S. Sookhai-Mahadeo, R. K. Storms, J. N. Strathern, G. Valle, M. Voet, G. Volckaert, C. Y. Wang, T. R. Ward, J. Wilhelmy, E. A. Winzeler, Y. Yang, G. Yen, E. Youngman, K. Yu, H. Bussey, J. D. Boeke, M. Snyder, P.

Philippsen, R. W. Davis, and M. Johnston. 2002. Functional profiling of the *Saccharomyces cerevisiae* genome. *Nature* 418:387-391.

Gietz, R. D., and R. A. Woods. 2002. Transformation of yeast by lithium acetate/single-stranded carrier DNA/polyethylene glycol method. Methods Enzymol. 350:87-96.

Gomes de Mesquita, D. S., H. R. ten Hoopen, and C. L. Woldringh. 1991. Vacuolar segregation to the bud of *Saccharomyces cerevisiae*: an analysis of morphology and timing in the cell cycle. *J. Gen. Microbiol.* 137:2447-2454.

Gonsalvez, G. B., J. L. Little, and R. M. Long. 2004. ASH1 mRNA anchoring requires reorganization of the Myo4p-She3p-She2p transport complex. *J. Biol. Chem.* 279:46286-46294.

Hammond, A. T., and B. S. Glick. 2000. Raising the speed limits for 4D fluorescence microscopy. *Traffic* 1:935-940.

Hill, K. L., N. L. Catlett, and L. S. Weisman. 1996. Actin and myosin function in directed vacuole movement during cell division in *Saccharomyces cerevisiae*. *J. Cell Biol.* 135:1535-1549.

Hoepfner, D., D. Schildknegt, I. Braakman, P. Philippsen, and H. F. Tabak. 2005. Contribution of the endoplasmic reticulum to peroxisome formation. *Cell* 122:85-95.

Hoepfner, D., B. M. van den Berg, P. Philippsen, H. F. Tabak, and E. H. Hettema. 2001. A role for Vps1p, actin, and the Myo2p motor in peroxisome abundance and inheritance in *Saccharomyces cerevisiae*. *J. Cell Biol.* 155:979-990.

Hollenbeck, P. J., and W. M. Saxton. 2005. The axonal transport of mitochondria. *J. Cell Sci.* 118:5411-5419.

Hoppins, S., L. Lackner, and J. Nunnari. 2007. The machines that divide and fuse mitochondria. *Annu. Rev. Biochem.* 76:751-780.

Huckaba, T. M., A. C. Gay, L. F. Pantalena, H. C. Yang, and L. A. Pon. 2004. Live cell imaging of the assembly, disassembly, and actin cable-dependent movement of endosomes and actin patches in the budding yeast, *Saccharomyces cerevisiae*. *J. Cell Biol.* 167:519-530.

Huh, W. K., J. V. Falvo, L. C. Gerke, A. S. Carroll, R. W. Howson, J. S. Weissman, and E. K. O'Shea. 2003. Global analysis of protein localization in budding yeast. *Nature* 425:686-691.

Huynh, T. V., R. A. Young, and R. W. Davis. 1985. DNA Cloning: A Practical Approach. IRL Press, Oxford.

Innis, M. A., and D. H. Gelfand. 1990. Optimization of PCRs. In PCR Protocols: A Guide to Methods and Applications. M. A. Innis, D. H. Gelfand, J. J. Sninsky, and T. J. White, editors. Academic Press, San Diego, pp. 3-12.

Ishikawa, K., N. L. Catlett, J. L. Novak, F. Tang, J. J. Nau, and L. S. Weisman. 2003. Identification of an organelle-specific myosin V receptor. *J. Cell Biol.* 160:887-897.

Ito, T., T. Chiba, R. Ozawa, M. Yoshida, M. Hattori, and Y. Sakaki. 2001. A comprehensive two-hybrid analysis to explore the yeast protein interactome. *Proc. Natl. Acad. Sci. U. S. A* 98:4569-4574.

Itoh, T., A. Watabe, E. Toh, and Y. Matsui. 2002. Complex formation with Ypt11p, a Rab-type small GTPase, is essential to facilitate the function of Myo2p, a class V myosin, in mitochondrial distribution in *Saccharomyces cerevisiae. Mol. Cell Biol.* 22:7744-7757.

Kaksonen, M., Y. Sun, and D. G. Drubin. 2003. A pathway for association of receptors, adaptors, and actin during endocytic internalization. *Cell* 115:475-487.

Kim, P. K., R. T. Mullen, U. Schumann, and J. Lippincott-Schwartz. 2006. The origin and maintenance of mammalian peroxisomes involves a de novo PEX16-dependent pathway from the ER. *J. Cell Biol.* 173:521-532.

Koch, A., G. Schneider, G. H. Luers, and M. Schrader. 2004. Peroxisome elongation and constriction but not fission can occur independently of dynamin-like protein 1. *J. Cell Sci.* 117:3995-4006.

Koch, A., M. Thiemann, M. Grabenbauer, Y. Yoon, M. A. McNiven, and M. Schrader. 2003. Dynamin-like protein 1 is involved in peroxisomal fission. *J. Biol. Chem.* 278:8597-8605.

Kuravi, K., S. Nagotu, A. M. Krikken, K. Sjollema, M. Deckers, R. Erdmann, M. Veenhuis, and I. J. van der Klei. 2006. Dynamin-related proteins Vps1p and Dnm1p control peroxisome abundance in *Saccharomyces cerevisiae*. *J. Cell Sci.* 119:3994-4001.

Li, X., and S. J. Gould. 2002. PEX11 promotes peroxisome division independently of peroxisome metabolism. *J. Cell Biol.* 156:643-651.

Li, X., and S. J. Gould. 2003. The dynamin-like GTPase DLP1 is essential for peroxisome division and is recruited to peroxisomes in part by PEX11. *J. Biol. Chem.* 278:17012-17020.

Long, R. M., R. H. Singer, X. Meng, I. Gonzalez, K. Nasmyth, and R. P. Jansen. 1997. Mating type switching in yeast controlled by asymmetric localization of ASH1 mRNA. *Science* 277:383-387.

Maniatis, T., E. F. Fritsch, and J. Sambrook. 1982. Molecular Cloning: A Laboratory Manual. Cold Spring Harbor Laboratory, Cold Spring Harbor.

Marshall, P. A., Y. I. Krimkevich, R. H. Lark, J. M. Dyer, M. Veenhuis, and J. M. Goodman. 1995. Pmp27 promotes peroxisomal proliferation. *J. Cell Biol.* 129:345-355.

McMahon, H. T., and J. L. Gallop. 2005. Membrane curvature and mechanisms of dynamic cell membrane remodelling. *Nature* 438:590-596.

Moseley, J. B., and B. L. Goode. 2006. The yeast actin cytoskeleton: from cellular function to biochemical mechanism. *Microbiol. Mol. Biol. Rev.* 70:605-645.

Motley, A. M., and E. H. Hettema. 2007. Yeast peroxisomes multiply by growth and division. *J. Cell Biol.* 178:399-410.

Needleman, R. B., and A. Tzagoloff. 1975. Breakage of yeast: a method for processing multiple samples. *Anal. Biochem.* 64:545-549.

Pashkova, N., N. L. Catlett, J. L. Novak, and L. S. Weisman. 2005. A point mutation in the cargo-binding domain of myosin V affects its interaction with multiple cargoes. *Eukaryot. Cell* 4:787-798.

Pashkova, N., Y. Jin, S. Ramaswamy, and L. S. Weisman. 2006. Structural basis for myosin V discrimination between distinct cargoes. *EMBO J.* 25:693-700.

Praefcke, G. J., and H. T. McMahon. 2004. The dynamin superfamily: universal membrane tubulation and fission molecules? *Nat. Rev. Mol. Cell Biol.* 5:133-147.

Pringle, J. R., A. E. Adams, D. G. Drubin, and B. K. Haarer. 1991. Immunofluorescence methods for yeast. *Methods Enzymol.* 194:565-602.

Pruyne, D., and A. Bretscher. 2000. Polarization of cell growth in yeast. *J. Cell Sci.* 113:571-585.

Pruyne, D. W., D. H. Schott, and A. Bretscher. 1998. Tropomyosin-containing actin cables direct the Myo2p-dependent polarized delivery of secretory vesicles in budding yeast. *J. Cell Biol.* 143:1931-1945.

Purdue, P. E., and P. B. Lazarow. 2001. Peroxisome biogenesis. *Annu. Rev. Cell Dev. Biol.* 17:701-752.

Rapp, S., R. Saffrich, M. Anton, U. Jakle, W. Ansorge, K. Gorgas, and W. W. Just. 1996a. Microtubule-based peroxisome movement. *J. Cell Sci.* 109:837-849.

Rapp, S., R. Saffrich, U. Jakle, W. Ansorge, K. Gorgas, and W. W. Just. 1996b. Microtubule-mediated peroxisomal saltations. *Ann. N. Y. Acad. Sci.* 804:666-668.

Raymond, C. K., P. J. O'Hara, G. Eichinger, J. H. Rothman, and T. H. Stevens. 1990. Molecular analysis of the yeast VPS3 gene and the role of its product in vacuolar protein sorting and vacuolar segregation during the cell cycle. *J. Cell Biol.* 111:877-892.

Rhodin, J. Correlation of ultrastructural organization and function in normal and experimentally changed convoluted tubule cells of the mouse kidney. 1954. Ph.D. Thesis, Karolinska Institutet Stockholm, Stockholm.

Rose, M. D., F. Winston, and P. Heiter. 1988. Laboratory Course Manual for Methods in Yeast Genetics. Cold Spring Harbor Laboratory, Cold Spring Harbor.

Rossanese, O. W., and B. S. Glick. 2001. Deconstructing Golgi inheritance. *Traffic* 2:589-596.

Rossanese, O. W., C. A. Reinke, B. J. Bevis, A. T. Hammond, I. B. Sears, J. O'Connor, and B. S. Glick. 2001. A role for actin, Cdc1p, and Myo2p in the inheritance of late Golgi elements in *Saccharomyces cerevisiae. J. Cell Biol.* 153:47-62.

Rottensteiner, H., K. Stein, E. Sonnenhol, and R. Erdmann. 2003. Conserved function of Pex11p and the novel Pex25p and Pex27p in peroxisome biogenesis. *Mol. Biol. Cell* 14:4316-4328.

Saiki, R. K. 1990. Amplification of genomic DNA. In: PCR Protocols: A Guide to Methods and Applications. M. A. Innis, D. H. Gelfand, J. J. Sninsky, and T. J. White, editors. Academic Press, San Diego. pp. 13-21.

Sakai, Y., H. Yurimoto, H. Matsuo, and N. Kato. 1998. Regulation of peroxisomal proteins and organelle proliferation by multiple carbon sources in the methylotrophic yeast, *Candida boidinii*. *Yeast* 14:1175-1187.

Sanger, F., S. Nicklen, and A. R. Coulson. 1977. DNA sequencing with chain-terminating inhibitors. *Proc. Natl. Acad. Sci. U. S. A* 74:5463-5467.

Schott, D., J. Ho, D. Pruyne, and A. Bretscher. 1999. The COOH-terminal domain of Myo2p, a yeast myosin V, has a direct role in secretory vesicle targeting. *J. Cell Biol.* 147:791-808.

Schrader, M., and H. D. Fahimi. 2006. Growth and division of peroxisomes. *Int. Rev. Cytol.* 255:237-290.

Schrader, M., and H. D. Fahimi. 2008. The peroxisome: still a mysterious organelle. *Histochem. Cell Biol.*

Schrader, M., J. K. Burkhardt, E. Baumgart, G. Luers, A.Volkl, and H. D. Fahimi. 1996. The importance of microtubules in determination of shape and intracellular distribution of peroxisomes. *Ann. N. Y. Acad. Sci.* 804:669-671.

Schrader, M., S .J. King, T. A. Stroh, and T. A. Schroer. 2000. Real time imaging reveals a peroxisomal reticulum in living cells. *J. Cell Sci.* 113:3663-3671.

Schrader, M., B. E. Reuber, J. C. Morrell, G. Jimenez-Sanchez, C. Obie, T. A. Stroh, D. Valle, T. A. Schroer, and S. J. Gould. 1998. Expression of *PEX11β* mediates peroxisome proliferation in the absence of extracellular stimuli. *J. Biol. Chem.* 273:29607-29614.

Schrader, M., M. Thiemann, and H. D. Fahimi. 2003. Peroxisomal motility and interaction with microtubules. *Microsc. Res. Tech.* 61:171-178.

Sesaki, H., and R. E. Jensen. 1999. Division versus fusion: Dnm1p and Fzo1p antagonistically regulate mitochondrial shape. *J. Cell Biol.* 147:699-706.

Simon, V. R., S. L. Karmon, and L. A. Pon. 1997. Mitochondrial inheritance: cell cycle and actin cable dependence of polarized mitochondrial movements in *Saccharomyces cerevisiae. Cell Motil. Cytoskeleton* 37:199-210.

Smith, J. J., M. Marelli, R. H. Christmas, F. J. Vizeacoumar, D. J. Dilworth, T. Ideker, T. Galitski, K. Dimitrov, R. A. Rachubinski, and J. D. Aitchison. 2002.

Transcriptome profiling to identify genes involved in peroxisome assembly and function. *J. Cell Biol.* 158:259-271.

Smith J. J., Brown T. W., Eitzen G. A., Rachubinski R. A. 2000. Regulation of peroxisome size and number by fatty acid beta-oxidation in the yeast *Yarrowia lipolytica.*

Steinberg, S. J., G. Dodt, G. V. Raymond, N. E. Braverman, A. B. Moser, and H. W. Moser. 2006. Peroxisome biogenesis disorders. *Biochim. Biophys. Acta* 1763:1733-1748.

Szilard, R. K., and R. A. Rachubinki. 2000. Tetratricopeptide repeat domain of *Yarrowia lipolytica* Pex5p is essential for recognition of the type 1 peroxisomal targeting signal but does not confer full biological activity on Pex5p. Biochem. J. 346:177-184.

Takizawa, P. A., A. Sil, J. R. Swedlow, I. Herskowitz, and R. D. Vale. 1997. Actin-dependent localization of an RNA encoding a cell-fate determinant in yeast. *Nature* 389:90-93.

Tam, Y. Y. C., A. Fagarasanu, M. Fagarasanu, and R. A.Rachubinski. 2005. Pex3p initiates the formation of a preperoxisomal compartment from a subdomain of the

endoplasmic reticulum in *Saccharomyces cerevisiae*. *J. Biol. Chem.* 280:34933-34939.

Tam, Y. Y. C., J. C. Torres-Guzman, F. J. Vizeacoumar, J. J. Smith, M. Marelli, J. D. Aitchison, and R. A. Rachubinski. 2003. Pex11-related proteins in peroxisome dynamics: a role for the novel peroxin Pex27p in controlling peroxisome size and number in *Saccharomyces cerevisiae*. *Mol. Biol. Cell* 14:4089-4102.

Tang, F., E. J. Kauffman, J. L. Novak, J. J. Nau, N. L. Catlett, and L. S. Weisman. 2003. Regulated degradation of a class V myosin receptor directs movement of the yeast vacuole. *Nature* 422:87-92.

Thoms, S., and R. Erdmann. 2005. Dynamin-related proteins and Pex11 proteins in peroxisome division and proliferation. *FEBS J.* 272:5169-5181.

Titorenko, V. I., H. Chan, and R. A. Rachubinski. 2000. Fusion of small peroxisomal vesicles in vitro reconstructs an early step in the in vivo multistep peroxisome assembly pathway of *Yarrowia lipolytica*. *J. Cell Biol.* 148:29-44.

Titorenko, V. I., D. M. Ogrydziak, and R. A. Rachubinski. 1997. Four distinct secretory pathways serve protein secretion, cell surface growth, and peroxisome biogenesis in the yeast *Yarrowia lipolytica*. *Mol. Cell Biol.* 17:5210-5226.

Titorenko, V. I., and R. A. Rachubinski. 1998. The endoplasmic reticulum plays an essential role in peroxisome biogenesis. *Trends Biochem. Sci.* 23:231-233.

Titorenko, V. I. and R. A. Rachubinski. 2001. Dynamics of peroxisome assembly and function. *Trends Cell Biol.* 11:22-29.

Towbin, H., T. Staehelin, and J. Gordon. 1979. Electrophoretic transfer of proteins from polyacrylamide gels to nitrocellulose sheets: procedure and some applications. *Proc. Natl. Acad. Sci. U. S. A.* 76:4350-4354.

van der Klei, I. J., and M. Veenhuis. 2006. Yeast and filamentous fungi as model organisms in microbody research. *Biochim. Biophys. Acta* 1763:1364-1373.

Vizeacoumar, F. J., J. C. Torres-Guzman, D. Bouard, J. D. Aitchison, and R. A. Rachubinski. 2004. Pex30p, Pex31p, and Pex32p form a family of peroxisomal integral membrane proteins regulating peroxisome size and number in *Saccharomyces cerevisiae. Mol. Biol. Cell* 15:665-677.

Vizeacoumar, F. J., J. C. Torres-Guzman, Y. Y. C. Tam, J. D. Aitchison, and R. A. Rachubinski. 2003. *YHR150w* and *YDR479c* encode peroxisomal integral membrane proteins involved in the regulation of peroxisome number, size, and distribution in *Saccharomyces cerevisiae. J. Cell Biol.* 161:321-332.

Wang, Y. X., N. L. Catlett, and L. S. Weisman. 1998. Vac8p, a vacuolar protein with armadillo repeats, functions in both vacuole inheritance and protein targeting from the cytoplasm to vacuole. *J. Cell Biol.* 140:1063-1074.

Warren, G., and W. Wickner. 1996. Organelle inheritance. *Cell* 84:395-400.

Weisman, L. S. 2003. Yeast vacuole inheritance and dynamics. *Annu. Rev. Genet.* 37:435-460.

Weisman, L. S. 2006. Organelles on the move: insights from yeast vacuole inheritance. *Nat. Rev. Mol. Cell Biol.* 7:243-252.

Wickner, W., and A. Haas. 2000. Yeast homotypic vacuole fusion: a window on organelle trafficking mechanisms. *Annu. Rev. Biochem.* 69:247-275.

Wiemer, E. A., T. Wenzel, T. J. Deerinck, M. H. Ellisman, and S. Subramani. 1997. Visualization of the peroxisomal compartment in living mammalian cells: dynamic behavior and association with microtubules. *J. Cell Biol.* 136:71-80.

Yan, M., N. Rayapuram, and S. Subramani. 2005. The control of peroxisome number and size during division and proliferation. *Curr. Opin. Cell Biol.* 17:376-383.

Yang, H. C., A. Palazzo, T. C. Swayne, and L. A. Pon. 1999. A retention mechanism for distribution of mitochondria during cell division in budding yeast. *Curr. Biol.* 9:1111-1114.

Young, M. E., J. A. Cooper, and P. C. Bridgman. 2004. Yeast actin patches are networks of branched actin filaments. *J. Cell Biol.* 166:629-635.

Zhu, H., M. Bilgin, R. Bangham, D. Hall, A. Casamayor, P. Bertone, N. Lan, R. Jansen, S. Bidlingmaier, T. Houfek, T. Mitchell, P. Miller, R. A. Dean, M. Gerstein, and M. Snyder. 2001. Global analysis of protein activities using proteome chips. *Science* 293:2101-2105.